INVESTIGATION OF A SLOPE INSTABILITY AT AMUAY, VENEZUELA

by

GARY ALAN PLATT
S.B., Rensselaer Polytechnic Institute
(1965)

Submitted in partial fulfillment
of the requirements for the degree of

MASTER OF SCIENCE

at the

MASSACHUSETTS INSTITUTE OF TECHNOLOGY

August 1966

Signature of Author.....
Department of Civil Engineering, August 23, 1966

Certified by.....
Thesis Supervisor

Accepted by.....
Chairman, Departmental Committee on Graduate Students

ABSTRACT

INVESTIGATION OF A SLOPE INSTABILITY
AT AMUAY, VENEZUELA

by

GARY ALAN PLATT

Submitted to the Department of Civil Engineering on August 23, 1966 in partial fulfillment of the requirements for the degree of Master of Science.

A shallow slide in the slope of an earth reservoir for storing fuel oil is investigated by means of field measurements and observations, laboratory tests and several theoretical analyses.

The peak and residual shear strength parameters of the clay in which the failure occurred, are obtained by repeated direct shear tests and compared to the shear strength parameters, obtained by theoretical analysis, that were required for equilibrium.

The residual factor is calculated for two possible soil conditons which may have existed in the shear zone at failure, and a value of residual factor, to be used as a future design criteria given.

Possible causes of the slide and recommendations for further surveillance and study are suggested.

Thesis Supervisor: Robert V. Whitman

Title: Professor of Civil Engineering

ACKNOWLEDGEMENT

The author is deeply indebted to Professor Robert V. Whitman for his inspiring guidance and suggestions, to Professor L. A. Wolfskill for his generous assistance, to Herbert G. Herrmann for his assistance in the experimental program and to Richard A. Schlumpf and William A. Bailey for their assistance and stimulating discussions concerning the computer solutions.

TABLE OF CONTENTS

LIST OF TABLES

LIST OF FIGURES

I. INTRODUCTION

This thesis is concerned with the slope failure (shown in Figure 1) of one wall of an oil storage reservoir. The slope was excavated into natural material in 1956, and remained stable until the spring of 1965, when the reservoir was emptied of oil. At this time, cracks were observed at the top of the failure area and the toe of the slope had moved horizontally. Movements occurred at a very slow rate during May, but major displacements resulted in early June. The slide involved a mass movement of approximately 1000 cubic yards.

Soil investigations, during and subsequent to the slide, yielded the soil conditions depicted in Figure 2. The major component of the mass slide was a fat "greasy" clay, with the bottom of the sliding mass being delineated by an old shear plane or joint. Subsequent to the initial movements of the slide, oil was readily seen to have seeped from this shear plane into excavations dug into the slide. Figure 2 shows the apparent phreatic line of soil within the slope, as observed in auger holes early in May.

The fat clay, being heavily overconsolidated, yielded a large difference between its peak and residual strengths, as determined by drained tests. In examining the results of repeated direct shear tests upon samples of the fat clay from a nearby location, the general nature of the strength behavior is indicated, rather than exact shear strength parameters. More and varied tests would be required to pinpoint these parameters. The strength parameters (shown in Figure 3) which were used for most of this investigation are:

	Angle of Friction	Cohesion
Peak Strength	$\overline{\phi} = 15.0°$	$\overline{c} = 3.2$ TSM
Residual Strength	$\overline{\phi} = 7.5°$	$\overline{c} = 0.0$ TSM

This slide was a typical progressive failure, after Skempton and Bjerrum, in which the strength of the clay in the most heavily stressed zone was gradually destroyed by a succession of drawdowns. In such situations, the strength is best described in terms of the residual factor*, an indicator of the degree to which the existing strength approaches its residual value.

The main objective of this thesis was to determine the residual factor of the clay as indicated by the failure, so as to provide a basis for the design of other cut slopes in this same material. This has been done by calculating the residual factor for two conditions.

(1) For the condition in May 1965, at which time the slope was just unstable. The residual factor for this condition is a lower bound for the residual factor an engineer should use for the design of other slopes in this material.

(2) For the reservoir full condition during the early part of 1965. The slope was apparently stable at this time. The residual factor for this condition is a reasonable value for the design of other slopes in this clay, although it is possible that the residual factor should be even higher for slopes which are to stand for much longer than 9 years.

In such a slope, the residual factor usually is not constant along the entire failure surface. In order to make

---

* Residual Factor (R), as defined by Skempton, is a quantitative expression for the amount by which the average strength of a clay has fallen below its peak strength.

the residual factor specific it is necessary to define some specific distribution of residual factor along the failure surface; two assumptions have been make herein:

(1) Residual factor is equal to 1.0 along the shear plane, but less than unity along the inclined portion of the failure surface through the clay.

(2) Residual factor is constant along the failure surface through the clay.

Further, the full frictional resistance of the granular rubble was assumed to have been mobilized.

A variety of analyses were made to calculate the residual factors, because at the start of the study it was not certain that any particular analysis was necessarily best. The Morgenstern-Price method, which breaks the failure mass into many slices with full consideration of the forces between the slices, was used as well as a version of the wedge method of analysis. The studies showed the Morgenstern-Price method to be versatile and very useful for the analysis of slopes in this type of situation.

The residual factors calculated from the Morgenstern-Price analysis are as follows.

	Residual Factor After drawdown	Residual Factor Before drawdown
Case 1 Residual factor along the inclined portion of the failure surface through clay when the residual factor equals unity all along the shear plane	.32	.62
Case 2 Residual factor is constant along the failure surface through clay	.70	.81

These factors were calculated using the lowest residual strength envelope in Figure 2; slightly higher factors would apply if a larger residual strength were used. The factors listed above can be used as a criteria for the design of slopes in similar materials, provided that corresponding assumptions are made regarding residual strength and the distribution of the residual factor.

II. BACKGROUND

II.1 History of FORS-2

During the summer of 1956, Fuel Oil Storage Reservoir No. 2 (FORS-2) was constructed at Amuay, Venezuela, for the Creole Petroleum Corporation. It is the second open and unlined reservoir of its kind for storing fuel oil.

Dr. T. William Lambe, acting as consulting soils engineer, and his Associates at M.I.T. designed and aided in construction control of the dam and reservoir. Details and specifications of the earthwork construction are given by Lambe (1957) in a soil engineering studies report of FORS-2. Performance records and observations are given by Lambe (1966).

II.2 Description of FORS-2

The reservoir was formed by constructing an 18 meter-high earth dam across a natural quebrada (u-shaped valley) yielding a capacity of 9 million barrels of oil. The dam proper, consisting of an upstream soil cement facing and an impervious core, is composed of the soil excavated from that portion of the natural plateau removed for the reservoir. The natural hills were excavated to an average slope between 2 to 1 and 3 to 1, horizontal to vertical.

To permit vehicular traffic during construction, operation and maintenance, and inspection, two berms were constructed. The lower one (elev. +12.0 meters) was added also for stability reasons. The upper berm was constructed along the crest of the reservoir (elev. +20.0 meters) to serve mainly as an access road.

The floor of the reservoir (elev. +2.0 meters) is covered with a clay blanket which is practically impervious

to the residual fuel oil that is stored (16 API weighing 60 lb/cu. ft., Lambe (1956) presents viscosity and surface tension data on the residual fuel oil).

II.3 Site Location

Amuay is located on the western side of the Paraguana Peninsula, Venezuela. The industrial area of the Creole Petroleum Corporation is situated adjacent to Amuay Bay.

For purposes of locating stability problems, the area has been divided into four zones. Three of these zones are indicated in the plan view of the refinery area given in Figure 4. As shown, FORS-2 falls within Zone D.

Figure 5 is a plan view of the completed dam and reservoir showing the location of the original cliff line into which the dam butts, the stationing along the crest, and the location of the slide and rubble zones which are to be analyzed. A photograph of the initial filling of FORS-2, Figure 6, illustrates the original design of the north wall. Figure 7 is another plan view of FORS-2. This figure indicates the shape of the reservoir after the north and south walls had been relined in the summer of 1965. The topography of the area and the location of some of the present field measurement installations are also shown.

II.4 Summary of Soil Types

Borings indicate a relatively uniform stratification or layering of the soil. From the boring logs around FORS-2, a generalized soil profile for the area has been approximated and is shown in Figure 8. The main soil types which were encountered and used in different phases of FORS-2

construction are described below.*

A. Caliche - A highly calcareous material (carbonate content of 88 per cent) in which the soil grains are cemented together. It is a non-plastic material and occurs naturally (in sizes ranging from clay to boulders) in the top few meters of the 20 meter high cliff.

B. Silty-Clay - A low plasticity material that was encountered in layers beneath the caliche for a distance of 5 - 10 meters (observed in boring logs).

C. Clay - Various types of clay were found in the lower portion of the cliff. These ranged from a very plastic clay (termed fat "greasy" clay) to a coarser, less plastic clay containing sea shells (termed "gritty" clay).

Table I summarizes the classification and index tests on the soils listed above. For this analysis, as will be explained later, we will mainly be concerned with the brown fat (greasy) clay.

The strength tests on this fat clay were run on a large sample obtained from the proposed FORS-3 area, which corresponds to that type of clay in which the slide took place.

---

* Soil descriptions and classifications (unless otherwise stated) have been taken from "Soil Engineering Studies for the Field Oil Storage Reservoir No. 2," by Lambe, March, 1957.

III. FORS-2 NORTH WALL SLIDE

III.1 Description of the Initial Cracking

In the spring of 1965, the oil in FORS-2 was drawn down to elevation +3.5 meters and on the morning of 22 April, four major longitudinal (parallel to the crest) cracks were observed on the north wall at approximately Station 14+30 (see Figure 5). One crack passed through the center of the lower berm; the second (major crack) through the reservoir edge of the lower berm; the third partially down the embankment; and the fourth, a horizontal crack, close to the reservoir floor. Figure 11 is a photograph which illustrates this initial cracking.

The upper material along crack no. 4 had heaved about 12 inches upward and toward the center of the reservoir (see Figure 13a) and crack no. 2 had opened at the center of its arc to dimensions of 12 inches vertically and 15 inches horizontally by 26 April 1965.

The movement seemed to have been restricted vertically to a zone between elevations +5.4 meters (crack no. 4 at the bottom) and +12.0 meters (cracks no.'s 1 and 2 through the berm). The maximum width of the zone of movement was about 50 - 60 meters longitudinally. Figure 9 illustrates the approximate shape and cross-section of the sliding mass.

III.2 Instrumentation and Field Investigation of the Slide Zone

In order to define and characterize the unstable zone, four kinds of information were required.

(1) Instrumentation and records of movement

(2) Types of soil in the slide zone

(3) Extent of cracks

(4) Extent of oil penetration

Four survey lines of closely spaced stakes were placed in the slope across the slide zone, as shown in Figure 10. The positions of the stakes were determined periodically by survey measurements and horizontal and vertical displacements calculated from them. It is from these measurements that the slope geometry to be used in the analysis was approximated.

On the days 3 May through 5 May, test pits were dug and auger borings attempted, in order to determine the type of soil in the slide zone, the extent of oil penetration and if possible, oil levels (which could be used in the analysis).

Due to oil seepage into the holes, the auger borings were abandoned. Identification of the soil was questionable and limits were not able to be run on those samples which were obtained because there was too much oil in them.

III.3 Engineer's Description of the Slide Zone Failure

The following paragraphs contain observations at the site, made by the soils engineer (Alton Davis), concerning the existing slide zone on the north wall of FORS-2, during the period 4 June to 20 June, 1965.

> By 4 June, 1965, a horizontal movement of about 2 cm. had occurred along a thin surface in test pit no. 1 at about elevation 5.4 meters.
>
> By noon time on 5 June, a further horizontal movement of 8 cm. was recorded in test pit no. 1. This sudden increase in the rate of movement corresponds to the first movement of heavy construction equipment along the berm. The combination of weight and vibration from these machines could account for this sudden movement. During

the period 6 to 7 June, there was no construction activity on the north wall, and the rate of movement observed in test pit no. 1 decreased to 5 cm. and 4 cm. per 24 hours, respectively.

On Monday the 8th of June, at about 9:00 a.m., a D-8 tractor started operating just above the slide mass. Between 9:10 and 9:25 complete failure of the slope occurred starting at the outside edge of the berm. During failure, wedge no. 1 of the slide (see Figure 15c) moved horizontally at about 1 meter per minute, and as it moved out over the edge (Point A), it disintegrated into blocks of about 1/2 meter on a side (average). As more of the mass broke up, the material flowed out onto the reservoir floor. Wedge no. III of the slide mass (see Figure 15a) moved vertically a maximum of about 2 meters near the center line of the slide mass.

During removal of the north wall slide mass, the bottom shear surface of the slide was found to be an oil covered, slightly undulating, horizontal surface at about elevation 5.6 meters. The material in the slide mass itself was stiff, fissured, fat clay with oil in all the fissures. The material outside of the slide mass consisted of medium fat clay with fewer fissures.

Just to the east of the slide on the north wall, a fault was uncovered which was filled with caliche rocks of up to 3 meter diameters (see Figure 9b). The fault appeared to be vertical and extended the full height of the dam. Complete excavation of the fault zone was not attempted since it appeared to penetrate well into the natural abutment.

Another area of oil penetration was uncovered at the western limit of the north wall repairs, corresponding to the bottom of the original abutment. This appeared to be a pocket of loose cobbles left during the original construction (see Figure 9b).

III.4 Discussion of the Slide Zone and the Mechanism of Failure

Although all movements of the sliding mass supposedly took place in natural ground, the soil in the failure zone

did not correspond with a typical soil profile of the area. Figure 1 illustrates this with a cross-section of the reservoir north wall. The soil profile shown is a simplified log of boring L-2-1 (a plan location of Boring L-2-1 is given in Figure 7). The upper portion of the slide zone was composed of a rubble material (loose, cohesionless soil) which had been smoothed off when the slope was originally excavated for the reservoir. This rubble indicates the presence of an old slide which had occurred naturally. Figure 12 shows an old slide surface in the south wall of FORS-2. It is possible that a similar slide surface existed in the upper region of our slide zone before excavation of the reservoir. The horizontal failure surface of the north wall slide zone seemed to be an old shear plane or joint in the fat "greasy" clay.

The mechanism of this slide exhibits the formation of 3 wedges which participated in the failure. These wedges are defined in the sketches of Figures 13c and 15c. Wedges II and III initially act as actuating blocks and wedge I as a neutral block. Figure 13 contains pictures of the early movements of the slide zone; the photograph in Figure 13a showing the initial toe bulge of wedge I and the photograph in Figure 13b showing the development of the wedges during early movements. Wedge II was the first one to undergo a large vertical displacement. This is shown by the photograph in Figure 13b and is illustrated schematically in Figure 13c.

Figure 14 depicts the test pit that was excavated in the toe region of the slide zone on 4 May 1965. At this time, as verified by the photograph in Figure 14a, oil was leaking from the horizontal slip surface beneath wedge I (the cigarette pack denotes the position of the shear plane).

From 4 May until 4 June, 1965, the failure body moved less than 2 cm. toward the center of the reservoir, but by

noon 5 June 1965, the movement had increased to 10 cm. This sudden increase has been attributed to the operating of heavy equipment along the berm directly above the slide zone. The photograph in Figure 14b, taken on 5 June 1965, is a close up of this horizontal failure surface that shows the movement to date, which has occurred since the excavation of the test pit.

Finally, on 8 June 1965, immediately after a bulldozer had been operating on the berm, complete failure occurred. The final shape of the slide zone is illustrated in Figure 15. Figure 15a is a photograph which indicates that wedge III was the actuating body which initiated the final movements. The relative movements of wedge II and wedge III, with respect to each other, caused the position of the inclined slip surface to change during increased movement of the failure body (i.e., first, wedge II moved vertically and came to rest and then wedge III dropped a distance of about 2 meters during failure). Figure 15b is a general view showing the debris on the reservoir floor and the scarp from the inclined failure surface. A schematic indicating the final positions of the wedges which participated in the failure is shown in Figure 15c.

IV. GENERAL ASSUMPTIONS AND CONSIDERATIONS IN THE STABILITY ANALYSIS

IV.1 Dimensions of the Failure Zone and Geometry of the Problem

One of the first steps in the stability analysis will be to define, as closely as possible, the boundaries of the slide zone. The approximate plan and cross-section of the three wedges have been given in Figures 9a and 9b respectively.

It should be explained that the failure surface, which we are going to analyze, is not the exact failure surface along which the initial movements took place. The dotted lines in Figure 9a depict what is thought to be a close estimate of the original failure surface shape. During the increase in displacement of wedge I along the horizontal slip surface, wedges II and III changed shape, causing a relocation of the position of the inclined portion of the failure surface.

We will perform our analysis on the final shape of the failure surface, shown by the dashed lines in Figure 9a, because it is along this surface that complete failure occurred. The final coordinates of the heel of wedge no. I were determined by field measurements and are noted in figure 9a. A scale drawing of the actual slope and failure surface has been given in Figure 2.

IV.2 Pore Pressure Considerations

"The principle of retaining fuel oil with compacted clay is based on the interfacial tension developed between oil and water" (Lambe, 1956). The pressure of the oil impounded in the reservoir is transferred to the soil by capillarity at the water-soil interface. Thus, this weight acts essentially as a surcharge or an applied total stress on the slope of the reservoir.

If the natural slopes acted as compacted clay, there would be no oil penetration, and the pore pressures would be taken as atmospheric or less at all points above the water table (located at elev. +2.0 meters). Actually, the pressures in the pore water above the water table would be less than atmospheric because of the capillary forces which may have developed at the air-water interfaces (Lambe, 1956).

However, in our problem we know from the test pits, auger borings, and experience with FORS-1, that oil has penetrated deeply into the slope at certain sections. The oil has entered through porous zones and along natural cracks and fissures, but has not penetrated the intact portions of the clay. In this case, the oil had penetrated the slope to such an extent that upon drawdown, a phreatic oil surface developed within the slope and oil was seeping back into the reservoir. This surface, approximated from the oil levels in 3 auger holes, was assumed to be a straight line as shown in Figures 1 and 2.

Ths oil, because of the seepage which had occurred previous to drawdown, can no longer be considered to act as a surcharge, but instead must be treated as an excess pore pressure. In the following analyses, the pore pressures will be computed as though the oil were equivalent to water. Because of the approximation in choosing the position of the oil surface, the error due to the difference in unit weight between water (62.4 pcf) and oil (60.0 pcf) is thought to be insignificant and will be neglected in the calculations. Treating the oil as water is a simplification in the conservative direction and therefore will not be critical if the assumption is not entirely correct.

The most critical condition for this problem is a rapid drawdown situation. Because we do not know the conditions of rapid drawdown for this case, but rather those at a later stage when the phreatic line was observed, we must analyze an after-drawdown situation.

IV.3 Three-Dimensional Effects and Corrections

All of our methods of analyses have assumed that the problem is two-dimensional. In many large land slides this may be true, but in the case which we are analyzing, the slide zone has a finite longitudinal dimension. Consequently, resisting shear forces act on the ends of the sliding mass and our assumption of a two-dimensional situation is conservative.

One may try and correct for the 3-D effects by dividing the wedge into a number of equal sections with the vertical planes perpendicular to the longitudinal axis, and analyze an average condition for each section. We may then compute a weighted factor of safety of the slide, by averaging the values of factor of safety obtained for each section.

In our case, the possible error in assumptions regarding dimensions of the failure surface for a number of sections would make questionable any improvement obtained by considering the 3-D effect. Therefore, we will not try and correct for it but will consider our estimate of the final equilibrium parameters and the residual factor conservative for the reasons stated above.

IV.4 Drained Failure

For the analyses of this slide, we have assumed drained conditions. It is thought for this failure, as is typical for long term failures, that the slow rate of movement of the sliding body justifies the assumption of a drained failure.

V. SHEAR STRENGTH

V.1 Definition of Shear Strength and Factor of Safety

The shear strength, resistance to sliding along a surface, may be expressed by the Coulomb-Terzaghi equation:

$s = \bar{c} + (\sigma - u) \times \tan(\bar{\phi})$

s = available shear strength of the soil

u = neutral force

$\bar{c}$ = effective cohesion intercept

$\bar{\phi}$ = effective angle of friction or shear resistance

$\bar{\sigma} = (\sigma - u)$ = effective normal stress acting on the slip surface at failure

If we analyze a stable slope, only a portion of the shear strength will be required to balance the shear stress and hold the slope in equilibrium. This particular slope is said to have a factor of safety with respect to failure.

We have defined our factor of safety as the ratio between the available shear strength and the actual shear stress.

Factor of safety (F) = shear strength (S)/shear stress (τ)

usually written as

$\tau = S/F = \bar{c}/F + \bar{\sigma} \times (\tan \bar{\phi})/F$

F = factor of safety

S = available shear strength

τ = actual shear stress

This definition assumes that the factor of safety is a constant for all points on a potential failure surface.

Failure occurs when the sum of the developed shear stresses along the failure surface is equal to the sum of the available shear strengths along the failure surface (i.e., when F = 1.0).

IV.2 Definition and Explanation of Residual Factor

When analyzing a slope stability problem, two of the first questions one asks are:

(1) What soil parameters are needed for the calculations?

(2) What laboratory tests will determine these soil parameters?

These are important questions when considering natural slopes in an over-consolidated clay. In most cases, the numerical value of the factor of safety in stability calculations varies greatly, depending on whether one uses peak, residual or some intermediate strength of the soil.

It has been pointed out (Skempton (1964), Bjerrum (1966)) that for analyses of slope failures in over-consolidated plastic clays, the strength parameters computed from the slide are almost independent of those observed in standard laboratory tests. It was found for these clays that the peak values of the cohesion intercept $\bar{c}$ and the angle of friction $\bar{\phi}$, obtained by conventional tests, had to be reduced in order to equal the values which must have been operative in the clay at the time of the failure.

The "problem" is to determine which soils fail at peak strength, which fail at residual strength, and which fail in between these two limits.

Skempton has formulated a "residual factor," which is a "quantitative expression for the amount by which the average strength of a clay has fallen" below its peak strength.

$$\text{Residual factor } (R) = (S_P - S)/(S_P - S_R)$$

or

$$\text{Shear stress } (S) = R \times S_R + (1 - R) \times S_P$$

S = average Shear Stress developed along the slip surface at a F.S = 1 condition

S_P = Peak Strength

S_R = Residual Strength

R = That portion of the total slip surface in the clay along which its shear strength has fallen to the residual value

For values of:

$R = 0$, there is no strength reduction and failure occurs at peak strength

$R = 1$, there is complete strength reduction and failure occurs at residual strength

Figure 16 gives a clearer concept of the definition of the residual factor by illustrating it on a $\bar{\sigma} - \tau$ plot.

Examining many case failures in overconsolidated clays, Skempton has tried to determine values of "R" and relate them to the type of clay in which the failure occurred. He believes that for a given set of conditions, the residual factor for the same type of clay will be constant.

We have calculated the residual factor of Amuay fat clay for both submerged and drawdown states for two different assumptions of residual factor distribution.

VI. EXPERIMENTAL INVESTIGATION

VI.1 Summary of Testing

The peak and residual shear strength parameters of undisturbed samples of Amuay brown fat clay were determined using the M.I.T. four-unit repeating direct shear apparatus.

The samples were taken from a large undisturbed chunk of Amuay fat clay (similar to that in which the major portion of the slide took place) which had been hand cut from an excavation in the proposed FORS-3 area.

Our test program consisted of running four direct shear tests in which three different consolidation pressures were used (10.0, 20.0, and 40.0 metric tons per square meter). Two tests were run at a consolidation pressure of 10.0 TSM. One of these, Test No. 4, after being consolidated, had a failure surface precut. Then, after one slow shear, nineteen rapid reversing shears, and a second slow shear, the sample was split apart. Oil was inserted on the failure surface and the sample put back together. Nine rapid reversing shears were run and then the final, thirty-first shear, was run at a slow rate. A more detailed testing procedure is described in Appendix A.

VI.2 Data Presentation

The results of the first, twenty-first and thirty-first forward shears of tests 1, 2, 3 and 4 are summarized on Figures A.1, A.3, A.5 and A.7 respectively. The stress-strain plots for the peak and residual shears for these tests are on Figures A.2, A.4, A.6 and A.8 respectively.

The peak strength has been obtained from the stress-strain plot of the first shear and the residual strength from the lowest drained shearing resistance mobilized along a

failure surface (Bjerrum (1966)).

A summary table of the four tests, the effective normal stresses, peak strengths and residual strengths is given in Table A.I. The values of strength are plotted in Figure 3 with open (peak) circles and solid (residual) circles. Through these two sets of data points, we have passed a peak strength envelope and three possible residual strength envelopes.

VI.3 Discussion of Data

Looking at Figure 3, the scatter of data points is quite noticeable for the peak strength envelope. This may be attributed to two possibilities.

(1) These are undisturbed soil samples and are not perfectly homogeneous. The fat clay contained sand lenses with occasional caliche stones.

(2) The four samples may have had slightly different orientation with respect to each other and the soil stratification. Taking our samples from undisturbed chunks of material made this error possible.

The data points of the residual envelope are in much better agreement, as would be expected. The truly residual condition of a clay is not affected by the stress history of the sample (Skempton). However, it is still possible for the sand lenses to cause some scatter in the results. Strict interpretation of the residual strength data points has led to three possible choices for the residual envelope. Actually, there are two possibilities for the untreated soil. Line No. 1, the lower-most one, has only one data point, which has been obtained from the sample with a precut and oil covered failure surface, whereas residual lines (2) and (3) each have at least three data points. Residual envelope (2) has a cohesion intercept and envelope (3) does not.

The results were not thought to be affected by caliche stones, in that none were visible upon inspection of the failure planes. We did notice that there was evidence of slickensides being developed on portions of the failure surface.

A comparison between Test #3 and Test #4 indicates that the residual strength of Amuay fat clay is slightly lower for a sample with a precut failure surface that has been split apart and had oil inserted on the failure plane.

The peak strength parameters and the three possible choices of the residual strength parameters are tabulated below.

Results of Direct Shear Testing Program

Strength Condition	Angle of Friction	Cohesion (TSM)
Peak strength	15.0	3.2
Oil residual#1	7.5	0.0
Residual #2	8.5	0.35
Residual #3	10.0	0.0

In summary, the test program is thought to have provided good representative results on the general strength behavior of Amuay fat clay.

VII. THEORETICAL INVESTIGATION

VII.1 Methods of Investigation

The two main methods of analysis which have been used are:

(1) Sliding Block or Wedge Method

Method in which the "equation of equilibrium of horizontal forces assumes the prominent position usually occupied by the equation of moment equilibrium" (Sherrard (1963)).

(2) Morgenstern and Price Method*

Slice method which completely satisfies equilibrium and boundary conditons. A computer is required for the useful application of this method.

The failure surface of the sliding mass may be closely defined by plane surfaces, and therefore our first approach to the problem is a wedge method of analysis. For purposes of this analysis, we have simplified the previously defined slope, soil, failure surface and oil surface information to that shown in Figure 17. Wedge I now has a horizontal base and the boundary between the two wedges is a vertical plane. Also, the slope of the reservoir has been assumed to be a straight line.

With this simplified wedge geometry as an approximation to the slide, we attack the problem from four different angles to see what may be learned from an investigation of this type of failure surface.

---

* Method of Morgenstern and Price will be referred to, in some cases, as "MGSTRN." This is a computer program solution which has been written for timesharing, with conversational input and output.

We then perform a stability analysis on the actual slope and failure surface geometry, approximated from field measurements, by the method of Morgenstern and Price.

The following is an outline of each method of analysis.

(1) Investigation of the average stresses developed along surface (2) of the simple wedge theory.
Given the soil conditions on surfaces (1) and (3):

(a) What are the average $\overline{N}_2$ and the average τ_2 required for equilibrium of the wedges?

(b) How do the values of average $\overline{N}_2$, average τ_2 and the residual factor along surface (2) change with different assumptions of $\overline{\phi}_1$, $\overline{c}_1$, $\overline{\phi}_3$ and $\overline{c}_3$?

(2) Factor of safety of the simple wedge by wedge theory for two conditions:

(a) F.S. = F on all surfaces

(b) F.S. = 1.0 on surface (1)
F.S. = F on surfaces (2) and (3)

(3) Factor of safety of the simple wedge by "MGSTRN."

(4) Side force investigation of the simple wedge geometry by "MGSTRN." We determine the effect of the side force assumption on:

(a) factor of safety

(b) residual factor

(c) position of the effective side thrusts

(d) $\overline{\phi}$'s developed on the sides of the slices

(5) Analysis of the actual slope and failure surface geometry by the method of Morgenstern and Price. Using the actual slope and failure surface geometry that was approximated from field measurements, we analyze the problem by "MGSTRN" for two soil conditions and two water conditions.

Case (1) Soil (1) is at Residual Strength

a) Before Drawdown

b) After Drawdown

Case (2) Soil (1) = Soil (2)

a) Before Drawdown

b) After Drawdown

The soil parameters and residual factors required for the equilibrium condition (F.S. = 1.0) in each of the four cases are compared.

VII.2 Analyses of the Problem

VII.2.1 Investigation of the average stresses developed along surface (2) of the simple wedge by wedge theory

The wedge geometry that is used in this investigation has been defined in Figure 17. We are interested in knowing how the average effective normal stresses ($\bar{N}$) and the average developed shear stresses (τ) along surface (2) vary for different assumptions of strength mobilized along surfaces (1) and (3). To do this, the author derived equations, using limiting equilibrium, for average $\bar{N}_2$ and average τ_2.

In the derivation of these equations, equilibrium of the wedges was satisfied with respect to horizontal and vertical translation but not with respect to moment. Moment equilibrium is not considered because of the assumptions required relative to the points of action of the external forces. Instead, in order to solve the equations for average $\bar{N}_2$ and average τ_2, we eliminate unknowns by assuming values of the soil parameters along surfaces (1) and (3).

Thus, we may readily substitute different values for the assumed parameters ($\bar{\phi}_1$, $\bar{c}_1$, $\bar{\phi}_3$ and $\bar{c}_3$) and observe changes in $\bar{N}_2$ and τ_2.

The equations for $\bar{N}_2$ and τ_2 are:

$$\bar{N}_2 = \frac{W_2 - \tau_3 - \tau_2 \times \sin\theta - U_2 \times \cos\theta}{\cos\theta}$$

$$\tau_2 = \frac{W_2 \times \tan\theta - \tau_3 \times \tan\theta - N_3}{\tan\theta \times \sin\theta + \cos\theta}$$

The derivation of these equations and the method in which they are solved are given in Appendix B.

Using the given wedge geometry and the above equations, we have computed for different assumed values of strength parameters along surfaces (1) and (3), the average $\bar{N}_2$ and τ_2 and the corresponding residual factor along surface (2) required for equilibrium of the wedges.

Figure 18 is a plot of average effective normal stress vs. average shear stress. For each assumption of $\bar{c}_1$, $\bar{\phi}_1$, $\bar{c}_3$ and $\bar{\phi}_3$ that is made, points corresponding to the values of the average $\bar{N}$ and the average τ developed along each of the three surfaces have been plotted.

The format of the method in which these points are obtained is as follows:

(1) A set of soil parameters is defined along surfaces (1) and (2) and designated by a small letter of the alphabet "a", "b", "c"...etc.

(2) Calculations are made of the average effective normal stress and the average shear stress developed along each of the three surfaces.

(3) Three points are plotted for each set of soil parameters:

i) Point (1) corresponds to the average stresses developed along surface (1)

ii) Point (2) corresponds to the average stresses developed along surface (2)

iii) Point (3) corresponds to the average stresses developed along surface (3)

This process was carried out for nine sets of parameters. A complete summary of the trials (soil parameters and developed stresses along each surface) is given in Table II.

We have also included on Figure 18 the peak strength envelope and three possible residual envelopes. For a given average effective normal stress acting on a surface, we may obtain from the proper envelopes the corresponding peak (S_p) and residual (S_R) values of available strength. For a given set of parameters, using these values of available strength along surface (2) with the corresponding calculated value of the average shear stress developed along that surface, we may compute the residual factor for surface (2).

In this investigation, we are primarily concerned with the residual factor and have made an assumption of its distribution. Because surface (1) was thought to be an old shear plane and is known to have been lubricated with oil, we have assumed a residual soil condition ($R = 1.0$) along that surface in all the trials of this section. Therefore, in the calculation of the residual factors, we use the envelope which corresponds to the parameters along surface (1) as the residual envelope. The results of the residual factor calculations are also included in Table II.

Looking at Figure 18, we can see how the average effective normal and shear stresses are changing. It should be noted that Figure 18 is at a much larger scale than Figure 3 (the results of the direct shear tests). Therefore, variations in $\bar{N}_2$ and τ_2 will seem greater when plotted on Figure 18. We have found that these changes of average effective normal stress and average shear stress along surface (2) which do occur are negligible, even on this enlarged scale. Consequently, these variations for different

assumptions of parameters could not be measured if the points were plotted on Figure 3.

Comparing the trials performed in this analysis, the following observations and conclusions have been made:

(1) For a given set of residual conditions ($\bar{\phi}_1$, $\bar{c}_1$) along surface (1).

(a) Small values of shear strength (compared to peak) are required along surface (2) for equilibrium.

(b) An increase in the assumed value of mobilized $\bar{\phi}_3$ from 7.5 to 10.0 degrees results in a negligible change in the value of the average $\bar{N}_2$ and the average τ_2 developed.

(c) An increase in the assumed value of mobilized $\bar{c}_3$ from 0.0 TSM to 0.35 TSM results in a small decrease in the average values of $\bar{N}_2$ and τ_2 which must be developed for equilibrium. This small change in the stresses (3-5%) is negligible for our purposes.

(d) There is a negligible change in the residual factor along surface (2) for the above increase in $\bar{\phi}_3$ and only a 2-3% change (which is also negligible) for the above increase in $\bar{c}_3$.

Thus, the residual factor along surface (2) may be considered to remain constant for small changes in the assumed parameters along surface (3).

(2) A small increase in the assumed residual friction angle mobilized along surface (1) (holding the cohesion constant), increases our residual factor along surface (2) by only 4-5%.

(3) The addition of a cohesion intercept (0.35 TSM)

to the residual parameters along surface (1), increases the residual factor along surface (2) substantially (30%).

(4) For an assumed value of R = 1.0 acting along surface (1), an average value of the residual factor = 0.66 along the entire length of surface (2) has been calculated for the drawdown condition.

VII.2.2 Factor of safety analysis by the wedge method

In this section we have analyzed the factor of safety of the simple wedge geometry for two conditions of factor of safety.

(1) F.S. = F on all surfaces

(2) F.S. = 1.0 on surface (1)
F.S. = F on surfaces (2) and (3)

VII.2.2.1 F.S. = F on all surfaces

The first condition which we analyze is with the factor of safety (F) constant throughout the entire failure body (i.e., the equations of equilibrium are solved such that the F.S. = F along surfaces (1), (2) and (3)).

In section VII.2.1, we assumed that the factor of safety with respect to shear strength was equal to 1.0 throughout the body. Now, using the same general equations of equilibrium, we leave the factor of safety term (F) in the equations as one of the unknowns. The equation for the developed shear stress along a surface becomes:

$$(\tau) = S/F = \bar{c}/F + \bar{N} \times \tan(\bar{\phi})/F$$

(as defined in section V.1)

In this investigation, we assume values of the soil parameters along all three surfaces of our sliding blocks.

We are left with four unknowns ($\bar{N}_1$, $\bar{N}_2$, $\bar{N}_3$ and F) and four equations of equilibrium. When solving these equations, we find that the unknown term "F" is not easily solved for in terms of the other unknowns. Therefore, we have set up the equations so that an iterative procedure is used in the determination of the factor of safety (F).

Appendix C has the derivation of the equations for this part of the analysis.

The final equations are given below:

$$\bar{N}_3 = \frac{(\gamma c_1 + (W_1 - U_1)\tan \bar{\phi}_1)(\frac{1}{F}) + \frac{\alpha c_3 \tan \bar{\phi}_1}{(F)^2} - U_3}{(1 - \frac{\tan \bar{\phi}_3 \tan \bar{\phi}_1}{(F)^2})}$$

$$A = W_2 \sin \theta - (\bar{N}_3 + U_3)\cos \theta$$

$$B = (U_2 - W_2 \cos \theta)\tan \bar{\phi}_2 - \beta c_2 - (\alpha c_3 + \bar{N}_3 \tan \bar{\phi}_3)\sin \theta - (\bar{N}_3 + U_3)\tan \bar{\phi}_2 \sin \theta$$

$$C = (\alpha c_3 + \bar{N}_3 \tan \bar{\phi}_3)\tan \bar{\phi}_2 \cos \theta$$

$$F_f = \frac{-B \pm \sqrt{B^2 - 4AC}}{2A}$$

To obtain a value of the factor of safety for a defined set of soil parameters along the three surfaces, we must assume an initial value of F.S. = F_i and insert this in our equation for $\bar{N}_3$. Using the value of $\bar{N}_3$ obtained, plug into the equations given for A, B, and C. Then put the values of A, B, and C into our final equation and compute a value of F_f. Using a trial and error iteration procedure, we quickly converge to values of F_i and F_f that are nearly identical. When this has been achieved, we have obtained the factor of safety for this particular set of soil conditions.

We have used the above equations to calculate factors of safety of the simple wedge drawdown condition for values of peak and residual strengths acting throughout the failure body. The results are summarized in the table below.

	Drawdown Condition F.S. = F on all surfaces		
Soil Condition	$\bar{\phi}_1 = \bar{\phi}_2 = \bar{\phi}_3$	$\bar{c}_1 = \bar{c}_2 = \bar{c}_3$ TSM	F.S.
Peak	15	3.2	3.79
Residual #1	7.5	0	.32
Residual #2	10.0	0	.43
Residual #3	8.5	0.35	.70
Residual #4	7.5	0.50	.80

Using a trial and error procedure, we may also obtain with these equations the parameters required to hold the two wedges in equilibrium (F.S. = 1.0). Assuming $\bar{\phi} = 7.5°$ for a constant soil condition, an equilibrium cohesion parameter ($\bar{c}$) = 0.75 TSM was computed. The corresponding residual factor along the entire length of the failure surface was equal to 0.78. This value of $\bar{c}$ was calculated using the $\bar{\phi} = 7.5°$ and $\bar{c} = 0.0$ TSM residual envelopes.

Later in the analysis, we determine the factors of safety and the residual factor for the same soil conditions using the high powered Morgenstern and Price method, and compare them with the results of the simple wedge.

VII.2.2.2 F.S. = 1.0 on surface (1) and F.S. = F on surfaces (2) and (3)

The second factor of safety condition that we investigate using the wedge analysis is with the F.S. = 1.0 along surface (1) and the F.S. = F along surfaces (2) and (3).

For this case, the definition of the shear strength mobilized along surface (1) is expressed as:

$$\tau_1 = S/1.0 + \frac{\bar{c}_1}{1.0} + \bar{N}_1 \frac{\tan(\bar{\phi}_1)}{1.0}$$

The other forces acting on the wedges are defined the same as those in the F.S. = F section (VII.2.2.1).

In this analysis, values of the soil parameters acting on surfaces (1), (2) and (3) of the sliding blocks are assumed in each trial. Thus we are left with the same four equations of equilibrium that we had in the previous section. To solve these equations for F_f, we must set up the same type of an iteration procedure.

The derivation of the final equations of this section is given in Appendix D.

The only difference between the equations derived in this section and those of section VII.2.2.1 is the equation for $\bar{N}_3$, and it is given below:

$$\bar{N}_3 = \frac{(W_1 - U_1)\tan\bar{\Phi}_1 + \gamma c_1 - U_3 + \frac{\alpha c_3}{F}\tan\bar{\phi}_1}{(1 - \frac{\tan\bar{\phi}_3 \tan\bar{\phi}_1}{F})}$$

The method of obtaining the factor of safety (F) for a given set of conditions is the same as in the previous section.

Using the final equations of this section, the factors of safety for trials with the same residual strength parameters as in the preceeding section have been calculated and are summarized below.

Drawdown Condition
F.S. = 1 on surface (1)
F.S. = F on surfaces (2) and (3)

Soil Conditions	$\bar{\phi}_1 = \bar{\phi}_2 = \bar{\phi}_3$	$\bar{c}_1 = \bar{c}_2 = \bar{c}_3$ TSM	F.S.
Residual #1	7.5	0	.186
Residual #2	10	0	.255
Residual #3	8.5	0.35	.554
Residual #4	7.5	0.50	.719

With the parameters along surface (1) already at the residual strength of the soil ($\bar{\phi}_1 = 7.5$, $\bar{c}_1 = 0.0$), we find that in order to obtain an equilibrium condition assuming $\bar{\phi}_2 = \bar{\phi}_3 = 7.5°$, we must have an average available cohesion along surfaces (2) and (3) equal to 1.0 TSM. These mobilized strength parameters correspond to a residual factor along surface (2) equal to .70.

A comparison of the residual factors calculated using wedge theory for the two possible soil conditions is given below.

Drawdown Condition

Case #1	$\bar{\phi}$	$\bar{c}$	F.S.	R
Residual Factor = 1.0 along surface (1) Residual factor = R along surfaces (2) & (3)	7.5	1.00	1.0	.70
Case #2				
Residual factor = R is constant along the failure surface	7.5	0.75	1.0	.78

Case #1 requires a higher equilibrium cohesion parameter and consequently has a lower residual factor. Therefore, a slope designed to be stable for the conditions of case 1 would be conservative for the conditions of case 2.

VII.2.3 Factor of safety of the simple wedge by "MGSTRN"

The factor of safety of the simple wedge failure surface may also be determined by the powerful method of Morgenstern and Price. Making different side force assumptions with "MGSTRN" we obtained three sets of factors of safety for three of the same soil conditions that were analyzed by the F.S. = F wedge method (see Table III for a tabulation of the results). The effects of these different side force assumptions will be explained in the next section. However, the small variation in the factor of safety with a change in the side force function should be noted at this time. Comparing the factors of safety computed by "MGSTRN" with those from the F.S. = F wedge method, we find very good agreement. The small difference between them indicates that the two methods will predict almost identical factors of safety for a constant soil condition.

Because a slope failure has occurred, we know that the correct factor of safety = 1.0 (that condition which exists when the actual average shear strength of the clay at the time of failure equals the actual average developed shear stress).

Using a trial and error procedure, we may also obtain with "MGSTRN" the strength parameters required to yield a F.S. = 1.0 in the stability analysis.

The first approach was for the drawdown condition with constant soil parameters throughout the slope (i.e., the same strength was mobilized along the entire failure surface). Assuming a $\overline{\phi}$ = 7.5°, the cohesion parameter required for equilibrium equaled 0.75 TSM and the corresponding residual factor along the entire failure surface equaled 0.77.

It is seen that the values of the equilibrium parameters and the calculated residual factor obtained with "MGSTRN" are also the same as those obtained for the wedge theory with the F.S. = F. Thus, these results seem to confirm a close correlation between "MGSTRN" and the simple wedge theory for a single soil condition.

The second approach more closely approximates the soil conditions of the slide zone. In this analysis, we use the simple wedge geometry and divide the slope into three soil zones as indicated in Figure 19. These three soil zones are believed to be representative of the soil conditions in the slide zone at the time of failure. We fix the soil parameters in zones (1) and (3), and vary those parameters in zone (2) in order to obtain a F.S. = 1.0. Because of the rubble zone discovered at the top of the slide and the manner in which the slip developed along surface (1), this seems to be a logical assumption of knowns and unknowns.

Thinking that in zone (2) the cohesion would be more critical than the friction angle of the soil (relative to stability), we chose a conservative estimate for the angle of friction ($\overline{\phi}_2 = 7.5°$) and varied the cohesion ($\overline{c}_2$) to obtain a factor of safety approximately equal to 1.0. The validity of this assumption is proven in section VII.2.5. (It is shown that doubling the assumed angle of friction ($\overline{\phi}_2$) decreases $\overline{c}_2$ by only about 15 per cent).

For equilibrium of the failure mass under these fixed soil conditions, the cohesion required in soil (2) was found to be $\overline{c} = 2.2$ TSM. The soil properties of the three zones which were used in this final trial are given below.

Soil Properties used in obtaining a F.S. = 1.0, by "MGSTRN," for the simple wedge with three soil zones for the after drawdown condition

Soil No.	Total	$\bar{c}$TSM	$\bar{\phi}$
1	2.08	0.0	7.5
2	2.08	2.2	7.5
3	2.17	0.0	25.0

The corresponding residual factor for this set of soil parameters = 0.36 along that portion of the inclined failure surface which falls in the clay (for this case, R = 1.0 along the horizontal portion of the failure surface and the full frictional resistance of the granular material in zone (3) has been mobilized).

Comparing this residual factor with those obtained, by both the wedge theory and "MGSTRN," for a more simplified soil condition, we observe that it is less than one half those values. This large difference points out the great effect that the residual factor distribution assumption and the soil conditions have on the results. It also indicates the versatility and advantage of "MGSTRN" in being able to define and handle complex soil conditions.

VII.2.4 Side force investigation of the simple wedge geometry by "MGSTRN"

When solving a slope stability problem using limiting equilibrium, assumptions must be made in order to obtain a statically determinate situation. Morgenstern and Price have solved their equilibrium equations such that the indeterminancy of the problem is placed on the internal forces. To remove this indeterminancy, assumptions are made concerning the relation between the normal and shear forces developed on the sides of the slices (see Bailey, 1966).

Consequently, for an analysis of a slope failure to be considered theoretically sound, we not only are required to have a F.S. = 1.0, but the internal stresses set up in the shear zone must satisfy the following conditions:

(1) The side force assumption throughout the failure zone must be reasonable.

(2) The line of action of the effective side thrust should fall between 1/3 to 1/2 the height of the slice.

(3) The friction angles which are developed on the sides of the slices should be less than the available friction angle.

An investigation by "MGSTRN" to determine the effects of a change in the side force assumption on results, was performed on the simplified wedge geometry shown in Figure 19. A description of this study is given in Appendix E. The main conclusions that were drawn from the investigation are given below.

(1) Numerically correct factors of safety and residual factors may be obtained using "MGSTRN" without concern of the side force assumption.

(2) In the determination of the most correct solution (that solution which completely satisfies equilibrium and boundary conditions), the side force assumption plays an important part.

(3) In the process of obtaining a most correct solution for the drawdown case of our problem, it was noted that a satisfactory side force assumption depends on the location of the phreatic surface, the shape of the failure surface, and the variation of soil parameters throughout the body.

(4) An off centered trapezoid + bell, with the

peak of the bell occuring at the intersection of the two segments of the failure surface, is thought to be the most correct side force assumption for this problem.

VII.2.5 Analysis of the actual slope and failure surface geometry by the method of Morgenstern and Price

In this section we have analyzed the actual slope and failure surface geometry that was approximated from field measurements. Figure 20 is a cross-section depicting the three soil zones, the phreatic oil surface and the failure surface of the slide which are used in this analysis. It should be mentioned that the strength parameters $\bar{\phi}_3 = 25°$ and $\bar{c}_3 = 0.0$ TSM have been assigned to soil (3). They are thought to be representative of the loose cohesionless rubble that was discovered in this zone.

We consider two possibilities of soil conditions and residual factor distribution which may have existed throughout the shear zone at the time of failure.

CASE 1 The soil in zone (1) is assumed to have a residual factor = 1.0 and the soil in zone (2) a residual factor < 1.0.

$\bar{\phi}_1 = 7.5°$ $\bar{c}_1 = 0.0$ TSM

$\bar{\phi}_2 =$ $\bar{c}_2 =$

$\bar{\phi}_3 = 25°$ $\bar{c}_3 = 0.0$ TSM

The mechanics of failure for CASE 1 are:

(1) Soil (1) reaches the residual condition because of oil entry along an old shear plane.

(2) Soil (3) is assumed to be experiencing a stress such that it is just below the failure condition (i.e., a $\bar{\phi}$ slightly less than 25° has been developed throughout zone (3)).

(3) Soil (2) is highly stressed upon drawdown and is undergoing a progressive weakening along surface β'.* When the strength in this zone has decreased to the point where it equals the developed shear stress along surface β', failure occurs.

CASE 2 The soil in zones (1) and (2) is assumed to have the same strength parameters and the same residual factor (R) along the failure surface through the clay.

$\bar{\phi}_1 = \bar{\phi}_2 =$ $\qquad$ $\bar{c}_1 = \bar{c}_2 =$

$\bar{\phi}_3 = 25°$ $\qquad$ $\bar{c}_3 = 0.0$ TSM

The mechanics of failure for CASE 2 are:

(1) Soil (3) is assumed, as in CASE 1, to be under a stress such that it is just below the failure condition.

(2) Soils (1) and (2) are assumed to act as one soil with progressive failure occurring along surfaces γ** and β'. When the average available strength along both of these surfaces has decreased enough such that it is equal to the average shear stress developed, failure will occur.

For each of these cases, we have calculated three sets of equilibrium parameters (F.S. = 1) for two possible oil conditions at failure.

(1) the after drawdown condition, during which the slope was just unstable.

(2) the before drawdown condition, during which the slope was stable.

Then, obtaining from the computer output for each trial, the average effective normal stress along surface β' (CASE 1) on

---

* β' = the steeply inclined portion of the failure surface located in soil (2).

** γ = the (almost) horizontal portion of the failure surface.

surface $\beta'+\gamma$ (CASE 2), we were able to calculate the residual factor for each set of equilibrium conditions.

The results of many sets of parameters for each case provide a good comparison of the residual factors between the before and after drawdown conditions and between the two cases of different residual factor distribution. They also familiarize us with the changes in the developed internal stresses for different possible combinations of equilibrium parameters $\bar{\phi}$ and $\bar{c}$.

The F(x) = constant side force assumption has been employed for the after drawdown condition and the F(x) = Bell side force assumption for the before drawdown condition. We use only one value of the side force function for a given oil condition so that the conclusions with respect to changes in the $\bar{\phi}$'s developed on the sides of the slices, the position of the effective side thrusts, and the value of the residual factor, for different sets of equilibrium parameters are not the result of a change in the side force assumption.

CASE (1) Soil (1) is at a Residual Condition

After Drawdown Condition

Using "MGSTRN" and a trial and error procedure, we obtained for the after drawdown case, for different assumed values of $\bar{\phi}_2$, the values of cohesion required in soil (2) for equilibrium of the failure zone. These values are given below in Table VII.2.5.1.

Table VII.2.5.1
Case (1)
Drawdown Condition

Assumed $\bar{\phi}_2$	$\bar{c}_2$ TSM	F.S.	Side Force Assumption	Residual Factor along β
7.5	2.4	1.00704	Constant	.37
10	2.25	1.00331	Constant	.36
15	2.0	1.00925	Constant	.32

As would be expected, for an increase in the assumed value of $\bar{\phi}_2$, there is a corresponding decrease in the value of $\bar{c}_2$ required for equilibrium. It is observed that doubling the value of $\bar{\phi}_2$ decreases the required value of cohesion by only 20%. Thus, it seems that the cohesion parameter is the most critical when analyzing a problem with the conditions of CASE (1).

We use the residual factor to compare strength developed along surface β', with the peak and residual strength values of the clay. To calculate the residual factor, we first compute the average effective normal stress acting on the β' portion of the failure surface and plot this value on the $\bar{\sigma}$ axis of $\bar{\sigma}$ -τ plot, as shown in Figure 21. Then, lay off the corresponding cohesion intercept ($\bar{c}_2$) along the shear stress axis. From this point, extend a line at a slope equal to the corresponding assumed value of the friction angle ($\bar{\phi}_2$). At the intersection of this $\bar{c}$ - $\bar{\phi}$ line with the value of average effective normal stress developed along β' is the average shear stress for this condition (repeat procedure for each trial).

For the after drawdown situation of Case (1), the average effective normal stress acting on β' does not change and the corresponding average shear stress on the same surface does not vary measureably (2.95 TSM to 3.11 TSM) for our three different sets of $\bar{\phi}_2$ and $\bar{c}_2$. This is verified by the group of points marked "1-D" on Figure 21. Consequently, for a fixed condition along surface (1), we obtain approximately the same residual factor along β' for three different sets of equilibrium parameters in soil (2). A conservative value of the residual factor for the drawdown case is equal to 0.32 (as shown in Table VII.2.5.1).

The plots of "MGSTRN"'s computer output (given in Figure 22) show that the position of the effective side thrusts

and the $\bar{\phi}$'s developed on the sides of the slices for the after drawdown condition of CASE (1) do not change for equilibrium attained with different assumed values of $\bar{\phi}_2$ and $\bar{c}_2$.

Before Drawdown Condition

Now, we obtain for the before drawdown condition, for different assumed values of $\bar{\phi}_2$, the cohesion parameter ($\bar{c}_2$) required for equilibrium. These values and the corresponding residual factors are shown below in Table VII.2.5.2.

Table VII.2.5.2
Case (2)
Before Drawdown Condition

$\bar{\phi}_2$	$\bar{c}_2$TSM	F.S.	Side Force Assumption	Residual Factor along β
7.5	1.25	1.00853	Bell	.64
10	1.20	1.00880	Bell	.63
15	1.05	1.00247	Bell	.62

We have calculated the residual factors for the before drawdown condition in the same manner as for the after drawdown condition. The points in Figure 21 from which the before drawdown values of Residual factor were calculated for CASE (1), are noted as 1-S.

It is found for this condition also that the residual factor remains approximately constant for different sets of equilibrium parameters ($\bar{\phi}_2$ and $\bar{c}_2$), and has a conservative value equal to 0.67 (as shown in Table VII.2.5.2).

CASE (2) Soil 1 = Soil 2

Performing almost the same operation for CASE (2), as done in CASE (1), we obtain for assumed values of $\bar{\phi}_1 = \bar{\phi}_2$, the following equilibrium cohesion parameters ($\bar{c}_1 = \bar{c}_2$),

factors of safety and residual factors for the after drawdown and before drawdown conditions.

Table VII.2.5.3
Case (2)
Drawdown Condition

$\bar{\phi}_1 = \bar{\phi}_2$	TSM $\bar{c}_1 = \bar{c}_2$	F.S.	Side Force Assumption	Residual Factor along $\gamma+\beta$
7.5	.95	1.01765	Constant	.75
10	.80	1.02504	Constant	.73
15	.50	1.01621	Constant	.70

Table VII.2.5.4
Case (2)
Submerged Condition

$\bar{\phi}_1 = \bar{\phi}_2$	TSM $\bar{c}_1 = \bar{c}_2$	F.S.	Side Force Assumption	Residual Factor along $\gamma+\beta$
7.5	.55	1.04495	Bell	.84
10	.45	1.02216	Bell	.84
15	.30	1.03830	Bell	.81

It is seen that the values of cohesion required for equilibrium in CASE (2) are much less than those in CASE (1). The reason, of course, being that there is now a much longer surface over which cohesion may be developed ($\gamma+\beta' > \beta'$). Consequently, the value of cohesion required for equilibrium should be smaller in this CASE.

For different equilibrium parameters ($\bar{\phi}$ and $\bar{c}$), there is no significant change in the average effective normal stress developed along the surface ($\gamma + \beta'$) for the after drawdown case and only a slight change for the before drawdown case. These small changes are not enough to greatly affect the values of the calculated residual factors and can therefore be neglected.

Once again we find that the value of residual factor is almost constant for a given oil condition. We obtained a residual factor approximately equal to 0.70 for the after drawdown condition and a value approximately equal to 0.81 for the before drawdown condition.. The points on Figure 21 corresponding to these residual factors are indicated by "2-D" and "2-S" respectively. It should be noted that when calculating the residual factor in CASE (2), we used the average effective normal stress along surface ($\gamma + \beta'$).

Figure 23 is a plot of the MGSTRN output data for the drawdown condition of CASE (2). For different sets of $\bar{\phi}$ and $\bar{c}$, each yielding a factor of safety approximately equal to 1.0, we obtain the same position of effective side thrust, within a few per cent. However, we do get a change in the $\bar{\phi}$'s developed on the sides of the slices. As we increase the angle of friction ($\bar{\phi}_1 = \bar{\phi}_2$) and decrease the value of cohesion ($\bar{c}_1 = \bar{c}_2$) in soils (1) and (2), the cohesion is no longer enough to hold the slices in equilibrium and higher $\bar{\phi}$'s must be developed in zones (1) and (2). The $\bar{\phi}$'s developed in zone (3) also increase very slightly with the above changes.

VII.2.5.1 Summary of analysis of actual slope and failure surface geometry by "MGSTRN"

It has been discovered that for a fixed assumption of the residual factor distribution and a given oil condition, one obtains almost the same value of the residual factor for different possible combinations of equilibrium parameters.

A summary table of the residual factors which will be used to represent each condition is given below.

	After Drawdown Residual Factor	Before Drawdown Residual Factor
Case #1		
Residual factor along the inclined portion of the failure surface through the clay, when R = 1.0 along surface (1).	.32	.62
Case #2		
Residual factor is constant along the failure surface through the clay.	.70	.81

Comparing the residual factors for the "after drawdown" and "before drawdown" conditions of CASE (2), we find an increase in "R" of approximately 15 - 20% for the "before drawdown" condition. Whereas, in CASE (1), it is observed that the residual factor for the "before drawdown" condition is approximately twice that of the "after drawdown" condition (i.e., for CASE (1), the strength of the clay along surface β' would have been required to decrease twice as far for failure to have occurred during a "before drawdown" condition). The small length of the failure surface along which the residual factor < 1 acts in CASE (1) is the cause of this large deviation in the value of R for a change in water conditions. The assumed distribution of R appears to be critical in this analysis.

If we assumed that the actual conditions of failure approximated those of CASE (2), we could try and use the residual factor obtained for the before drawdown condition as a design criteria for a future drawdown situation. The average strength of the clay along surfaces γ and β' would need to decrease approximately 20% more than it has in this problem, for failure to occur during a drawdown situation. Thus, this slope should be stable for considerably more than

9 years. How much longer is a function of the number of drawdowns and the change in rate of progressive failure as we approach the residual condition.

It is the author's belief that the conditions of this slide more closely typified those in CASE (1). This reasoning is supported by the fact that the bottom portion of the failure surface was a horizontal, oil covered shear plane at the time of failure. It is thought that this plane was an old shear surface which had been weakened by oil entry into the adjacent fissures and along the plane itself.

The R = 0.32 calculated in Case (1) for the drawdown condition corresponds to a design in which the developed $\bar{\sigma}$ and τ stresses along β' were high enough so that it took only 9 years for the strength of the clay to decrease to a drawdown failure situation. However, it should be noted that a substantial value of R may have been developed by the end of construction and thus the residual factor would not have increased a full 0.32 in 9 years.

When the slope was submerged just prior to drawdown, an equilibrium analysis would have yielded an $R \approx 0.62$. We know that failure did not occur at this time and therefore, this value of residual factor would be conservative for design of a drawdown situation for a structure life span of 9 years. It would most likely be conservative for a much longer period of time than this, but we cannot say how long for sure. It depends on how fast the strength of the clay drops between R = 0.32 and R = 0.62 and, once again, this would be a function of the number and duraction of drawdowns.

The following is a summary of the results used in calculating the residual factor for the drawdown situation of Case (1).

Assuming that the residual factor is = 1.0 along the horizontal portion of the failure plane and that full frictional resistance is mobilized throughout zone (3), we find that an analysis of the slide at failure (F.S. = 1.0, for after drawdown situation) yields an average effective normal stress ($\bar{\sigma}_{\beta}'$) = 4.2 TSM and an average developed shear stress (τ_{β}') = 3.0 TSM along surface β'.

To be conservative in our extimation of the residual strength and the residual factor, we used the strength envelope which corresponded to the oil residual condition ($\bar{\phi}$ = 7.5°; $\bar{c}$ = 0.0 TSM) in the calculations.

The peak (S_P) and residual (S_R) strengths corresponding to a ($\bar{\sigma}_{\beta}'$) = 4.2 TSM are:

S_P = 4.32 TSM

S_R = 0.55 TSM

Residual Factor along Surface β' = $R = \dfrac{S_{P_{\beta}'} - \bar{S}_{\beta}'}{S_{P_{\beta}'} - S_{R_{\beta}'}} = 0.32$

Thus, for this failure to have occurred in the manner described above, the strength of the clay along surface β' would need to decrease 32% of the way from its peak value to its residual value.

In conclusion, it is thought that an R = 0.65 would be a reasonable value of the residual factor that could be used in future design of a slope depicting the conditions of Case (1).

VIII. CAUSES OF THE SLIDE

VIII.1 Types of Earth Movement

Figure 24 illustrates six types of earth movement. The FORS-2 North wall failure is a combination of three or more of these movements (No.'s 2, 3, 5 and possibly 1).

The rubble in zone (3) is evidence that an old slide of some kind has taken place along the upper portion of the inclined failure surface. This rubble may have been placed by movement along an old shear surface or possibly by erosion.

The (almost) horizontal portion of the failure surface indicates movement along a weak layer. In this failure, the weak layer was an oil covered shear plane.

The soil of zone (2), which is the last to lose its strength, fails due to an overstressing and progressive "strain softening" of the desiccated, oil soaked region.

VIII.2 Causes of Earth Movement

Figure 25 lists and illustrates some of the reasons why earth movement took place. All of these have occurred either during construction or throughout the life of the structure.

When the slope was originally excavated for the reservoir, an overburden or counterweight was removed from the potential slide zone.

The area of the shear surface was reduced by the presence of an old shear plane and desiccation cracks and fissures within the failure zone. These imperfections may be a result of tectonic movements, unequal expansion during excavation or during the loading and unloading imposed by filling and emptying the reservoir. The strength of a clay is greatly diminished by the presence of fissures and cracks for they not only cause a lowering of the average shear strnegth, but an acceleration of localized failure.

The actuating and resisting forces were both increased when the reservoir was filled with oil, but each time the level of the reservoir was drawn down below the elevation of the slide zone, the strength of the clay in the failure zone decreased because the effective stress decreased along the potential failure surface. This decrease was caused by an increase in pore pressure set up by the oil trapped in the slope (i.e., a "rapid drawdown" situation). A "rapid drawdown" condition also increases the actuating force by increasing the shear stress that is acting throughout the slope.

During the unstable condition before complete failure, oil was seeping from the surface of the slope (through porous sand lenses and cracks) and also into excavations (permeating through desiccation cracks and along the horizontal shear plane). The movement of the oil along the shear plane, caused by either gravity or expansion of the entrapped air in the fissures or a combination of the two, would create a lubricating effect along this surface, thus reducing its strength and also contributing to the over-stressing of the clay in zone (2).

When the reservoir was drawn down in April 1965, the strength of the clay in the failure zone had decreased to the point that the actuating forces were approximately equal to the resisting forces. These conditions remained approximately constant during May; consequently, only a small movement took place. Finally, on 8 June 1965, a combination of the weight and vibrations from a D-8, operating on the berm above the slide zone, increased the actuating force enough to trigger the failure.

IX. RECOMMENDATIONS

IX.1 Use a Large F.S. in the Design of Slopes in Over-Consolidated Clays

The stability of a body of soil refers to complete equilibrium of all external and internal forces. As long as the developed shear stresses within the slope are considerably below the strength of the soil (in Case (1) R = 0.65), the body will remain stable. With the fissures and excess pore pressures present, a strength decrease during a drawdown situation, coupled with a deformation or volume change, results in the value of the shear strength available approaching the value of the shear stress developed. After a number of drawdowns, we reach an unstable situation and failure occurs. Therefore, when designing a cut slope of a reservoir in an over consolidated soil, which is to stand for a long period of time, a large factor of safety against failure must be employed.

IX.2 Construction Inspection

In an area such as Amuay, which has a relatively horizontal bedding and occasional weak layers, one should be cautious of possible horizontal slip surfaces. Evidence of ancient shear deformations tend to indicate that this slide was not a slope failure that would have been predicted. The rubble zone, horizontal shear plane and the nearby vertical caliche fault were all unconservative elements that contributed to this failure. It is not likely that the original design could have been conservative enough (economically speaking) to account for such a combination of unknowns.

It is proposed that a program for careful inspection of the slopes during construction be set up for future work

in the Amuay area. This type of program should reveal such soil imperfections as caused this slide. These imperfections could then be removed (if within the scope of the work) or accounted for in the design of a specific section of the slope.

IX.3 Possible Extended Study

It is recognized from the slides which have already occurred that the cliffs adjacent to Amuay Bay are naturally unstable. If a detailed study and comparison of all the well defined natural slope failures in the area were made, the strengths of the involved soils determined, and the ground water and other failure conditions noted, a correlation of these factors with the susceptibility of a slope or cut to failure should be possible. Information of this type would be valuable in future remedial work of the existing structures and in the design of new structures, by helping us predict the "where," "when," and "why" of failures and possible methods of their prevention.

The following factors should be noted, if possible, in the analysis of each slide.

(1) Description of the slope or cut in which the slide took place.
(2) Dimensions of the failure zone.
(3) Shape of failure surface.
(4) Ground water conditions.
(5) Soils involved - strength, bedding.
(6) Rate of movement.
(7) Causes.

A more extensive testing program is also proposed. Since only a few tests were run in this investigation, exact soil

parameters were not obtained. Lower intensity repeated direct shear tests should be run, so that the strength parameters at these low pressures could be checked. Also more tests are needed to better determine the effect of oil on the strength of an overconsolidated clay.

X. SUMMARY AND CONCLUSIONS

X.1 Wedge Method vs. Morgenstern and Price Method

The investigations and analyses on the simplified wedge geometry were performed to discover possible relationships and differences between a wedge theory and the powerful method developed by Morgenstern and Price.

In comparing the results of the wedge theory with that of Morgenstern and Price, we find good agreement in the values of the factor of safety, equilibrium parameters and the residual factor for simplified soil conditions. However, in order to obtain the correct answer for a given problem, one must define, as closely as possible the actual soil conditions. Using the wedge method we cannot easily do this, whereas the versatility of the Morgenstern and Price method does enable us to efficiently analyze very complex failure conditions (slope, failure surface, phreatic surface, soil) thus giving us the best solution and "most" correct values for the factor of safety, equilibrium parameters and the residual factor.

We found that the side force assumption, used in the Morgenstern and Price method, is not critical in the determination of the factor of safety, equilibrium parameters or the residual factor, but that it is important when trying to obtain a theoretically correct solution (i.e., an equilibrium that satisfies the boundary conditions imposed by the soil).

X.2 Results of Residual Factor Analysis

One of the main considerations of this analysis has been a comparison between two possible residual factor distributions

for an after drawdown condition.

Case (1) Residual factor is equal to 1.0 along the horizontal shear plane but less than unity along the inclined portion of the failure surface through the clay.

Case (2) Residual factor is constant along the failure surface through the clay.

We computed a residual factor for Case (1) equal to 0.32 and a residual factor for Case (2) equal to 0.70.

For a slope having the same conditions as those depicted in Case (1) of our analysis on the actual failure surface and slope geometry, it is thought that a residual factor (R) = 0.65 is a reasonable value which may be used in future design considerations.

X.3 Recommendations

It is apparent that a combination of soil and geologic imperfections were the cause of this slide. The failure may have been prevented if these imperfections has been discovered and removed during construction. Therefore, careful site inspection of slopes during future construction at Amuay is proposed.

BIBLIOGRAPHY

Bailey, W. A. (1966), "Stability Analysis by Limiting Equilibrium," Civil Engineering Degree Thesis, M.I.T.

Bjerrum, L. (1966), "Mechanisms of Progressive Failure in Slopes of Overconsolidated Plastic Clays and Clay Shales," Preprint of the Third Terzaghi Lecture, ASCE Structural Engineering Conference.

Herrmann, H. G. (1966), "Residual Shear Strength of Clay Shales," Master of Science Thesis, M.I.T.

Lambe, T. W. (1956), "The Storage of Oil in an Earth Reservoir," Journal B.S.C.E., Vol XLIII, No. 3, July.

Lambe, T. W. (1957), "Soil Engineering Studies for the Fuel Oil Storage Reservoir No. 2," March.

Lambe, T. W. (1963), "An Earth Dam for the Storage of Fuel Oil," Proceedings of the Second Pan-American Conference on Soil Mechanics and Foundation Engineering.

Lambe, T. W. and Whitman, R. V. (1964), An Introduction to Soil Mechanics, Notes printed at M.I.T. under Sponsorship of the Ford Foundation.

Lambe, T. W. (1965), "Proposed Program of Investigation and Surveillance of the Natural Slopes and Earth Structures at the Refinery of the Creole Petroleum Corporation, Amuay, Venezuela," August.

Lambe, T. W. (1966), "Report on the Performance of the FORS-1 and FORS-2 Reservoirs, Amuay, Venezuela," February.

Morgenstern, N. R. and Price, V. E. (1965), "The Analysis of the Stability of General Slip Surfaces," Geotechnique, Vol. XV.

Sherrard, J. L., Woodward, R. J., Gizienski, S. F. and Clevenger, W. A. (1963), Earth and Earth Rock Dams, John Wiley and Sons.

Skempton, A. W. (1964), "Long-term Stability of Clay Slopes," Fourth Rankine Lecture, Geotechnique, Vol. XIV.

Terzaghi, K. and Peck, R. B. (1948), Soil Mechanics in Engineering Practice, John Wiley and Sons.

Whitman, R. V. and Moore, P. J. (1963), "Thoughts Concerning the Mechanics of Slope Stability Analysis," Proceedings of the Second Pan-American Conference on Soil Mechanics and Foundation Engineering.

Whitman, R. V. and Bailey, W. A. (1966), "Use of Computers for Slope Stability Analysis," ASCE Specialty Conference, Stability and Performance of Slopes and Embankments.

TABLE I

CLASSIFICATION OF SOILS FROM FORS-2

Soil	Name	Atterberg Limit			Specific Gravity	Particle Size Per Cent Finer		
		w_l	w_p	w_n		1.0	.074	.002MM
A.	Caliche							
	1. White Caliche	*29	23	4-8	2.85	100	98	12
	2. Brown Caliche	*19		5-10	2.76	99	56	10
B.	Silty Clay	35	23	12	2.78	100	98	45
C.	Brown Fat Clay	53.5	23.3	21.6	2.75	100	98	62

* Test run on the material passing the No. 40 sieve.

TABLE II

AVERAGE STRESSES DEVELOPED ALONG THE 3 WEDGE SURFACES
AND THE RESIDUAL FACTOR DEVELOPED ALONG SURFACE (2)
USING WEDGE ANALYSIS
After Drawdown Condition

TRIAL	Assumed Soil Parameters				Surface (1)		Surface (2)			Surface (3)	
	$\bar{\phi}_1$	$\bar{c}_{TSM}$	$\bar{\phi}_3$	$\bar{c}_{3\,TSM}$	$\bar{N}_{1\,TSM}$	$\tau_{1\,TSM}$	$\bar{N}_{2\,TSM}$	$\tau_{2\,TSM}$	"R_2"	$\bar{N}_{3\,TSM}$	$\tau_{3\,TSM}$
a	7.5	0	7.5	0	3.01	0.40	1.84	1.43	0.66	0.61	0.08
b	7.5	0	10.0	0	3.02	0.40	1.83	1.42	0.66	0.61	0.11
c	7.5	0	8.5	0.35	3.20	0.42	1.77	1.35	0.67	0.66	0.45
d	8.5	0.35	7.5	0	3.06	0.81	1.96	1.24	0.81	1.41	0.19
e	8.5	0.35	10.0	0	3.10	0.81	1.95	1.23	0.81	1.42	0.25
f	8.5	0.35	8.5	0.35	3.26	0.84	1.90	1.16	0.83	1.47	0.57
g	10.0	0	7.5	0	3.02	0.53	1.88	1.37	0.69	0.88	0.12
h	10.0	0	10.0	0	3.05	0.54	1.87	1.36	0.69	0.88	0.12
i	10.0	0	8.5	0.35	3.22	0.57	1.81	1.28	0.71	0.94	0.49

TABLE III

WEDGE F.S. VS MGSTRN F.S.

Drawdown Condition

One Soil throughout the Failure Zone

Strength Parameters	Wedge F.S.	Morgenstern and Price Factor of Safety		
		F(x)=Constant	F(x)=H.S.W.	F(x)=Clipped H.S.W.
Peak $\bar{\phi} = 15°$ $\bar{c} = 3.2$ TSM	3.79	3.48	3.47	3.47
Residual $\bar{\phi} = 8.5°$ $\bar{c} = 0.35$ TSM	0.70	0.69	0.70	0.69
Oil Residual $\bar{\phi} = 7.5°$ $\bar{c} = 0.0$ TSM	0.32	0.34	0.35	0.34

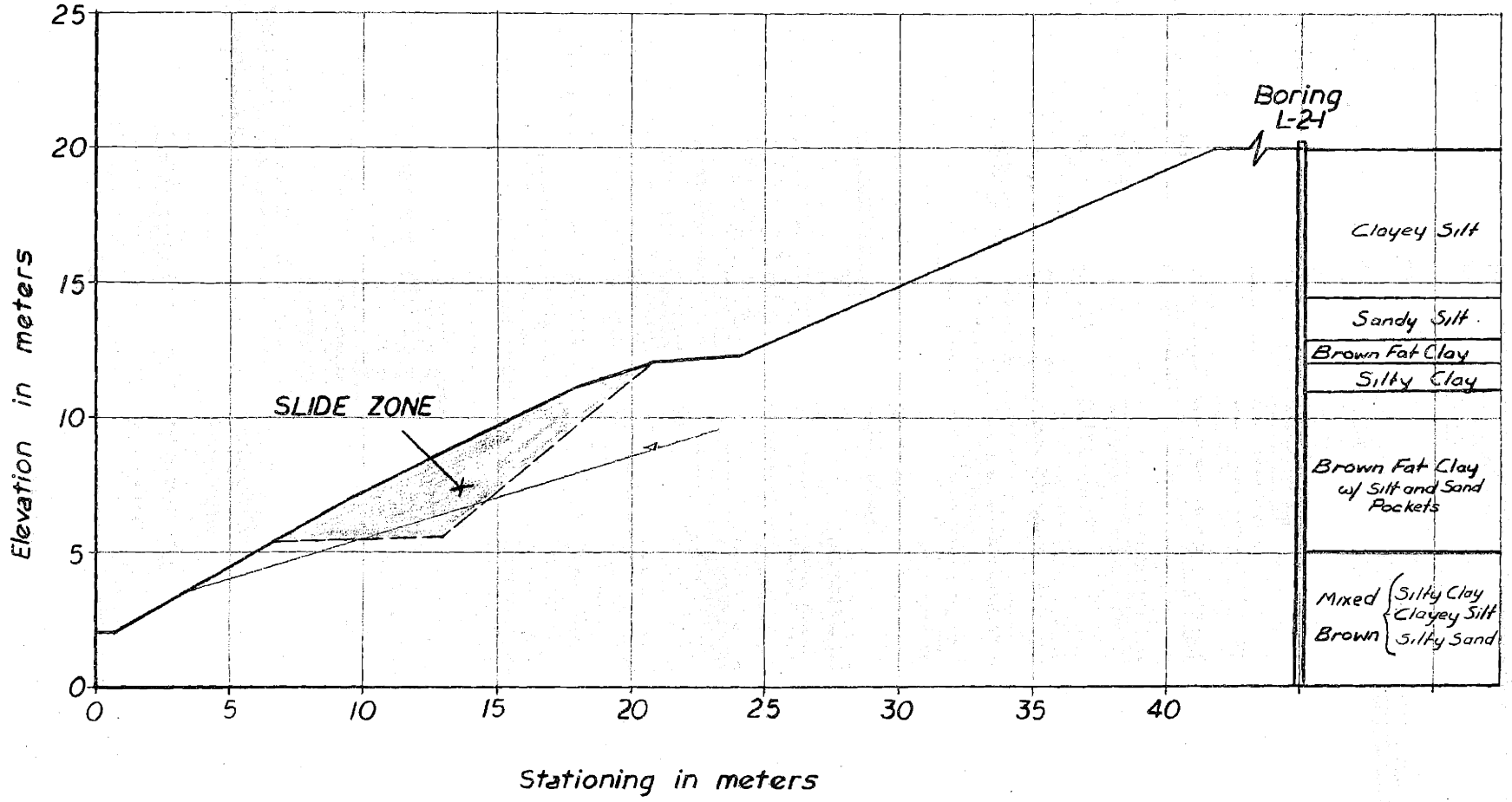

FIGURE 1 CROSS-SECTION OF FORS-2 NORTH WALL AT ℄ OF 1965 SLIDE ZONE

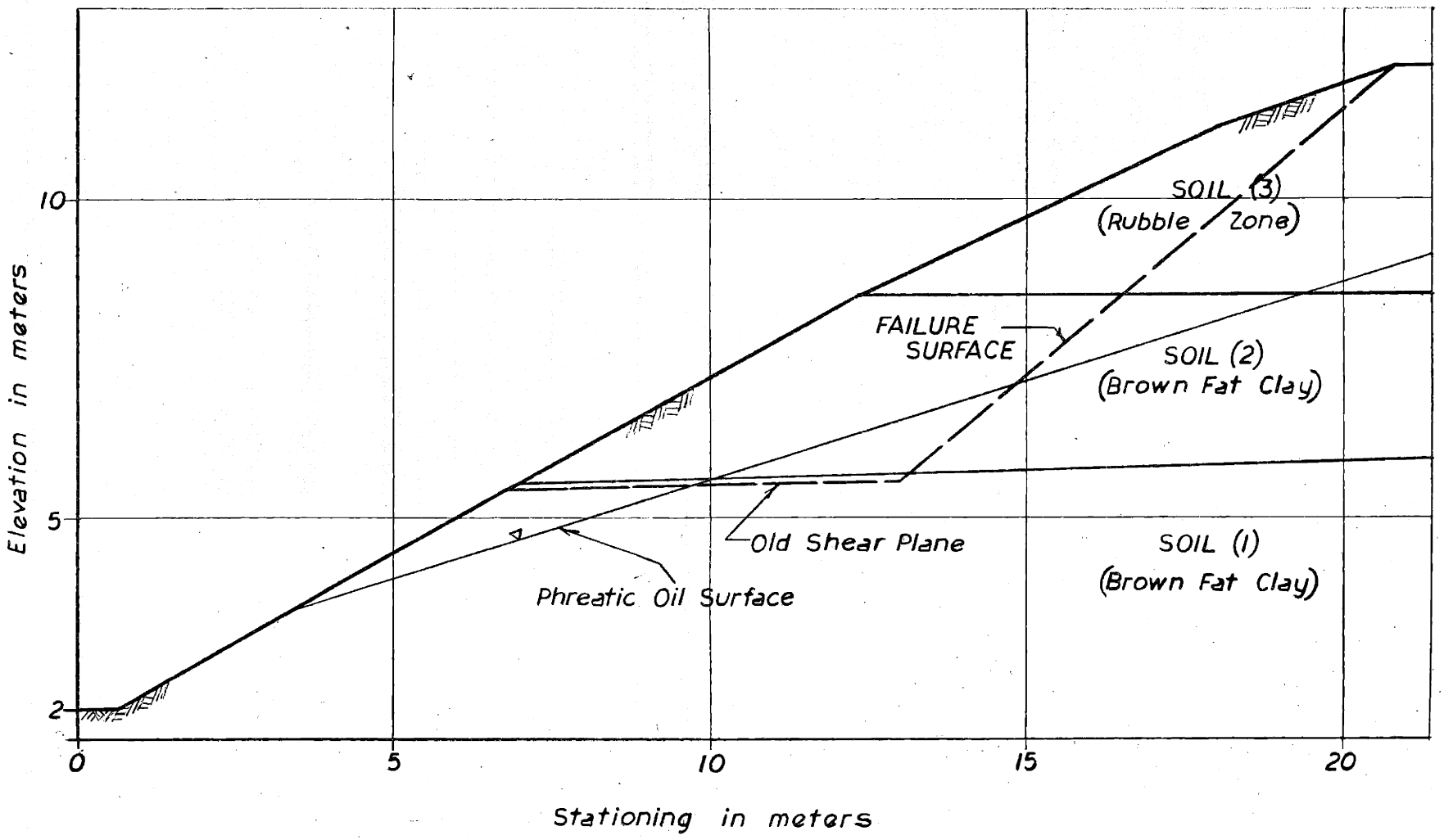

FIGURE 2 CROSS-SECTION AT CENTERLINE OF SLIDE ZONE

Peak Strength	ϕ = 15°	$\bar{C}$ = 3.2 tsm
Residual Strength #1	ϕ = 7.5	C = 0 tsm
Residual Strength #2	ϕ = 10.0	C = 0 tsm
Residual Strength #3	ϕ = 8.5	C = 0.35tsm

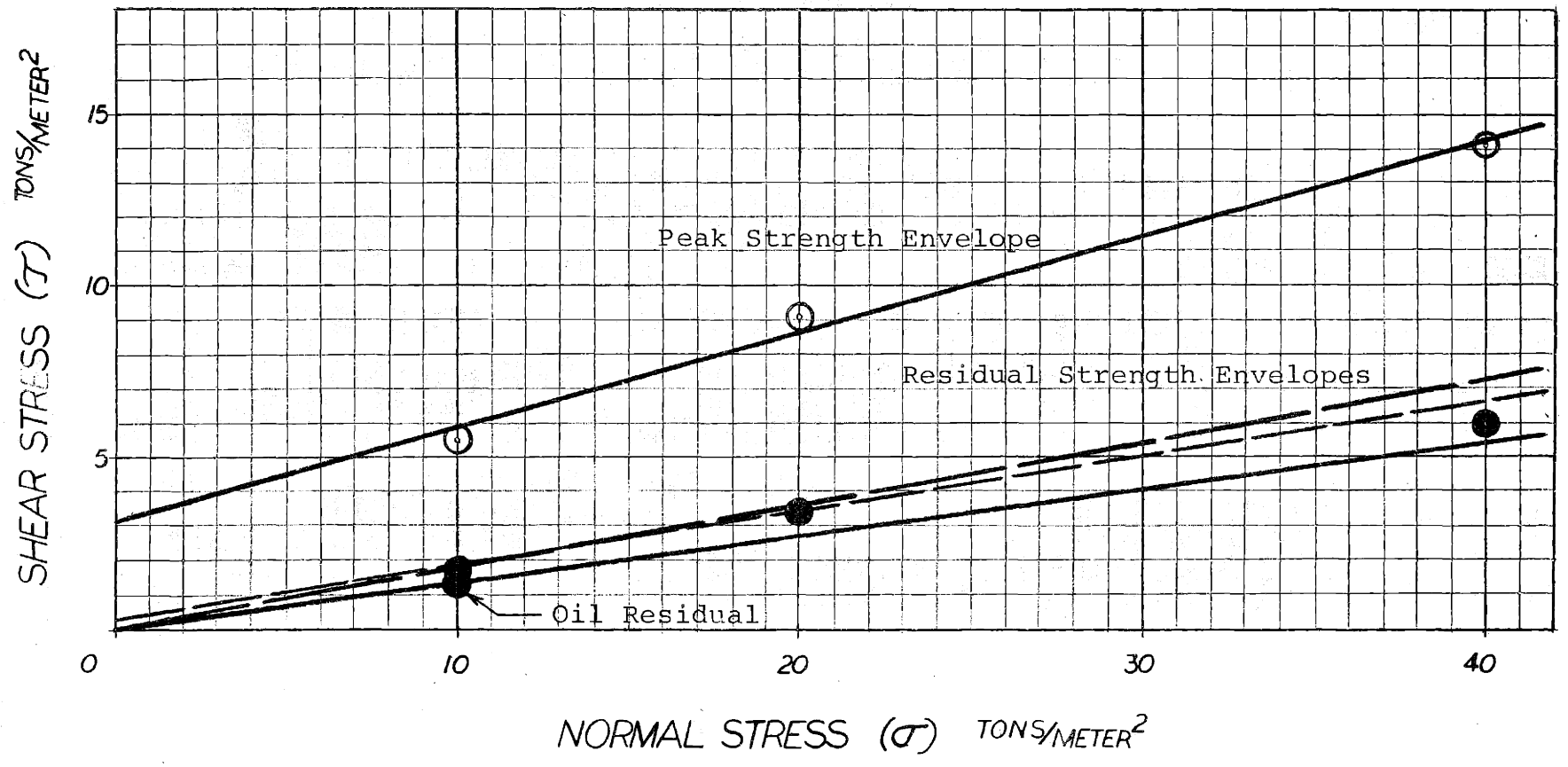

FIGURE 3 DIRECT SHEAR TEST RESULTS

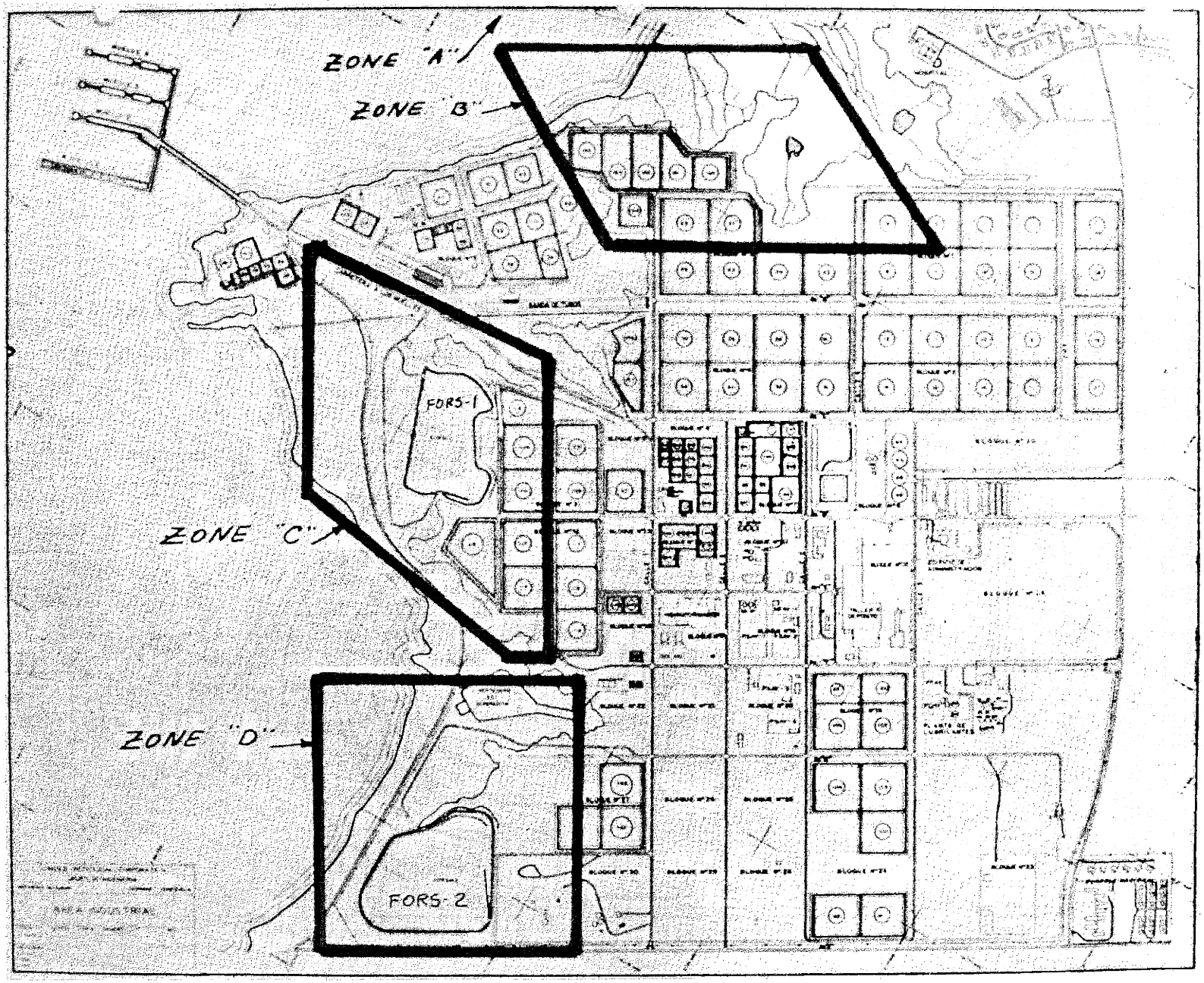

FIGURE 4 Plan View of the Refinery Area

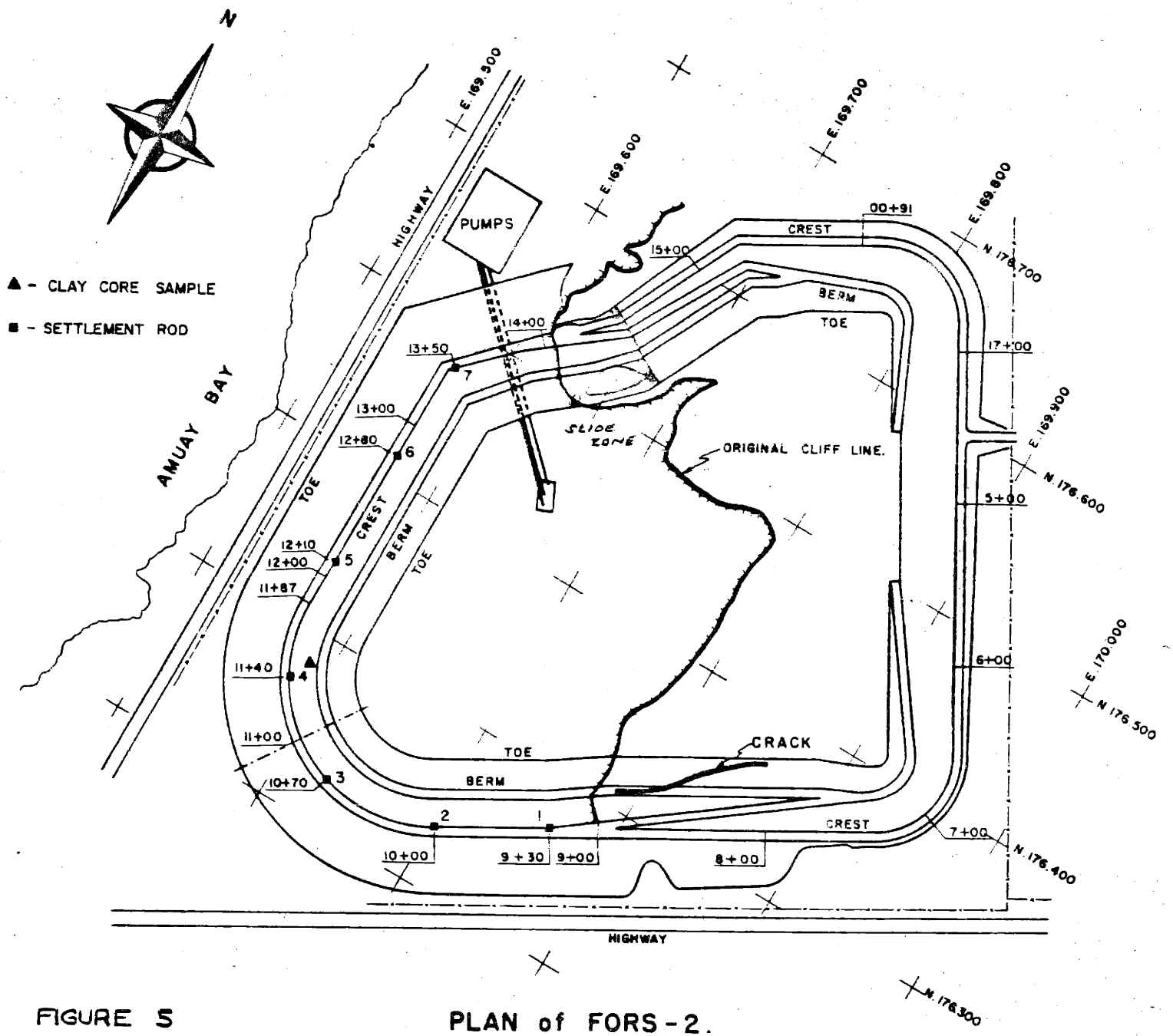

FIGURE 5 PLAN of FORS-2.

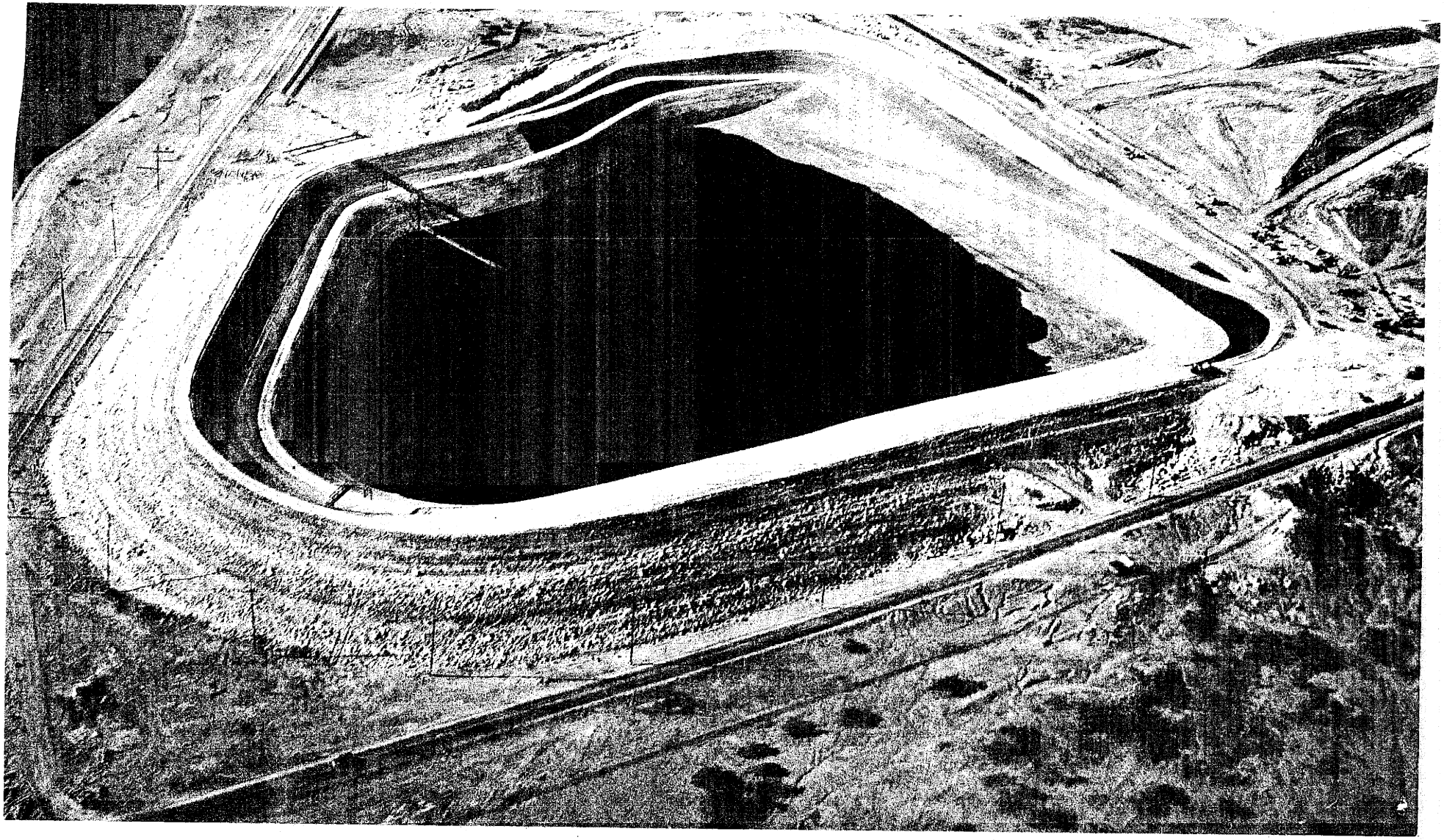

FIGURE 6 A View Looking North During the Initial Filling of FORS-2

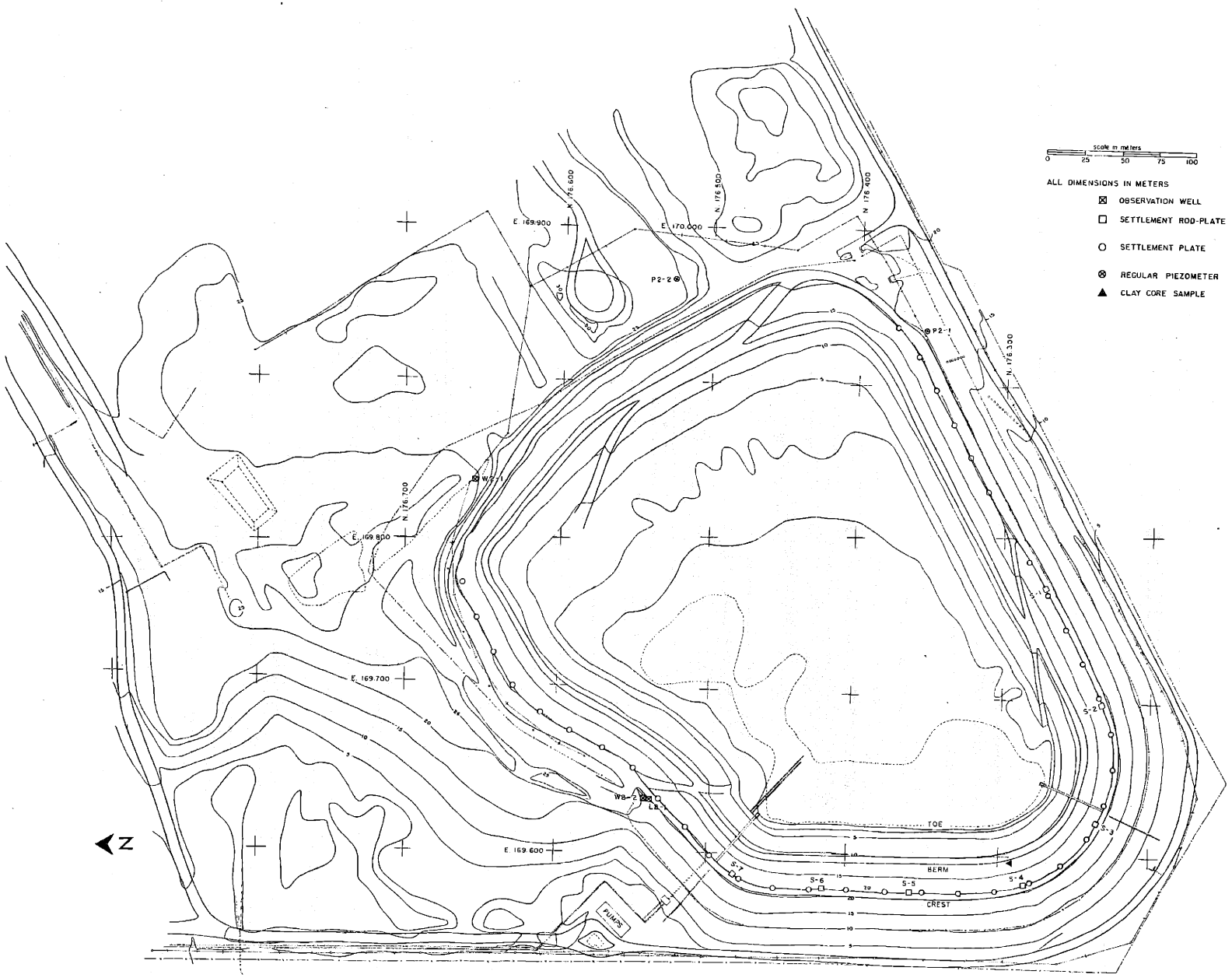

Figure 7

PLAN OF FORS-2

SHOWING LAYOUT OF FIELD-MEASUREMENT INSTALLATIONS

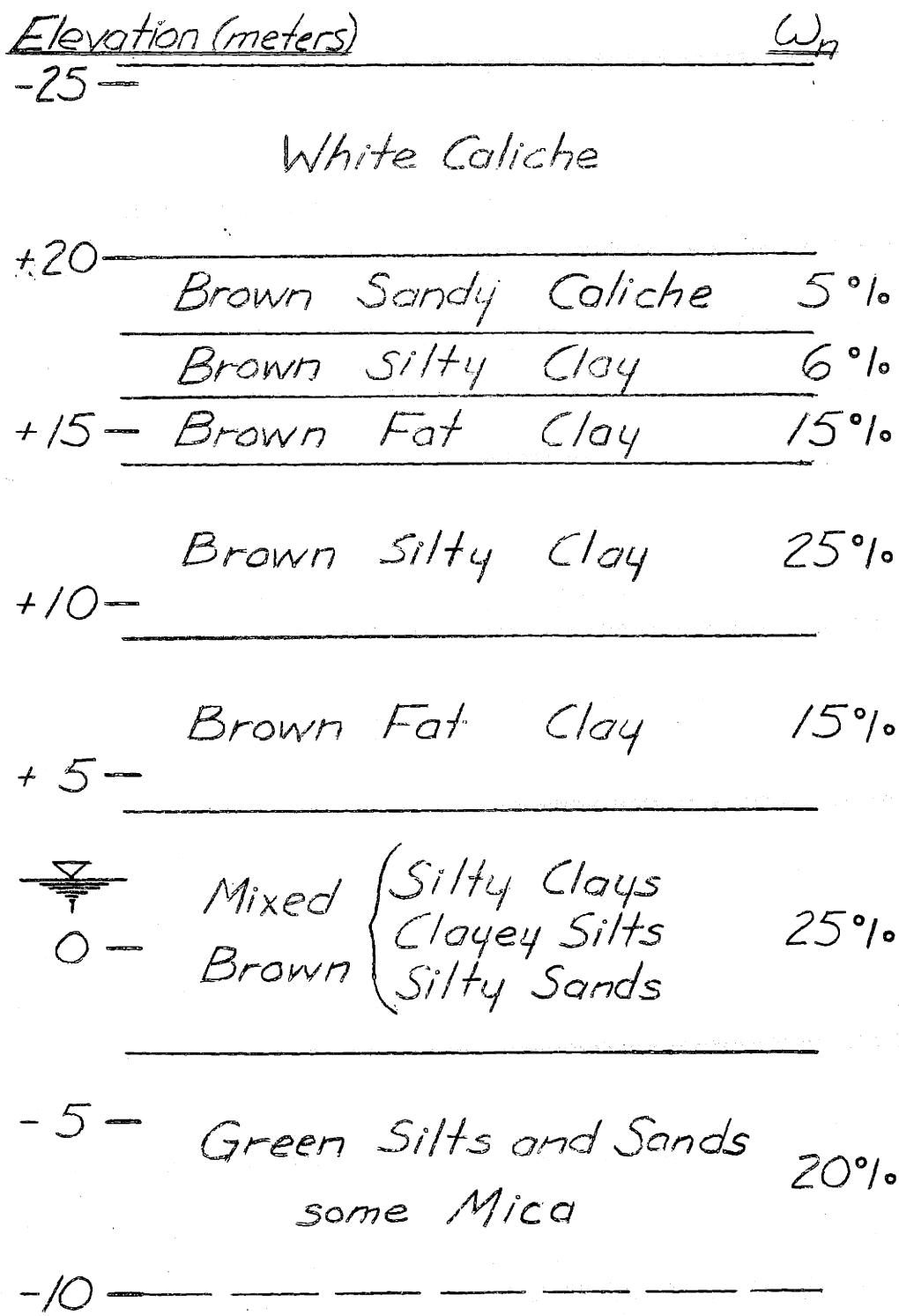

FIGURE 8 Generalized Soil Profile of Amuay Refinery Area -LAW

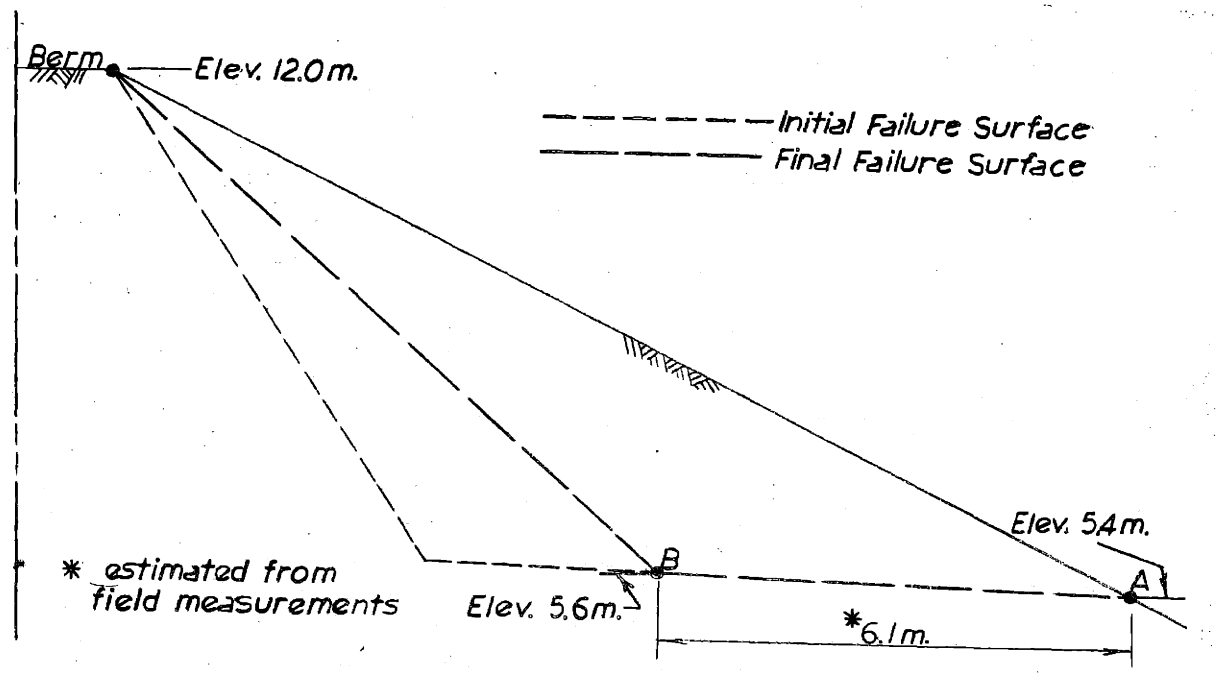

No Scale:

(a) SECTION A-A

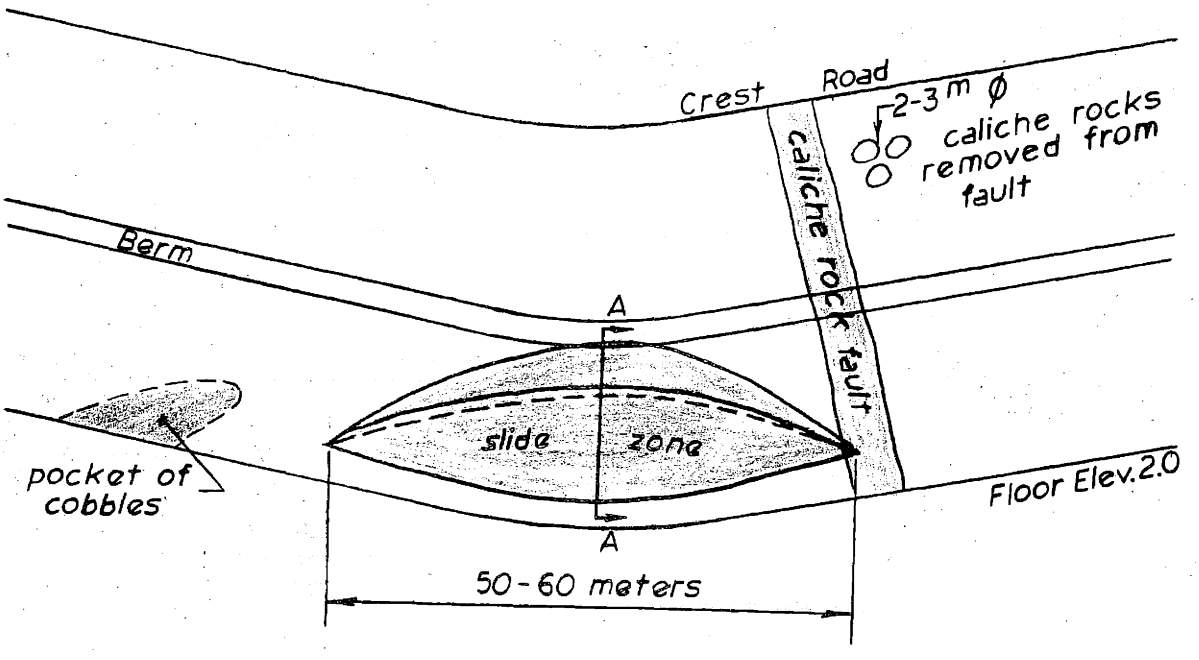

No Scale:

(b) PLAN

FIGURE 9 DETAIL OF NORTH WALL SLIDE ZONE

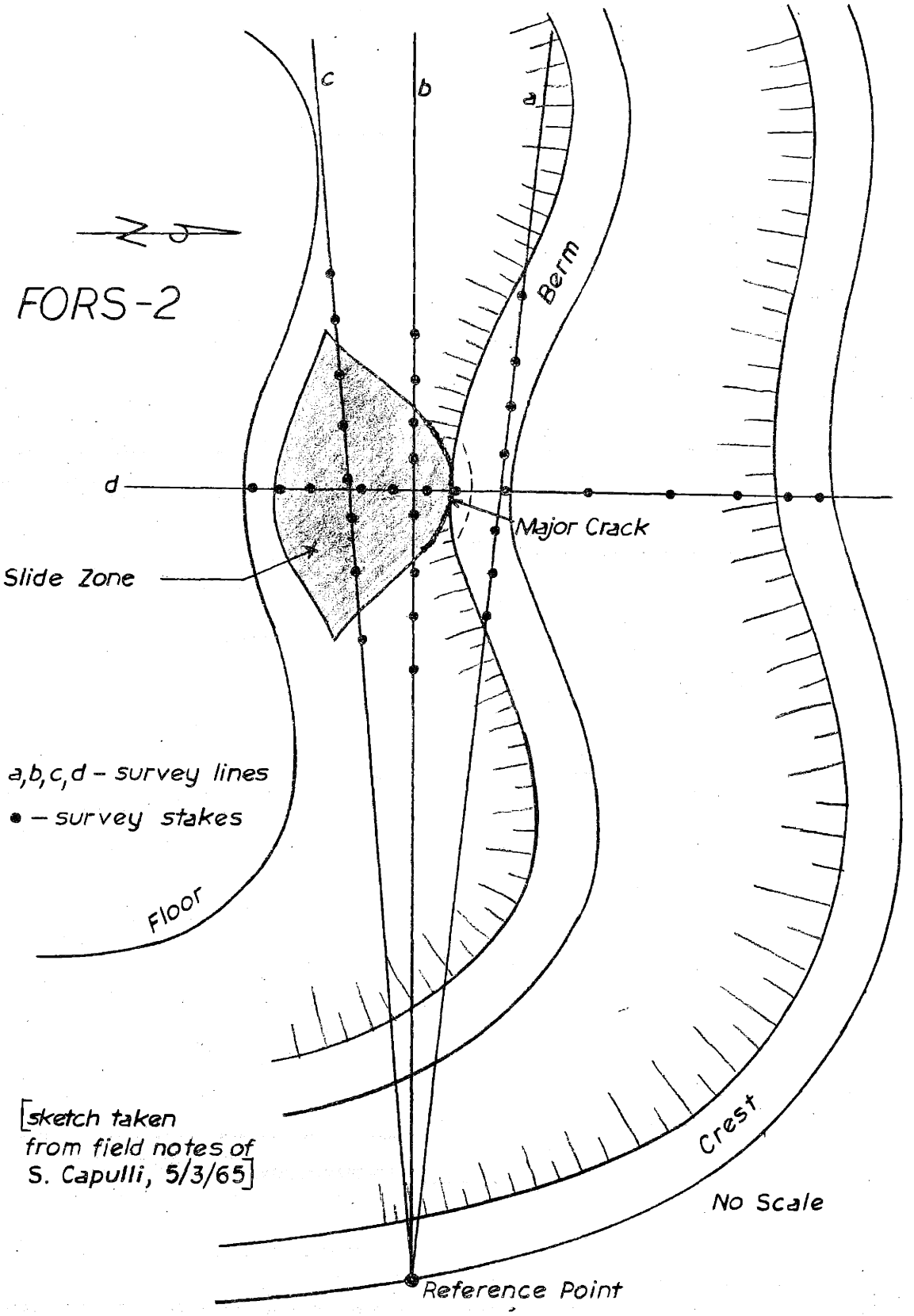

FIGURE 10 INSTRUMENTATION OF SLIDE ZONE

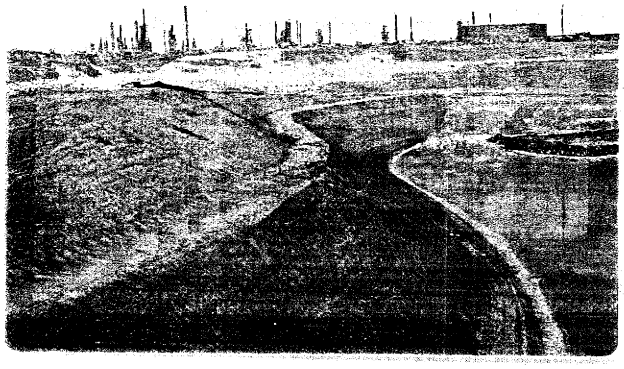

FIGURE 11 Initial Cracking in the North Abutment of FORS-2
April 1965

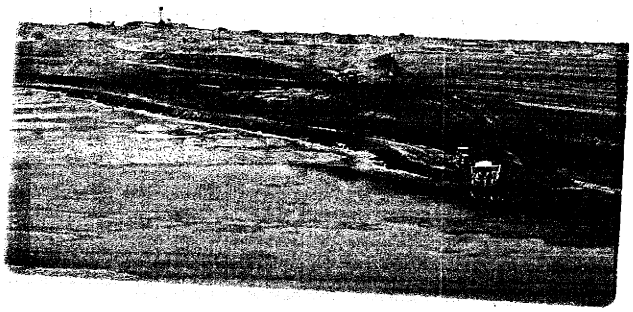

FIGURE 12 View of the South Wall of FORS-2
Showing an Old Slide Surface in the Natural Slope

a) Initial toe bulge

May 1965

b) Development of wedges during the slide

May 1965

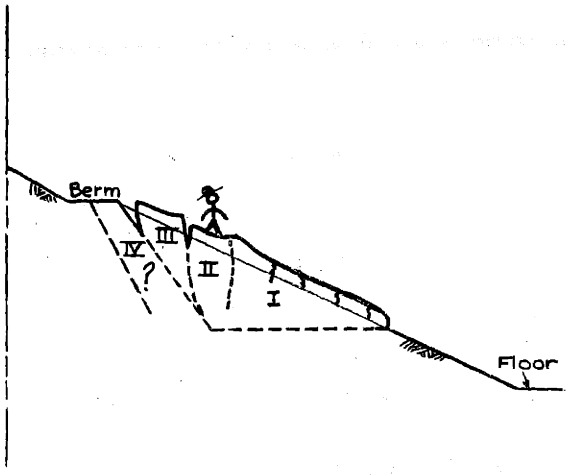

c) Schematic showing the formation of the wedges

FIGURE 13 Early Movements of the FORS-2 North Abutment Slide

a) General view showing the seepage of oil from the horizontal slip surface

May 1965

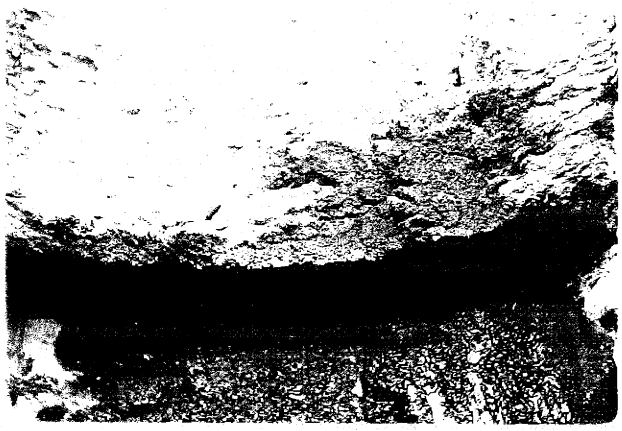

b) Close up showing the movement of the sliding block which has taken place, along the horizontal failure surface

5 June 1965

FIGURE 14 Looking North into Test Pit No. 1 at the Bottom of the North Wall Slide Zone

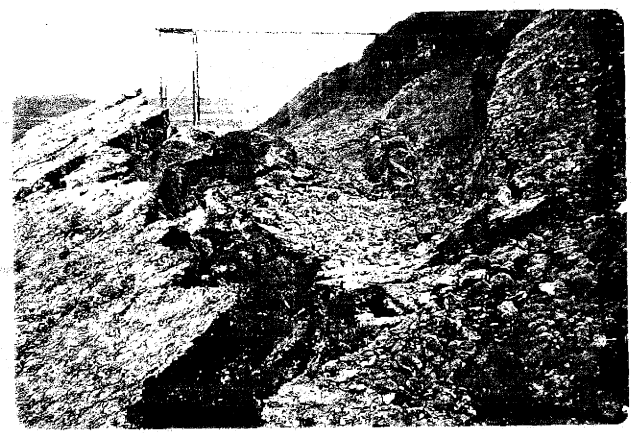

a) Head of slide zone after failure occurred

May 1965

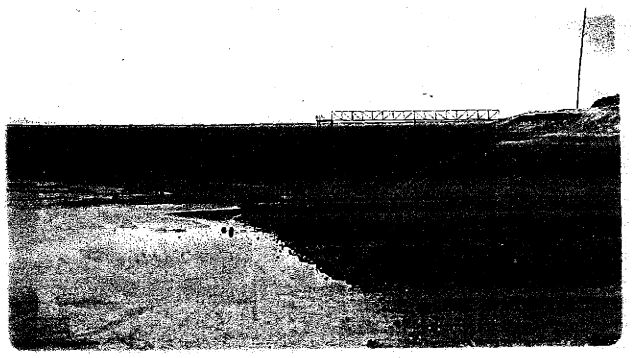

b) General view after failure showing the toe debris

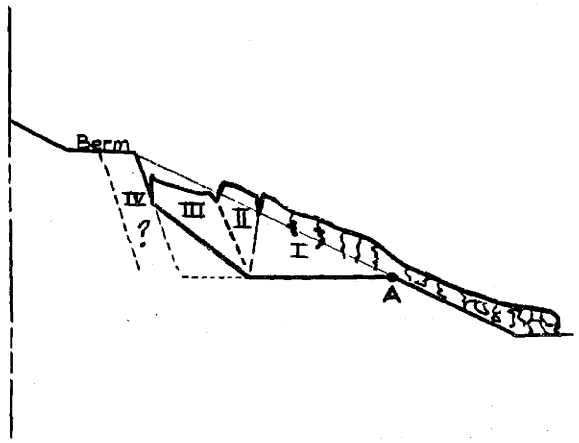

c) Schematic showing the approximate positions of the wedges participating in the failure

FIGURE 15 Final Movements of the FORS-2 North Abutment Slide

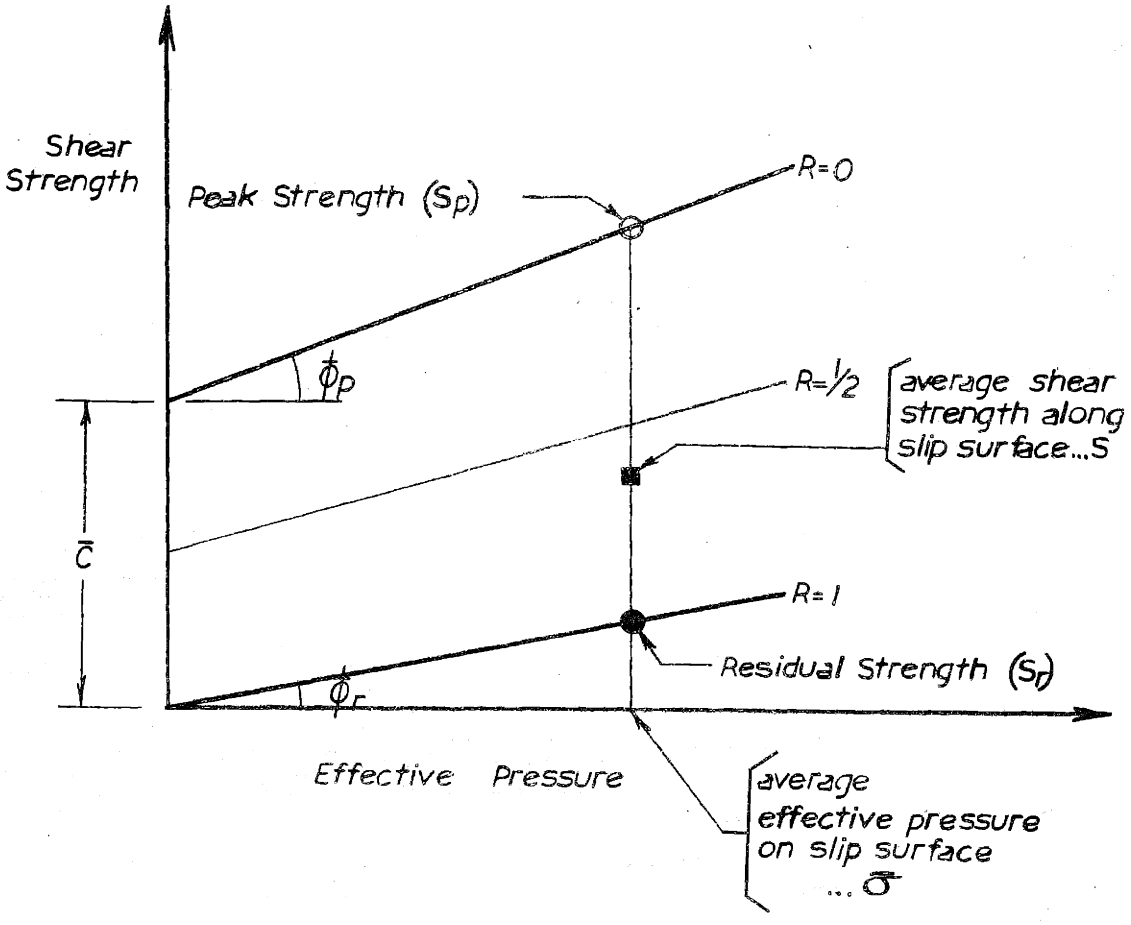

$$\text{Residual Factor } (R) = \frac{S_p - S}{S_p - S_r}$$

FIGURE 16 DEFINITION OF RESIDUAL FACTOR

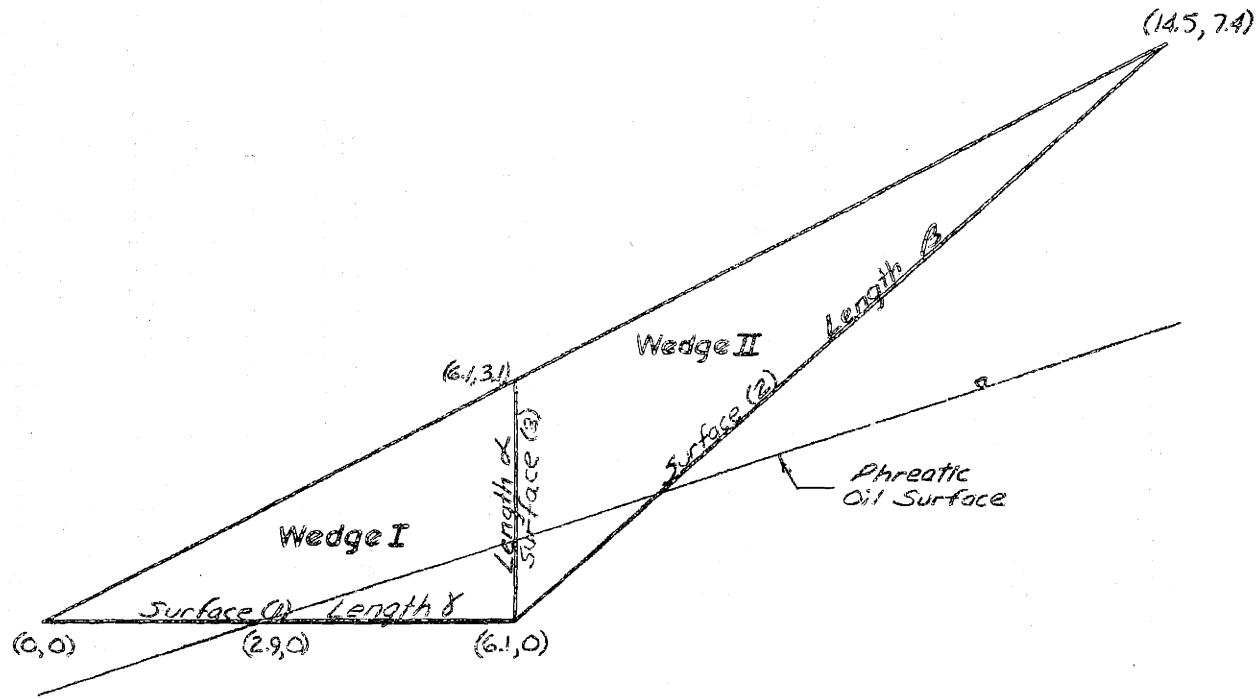

FIGURE 17 SIMPLIFIED WEDGE GEOMETRY OF SLIDE ZONE

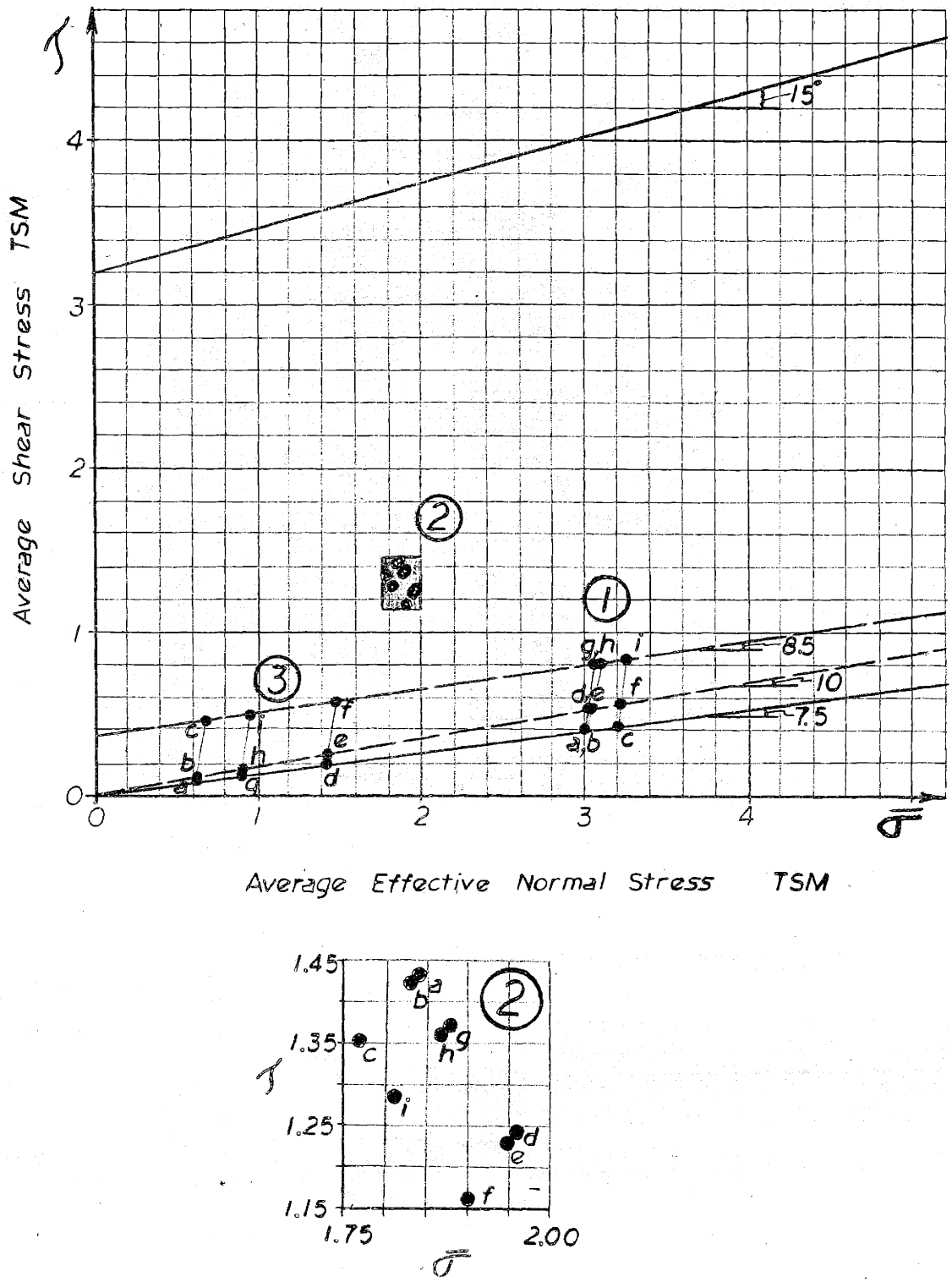

FIGURE 18 AVERAGE STRESSES BY WEDGE ANALYSIS

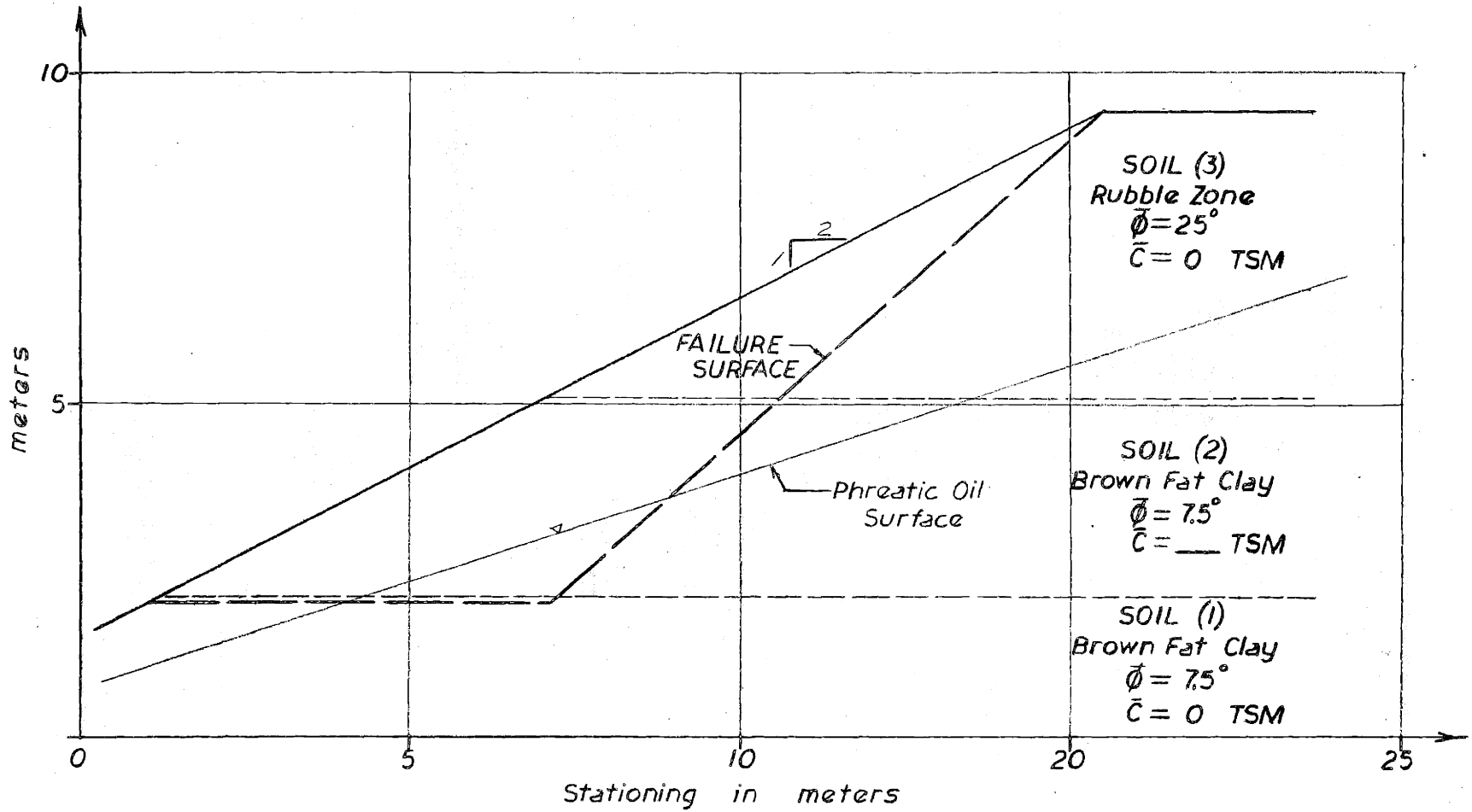

FIGURE 19 SIMPLIFIED WEDGE GEOMETRY FOR "MGSTRN" ANALYSIS

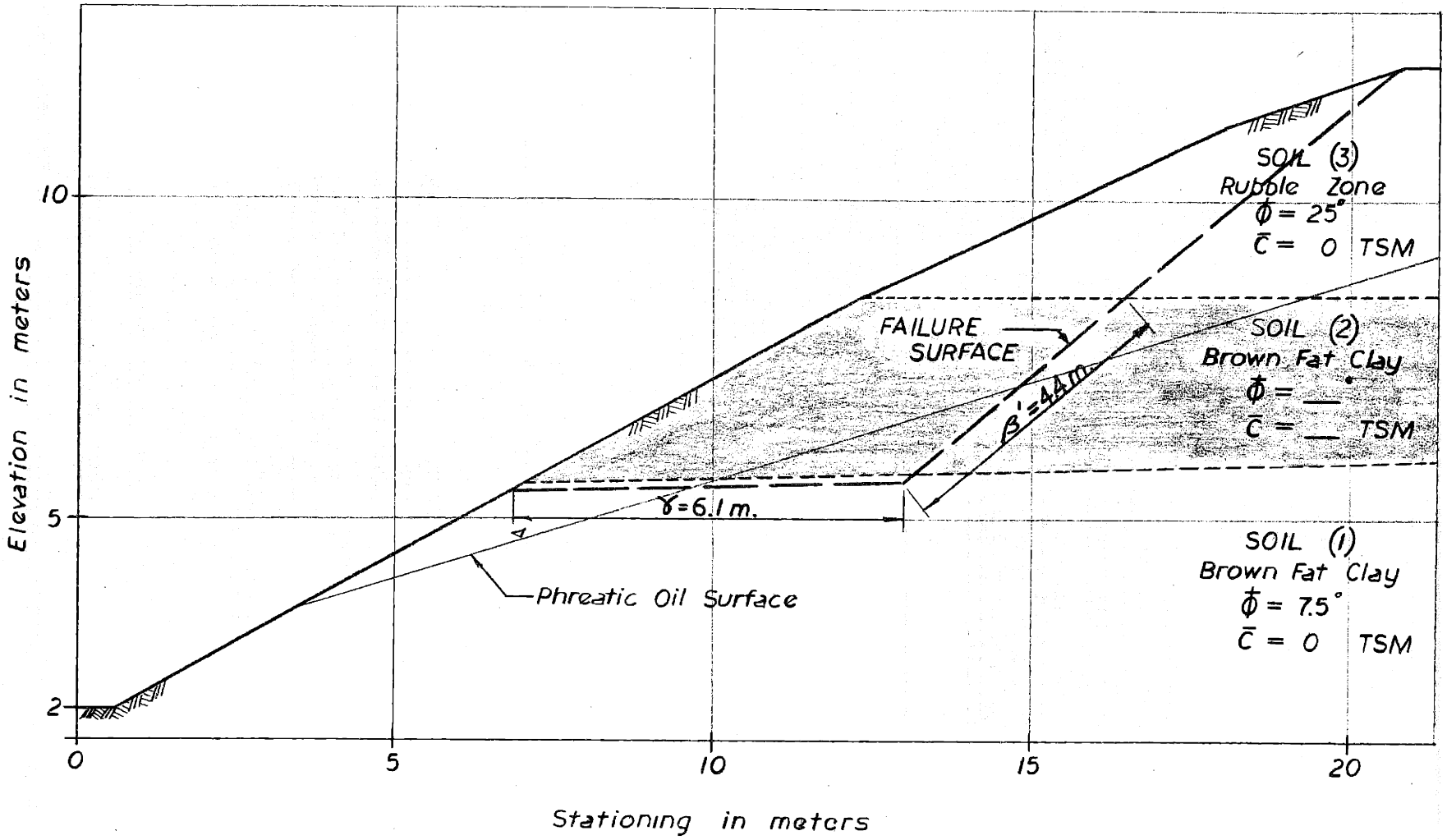

FIGURE 20 GEOMETRY USED IN "MGSTRN" ANALYSIS OF THE ACTUAL SLIDE ZONE

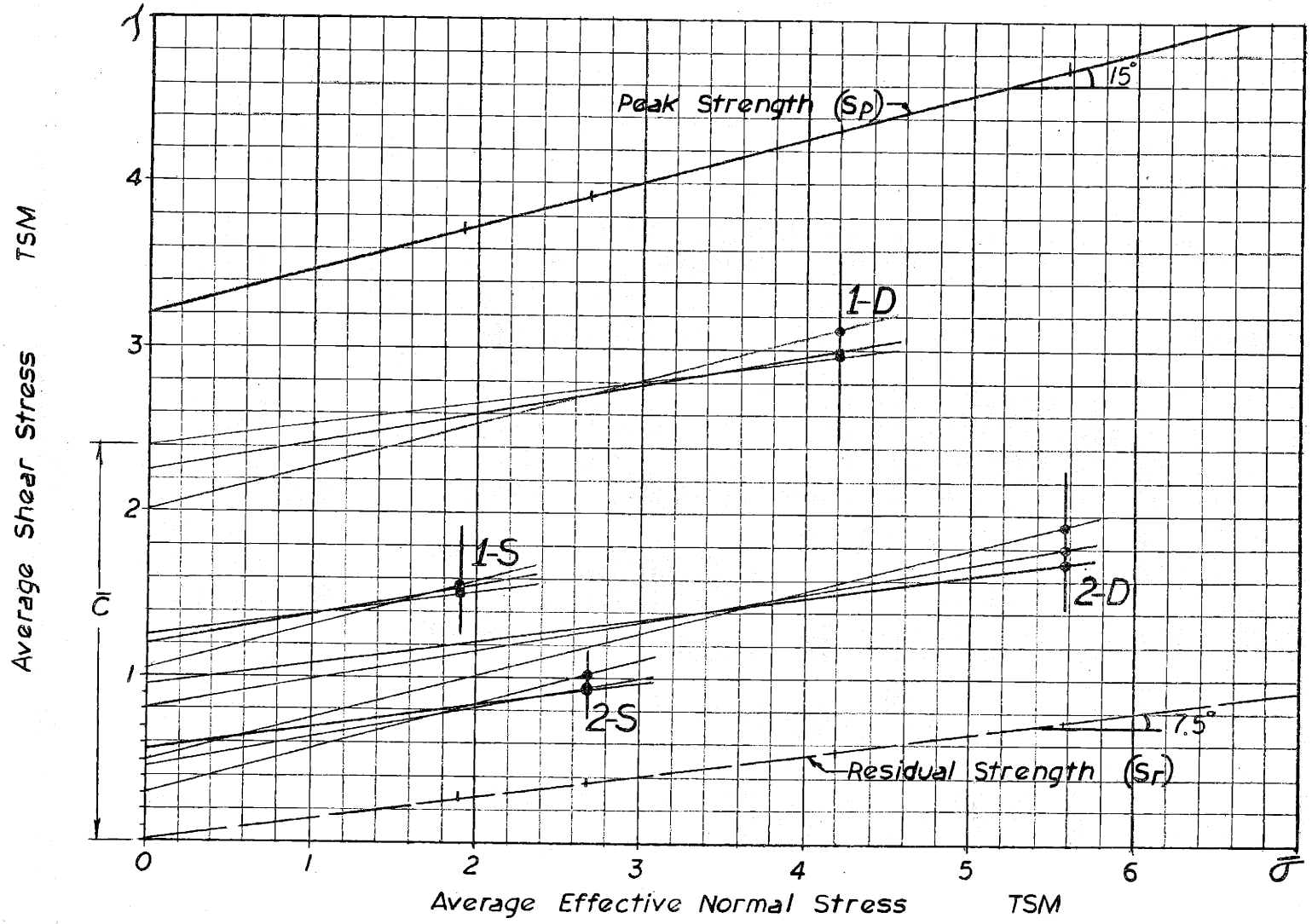

FIGURE 21 AVERAGE STRESSES BY "MGSTRN" ANALYSIS

"MGSTRN" OUTPUT

Trial	Side Force	ϕ_2	C_2	F. S.
a	CONSTANT	7.5°	2.4 TSM	1.007
b	"	10.0°	2.25 TSM	1.003
c	"	15.0°	2.2 TSM	1.009

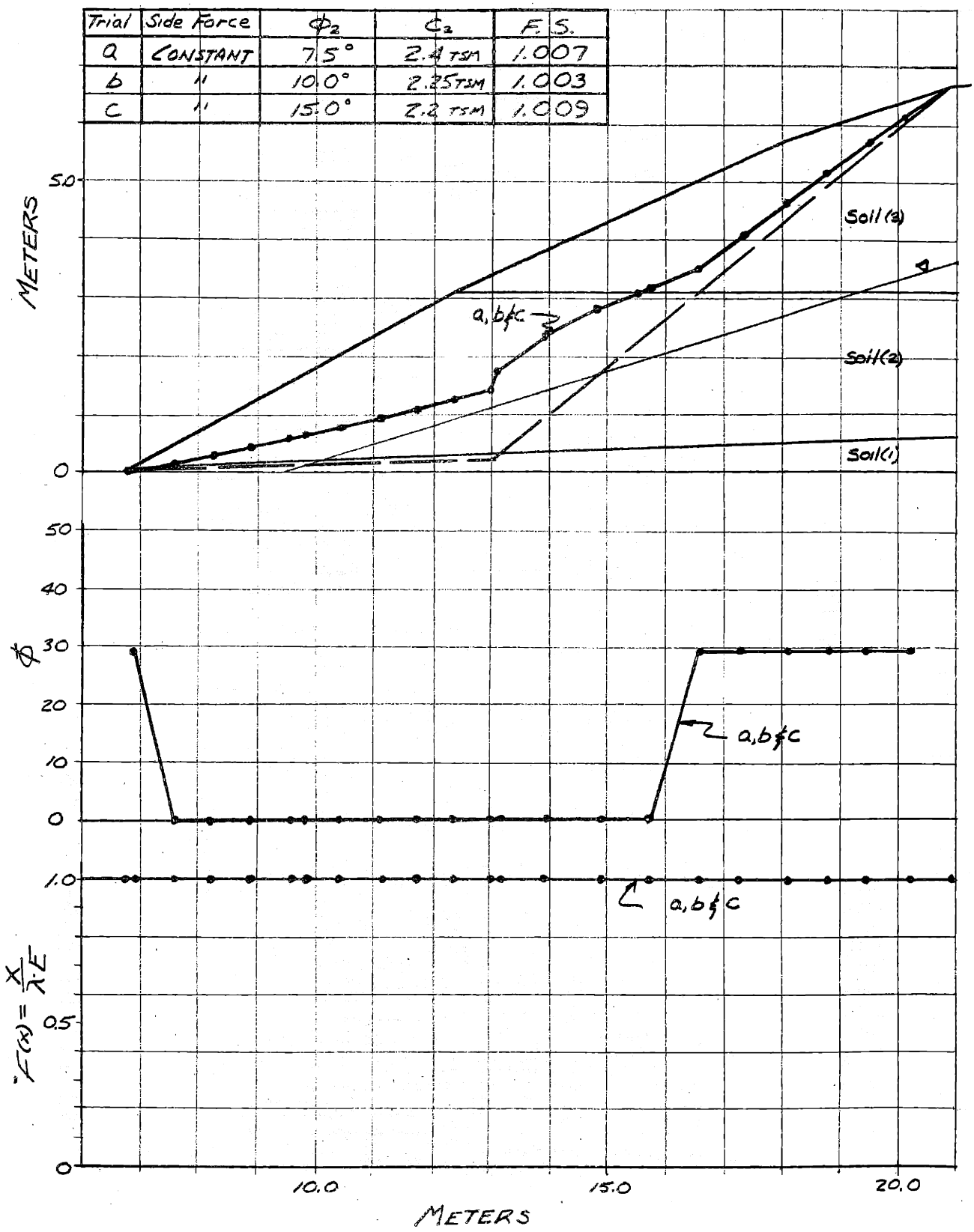

FIGURE 22

"MGSTRN" OUTPUT

Trial	Side Force	$\phi_1 = \phi_2$	$c_1 = c_2$	F.S.
a	CONSTANT	7.5°	.95 TSM	1.018
b	"	10.0°	.80 TSM	1.025
c	"	15.0°	.50 TSM	1.016

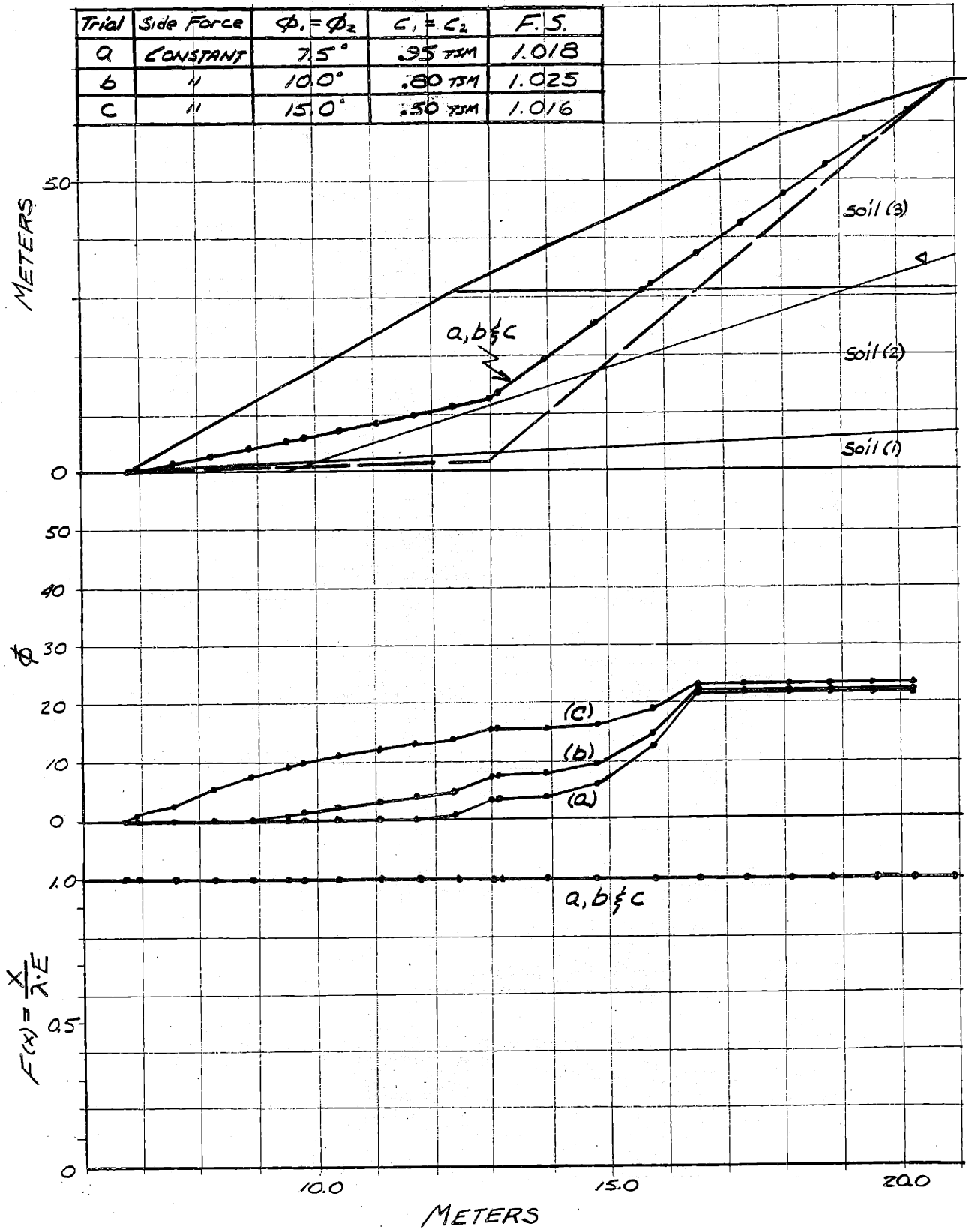

FIGURE 23

1) UNDERCUTTING BY EROSION

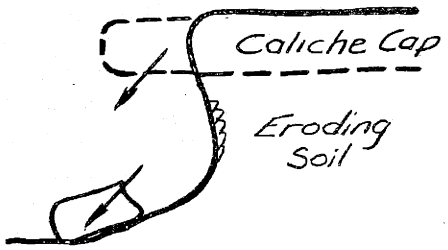

2) MOVEMENT ALONG OLD SHEAR SURFACES

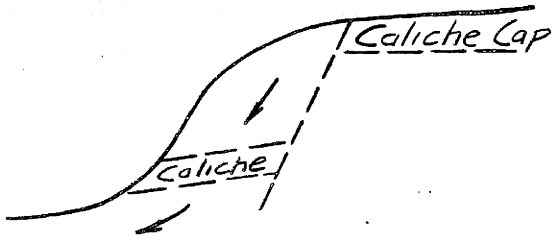

3) MOVEMENT ALONG DESSICATION CRACKS

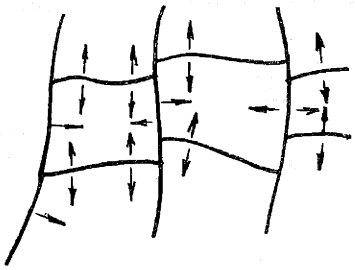

4) MOVEMENT ALONG TENSION CRACKS

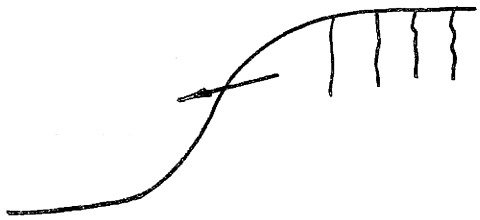

5) MOVEMENT ALONG WEAK LAYER

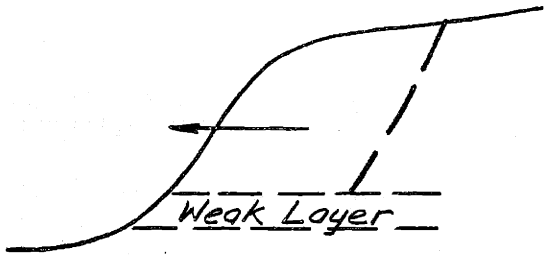

6) DEEP-SEATED SHEAR SLIDE

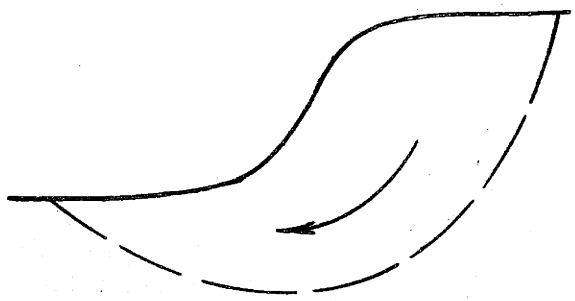

FIGURE 24 TYPES OF EARTH MOVEMENT TWL-LAW

Increase Actuating Force

1. Oil

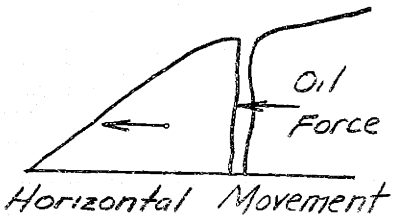

2. Surcharge

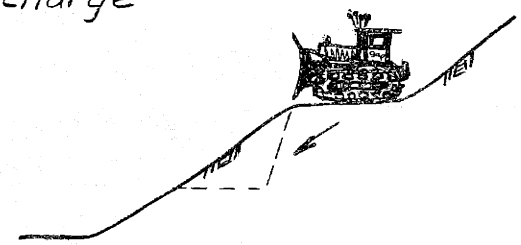

3. Earthquake or Vibratory Force

Decrease Resisting Force

1. Reduce area of shear surface by cracking

2. Reduce effective stress by removing total stress or by increasing pore pressure

3. Removal of counterweight

FIGURE 25 CAUSES OF EARTH MOVEMENT TWL-LAW

APPENDIX A

TESTING PROCEDURE
(Developed by Herrmann (1966))

The samples were prepared by first cutting to near size with a thin saw. They were then cut to exact size (2 in. sq. by .75 in. thick) using a standard sample cutter (specifically coated with teflon to reduce disturbance). Water contents were determined from the sample trimmings. The samples were then extruded from the sample cutter into the direct shear box, and the top loading plate with porous stones and sample grippers, loading cap, and pivot ball added. The weight hanger with weights equivalent to the normal load desired were then lowered and consolidation or swell data of volume change taken.

When consolidation was complete, the "stay" screws, which hold the two halves of the box together and in line, were removed and the top half of the direct shear box separated from the bottom half ten-thousandths of an inch by means of the three "elevator" screws mounted in the top half. A failure surface was cut through sample no. 4 using piano wire, while the halves of the shear box were separated. "Zero" or "initial" readings were taken of the load and shear deflection and the tests started by turning the motor on and tightening the connection between the load cell and the shear box yoke. Readings were taken as often as necessary to insure a complete record of the sample's behavior (i.e., obtain a good "peak" and a good "minimum" on the "$\tau/\overline{\sigma}$ vs. Displacement" curve). The standard "slow" shearing speed for monitored shears was a tenth of an inch per day. The fast speed used for unmonitored forward shears and all reverse shears was a tenth of an inch per hour.

After the first shear was completed, the driving mechanism was reversed and set at the "fast" strain rate by changing the "vibration free connection" to the fast output shaft. The machine was left in the automatic reversing mode until the end of the twentieth shear. The twenty-first shear was a slow monitored shear and the "vibration free connection" had to be switched back to the slow output shaft, the shear boxes separated, initial readings taken, motor turned on, and the load cell shear box yoke connection tightened as before.

After the twenty-first shear, the sample in test no. 4 was unloaded and split apart along the precut and, now, polished failure surface. Residual fuel oil was poured on the failure surface and the sample was put back together and reloaded. Then, the machine was, once again, changed to the "fast" strain rate until completion of the thirtieth shear. The thirty-first shear was the final slow monitored shear.

The samples were then removed from the shear boxes and water content trimmings taken from both the failure plane and the outer portions of the sample.

TABLE A.I

DIRECT SHEAR TEST RESULTS

ON AMUAY FAT CLAY

Test Number	$\bar{\sigma}_N$ TSM	Peak Strength (1st Shear) TSM	Residual TSM	Shear Number TSM
1	20	9.08	3.37	21st
2	40	14.12	6.00	21st
3	10	5.50	1.66	31st
4*	10	2.96	1.38	31st

* This sample had a failure surface precut after consolidation and oil placed on the failure surface after the 21st shear.

REPEATED DIRECT SHEAR TEST ON AMUAY FAT CLAY

Sample Number: 1

Duration of Consolidation:
2 days

Duration of Shearing:
9 days

Sample Size:
2"x2"x0.750"

w_i = 20.2%

w_f = 23.0-25.7%

*ALL FORWARD AND REVERSE SHEARS IMPLIED BUT NOT LISTED WERE RUN AT A STRAIN RATE OF 0.1 INCH PER HOUR.

REMARKS;

Sample separated easily along failure surface which was polished and had slickensides.

* Shear Number	* Strain Rate V_S (0.1 inch per)	$\bar{\sigma}_N$ T/Sq.M.	(τ/σ) Initial Maximum	$\delta_{I.M.}$ Inches	(τ/σ) Residual	δ_R Inches
1	DAY	20.0	0.454	0.0325	0.302	0.166
21	DAY	20.0	0.197	0.0110	0.168	0.0185
31	DAY	20.0	0.208	0.0120	0.170	0.0242

FIGURE A. 1

DIRECT SHEAR TEST ON AMUAY FAT CLAY

SAMPLE NUMBER 1 SHEAR NUMBER 1 & 21 $(\tau/\sigma)_{IM} = 0.454$ $\delta_{IM} = 0.0325$ in.

SHEARING SPEED = 0.1 in/DAY NORMAL STRESS = 20 T/M² $(\tau/\sigma)_R = 0.168$ $\delta_R = 0.0185$ in.

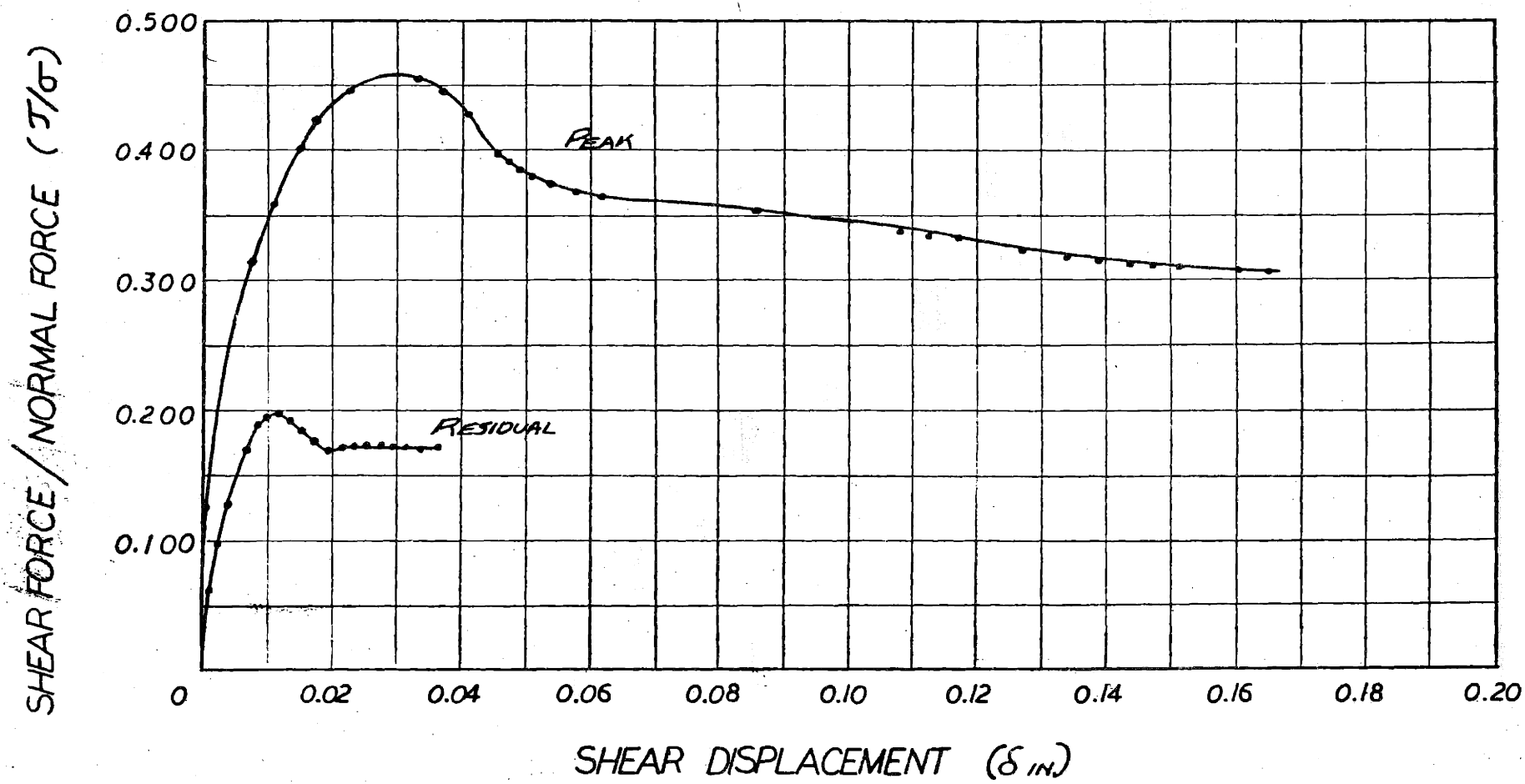

FIGURE A.2

REPEATED DIRECT SHEAR TEST ON AMUAY FAT CLAY

Sample Number: 2

Duration of Consolidation: 2 days

Duration of Shearing: 9 days

Sample Size: 2"x2"x0.750"

w_i = 19.7%

w_f = 25.5-28.70%

*ALL FORWARD AND REVERSE SHEARS IMPLIED BUT NOT LISTED WERE RUN AT A STRAIN RATE OF 0.1 INCH PER HOUR.

REMARKS:

Sample separated easily along failure surface which was polished and had slickensides

Shear Number	Strain Rate V_S (0.1 Inch per)	$\bar{\sigma}_N$ T/Sq.M.	(τ/σ) Initial Maximum	$\delta_{I.M.}$ Inches	(τ/σ) Residual	δ_R Inches
1	DAY	40.0	0.353	0.041	0.231	0.1604
21	DAY	40.0	0.173	0.0171	0.150	0.0270
31	DAY	40.0	0.174	0.0164	0.155	0.0248

FIGURE A.3

DIRECT SHEAR TEST ON AMUAY FAT CLAY

SAMPLE NUMBER 2 SHEAR NUMBER 1 & 21 $(\tau/\sigma)_{IM} = 0.353$ $\delta_{IM} = 0.041$

SHEARING SPEED = 0.1 in/DAY . NORMAL STRESS = 40 T/M² $(\tau/\sigma)_R = 0.150$ $\delta_R = 0.027$

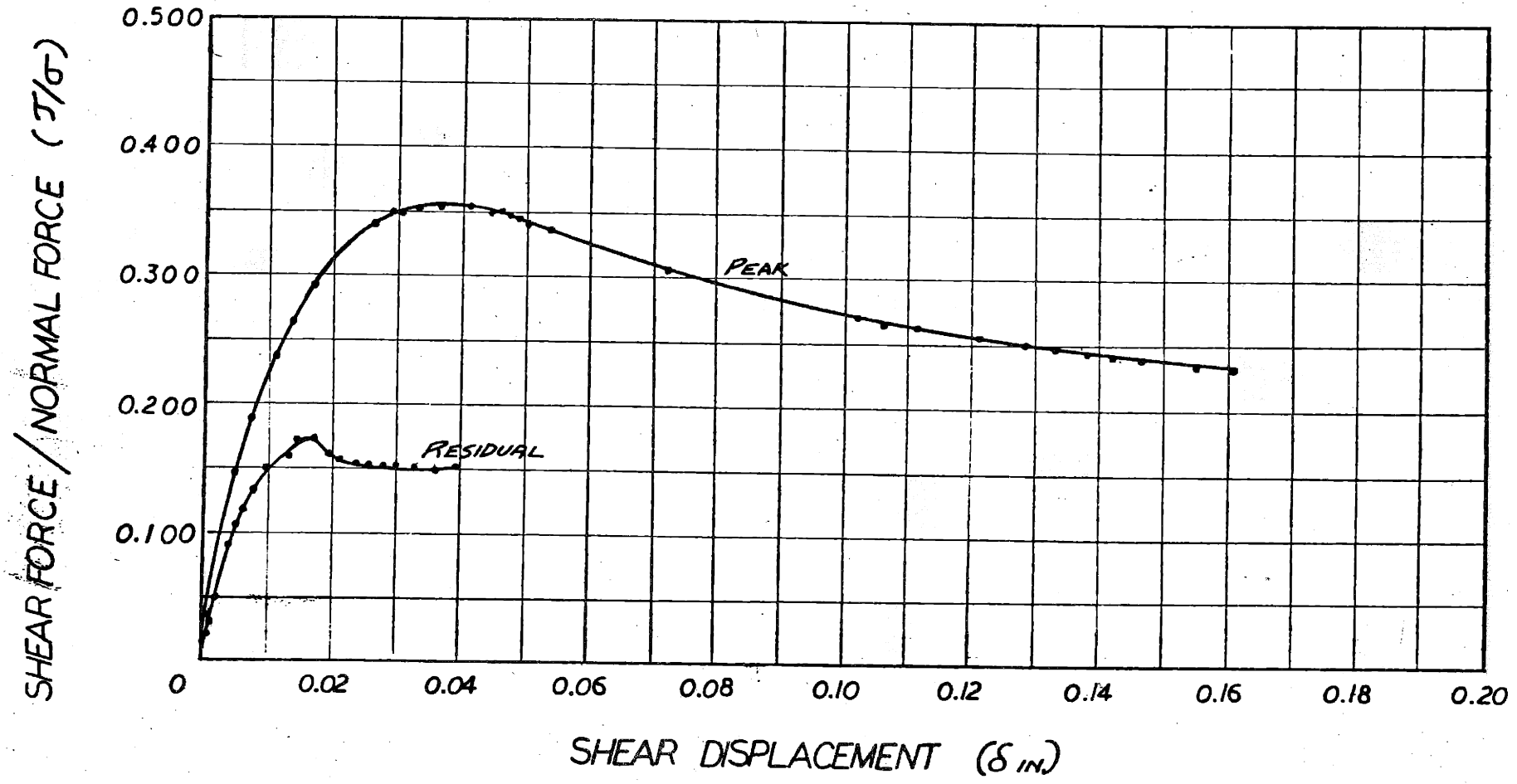

FIGURE A.4

REPEATED DIRECT SHEAR TEST ON AMUAY FAT CLAY

Sample Number: 3

Duration of Consolidation: 2 days

Duration of Shearing: 9 days

Sample Size: 2"x2"x0.750"

w_i = 21.%

w_f = 26.5-28.0%

*ALL FORWARD AND REVERSE SHEARS IMPLIED BUT NOT LISTED WERE RUN AT A STRAIN RATE OF 0.1 INCH PER HOUR.

REMARKS;

Sample separated easily along failure surface which was polished and had slickensides.

* Shear Number	* Strain Rate V_S (0.1 Inch per)	$\bar{\sigma}_N$ T/Sq.M.	(τ/σ) Initial Maximum	$\delta_{i.m.}$ Inches	(τ/σ) Residual	δ_R Inches
1	DAY	10.0	0.550	0.0204	0.350	0.1469
21	DAY	10.0	0.1905	0.0103	0.173	0.0159
31	DAY	10.0	0.1950	0.0109	0.166	0.0189

FIGURE A.5

DIRECT SHEAR TEST ON AMUAY FAT CLAY

SAMPLE NUMBER 3 SHEAR NUMBER 1 & 31 $(\tau/\sigma)_{IM} = 0.550\ \delta_{IM} = 0.0204$ in.

SHEARING SPEED = 0.1 in./DAY NORMAL STRESS = 10 T/M² $(\tau/\sigma)_R = 0.166\ \delta_R = 0.0189$ in.

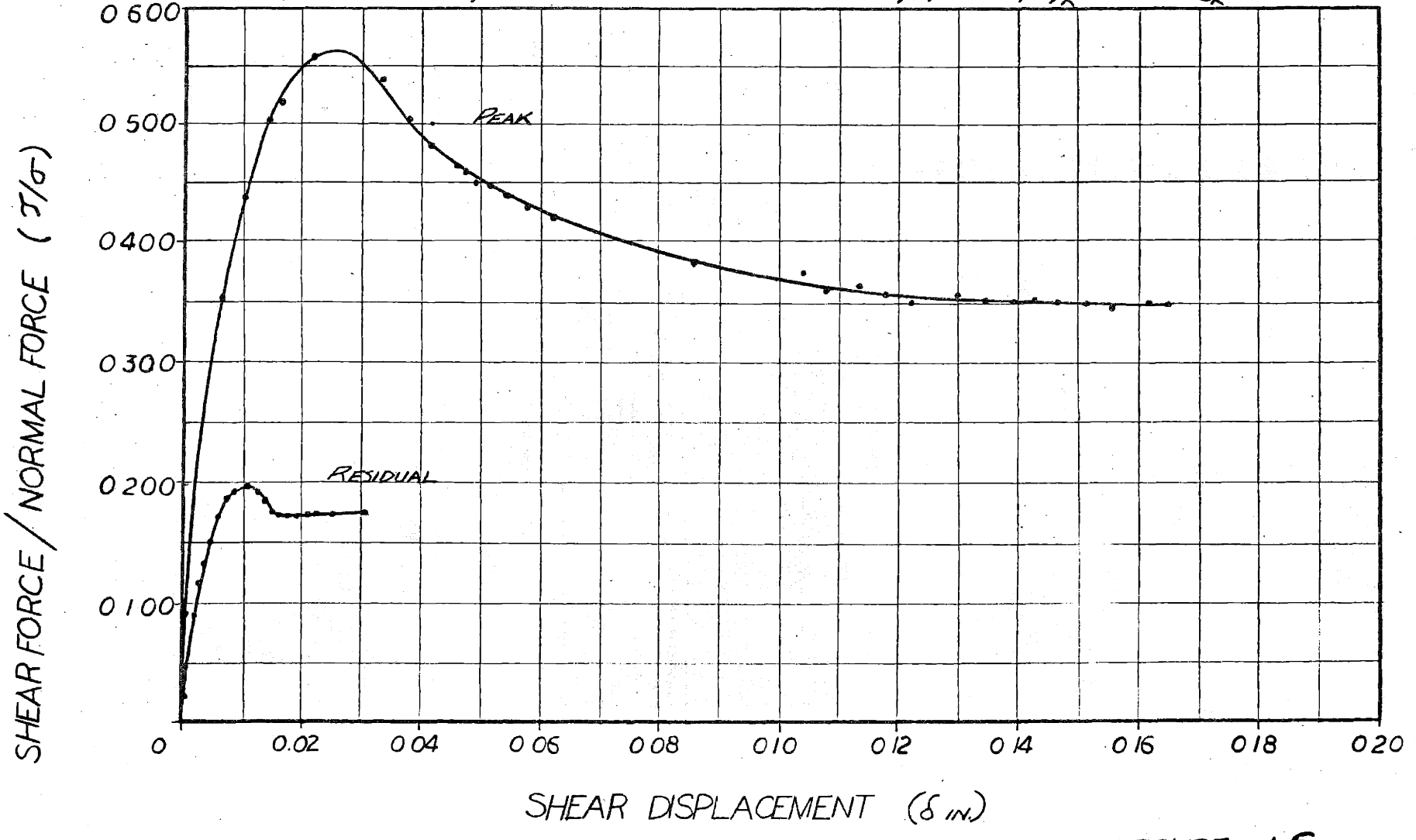

FIGURE A.6

REPEATED DIRECT SHEAR TEST ON AMUAY FAT CLAY

Sample Number: 4

Duration of Consolidation: 2 days

Duration of Shearing: 9 days

Sample Size: 2"x2"x0.750"

w_i = 21.4%

w_f = 28.6-30.0%

*ALL FOWARD AND REVERSE SHEARS IMPLIED BUT NOT LISTED WERE RUN AT A STRAIN RATE OF 0.1 INCH PER HOUR.

REMARKS;

After consolidation of the sample, a failure surface was precut using piano wire. After the 21st shear the sample was: unloaded, split apart, and had residual fuel oil placed on the failure surface; and then put back together, reloaded and sheared. When sample was split apart at end of test, there were only slight traces of oil on the failure surface.

* Shear Number	* Strain Rate V_S (0.1 Inch per)	$\bar{\sigma}_N$ T/Sq.M.	(τ/σ) Initial Maximum	$\delta_{i.m.}$ Inches	(τ/σ) Residual	δ_R Inches
1	DAY	10.0	0.296	0.0058	0.200	0.042
21	DAY	10.0	0.190	0.0070	0.170	0.028
31	DAY	10.0	0.1578	0.0065	0.138	0.034

FIGURE A.7

DIRECT SHEAR TEST ON AMUAY FAT CLAY

SAMPLE NUMBER 4 SHEAR NUMBER 1 & 31 $(\tau/\sigma)_{IM} = 0.296\ \delta_{IM} = 0.0058$ in.

SHEARING SPEED = 0.1 in/DAY. NORMAL STRESS = 10 T/M² $(\tau/\sigma)_R = 0.138\ \delta_R = 0.034$ in.

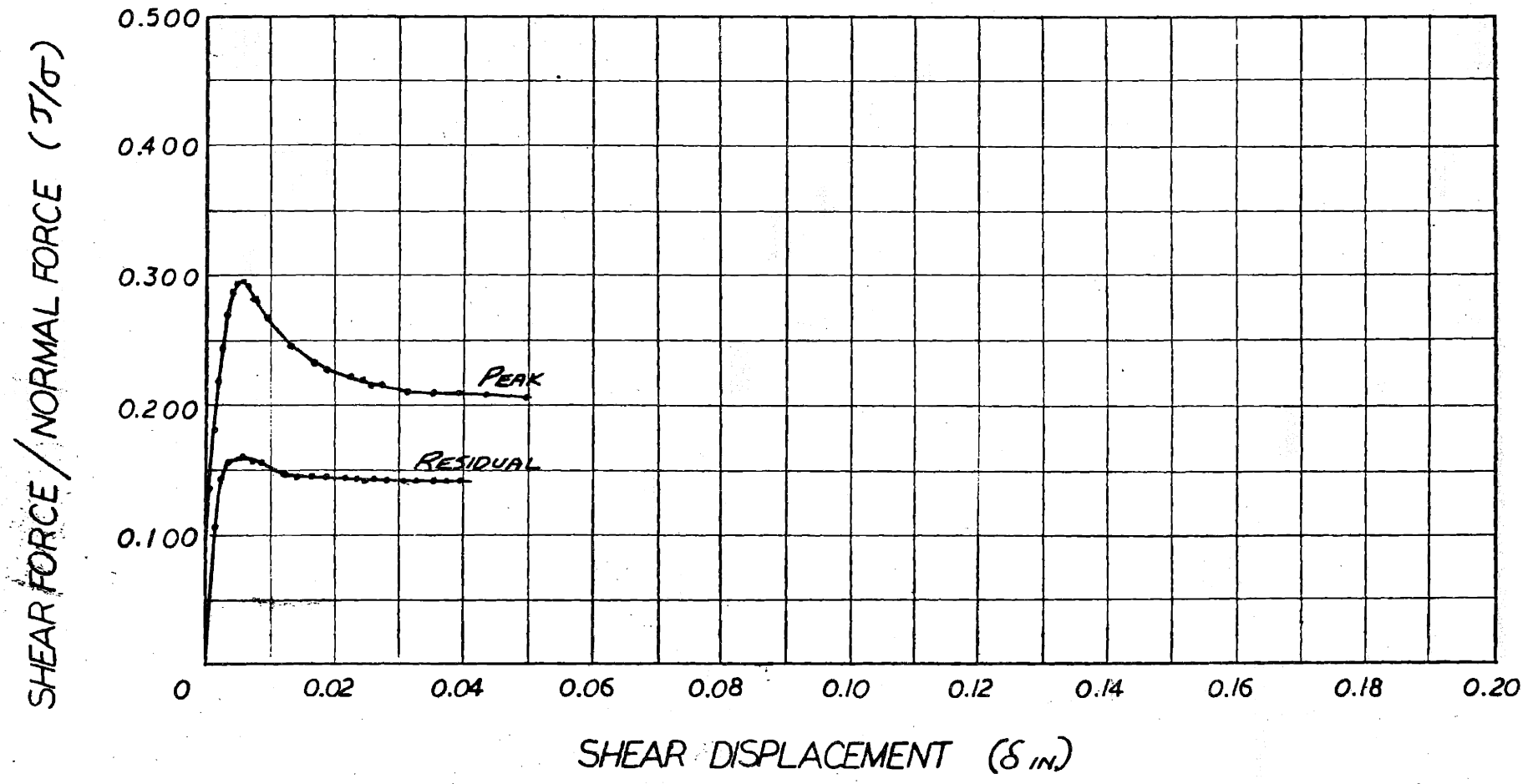

FIGURE A.8

APPENDIX B

DERIVATION OF EQUATIONS FOR THE WEDGE ANALYSIS OF THE STRESSES ALONG SURFACE (2)

Figure B.1 shows wedges I and II in free body form. The forces acting on the wedges are defined in terms of the following quantities:

W_1, W_2, U_1, U_2, U_3.....Knowns
$\overline{N}_1$, $\overline{N}_2$, $\overline{N}_3$, τ_2.....Unknowns
$\overline{c}_1$, $\overline{c}_3$, $\overline{\phi}_1$, $\overline{\phi}_3$.....Assumed Values

Knowing the coordinates of the wedges, the unit weight of the soil (total) and the position of the phreatic surface, we have calculated respectively the weight of the wedges and the neutral forces acting on the three surfaces (given in Figure B.1).

There are two equations of equilibrium for each wedge:

1) Setting the sum of the forces in the vertical direction equal to zero, $\Sigma F_v = 0$.

2) Setting the sum of the forces in the horizontal direction equal to zero, $\Sigma F_h = 0$.

If we assume values of the cohesion and the angle of friction for surfaces (1) and (3) (i.e. $\overline{c}_1$, $\overline{c}_3$, $\overline{\phi}_1$ and $\overline{\phi}_3$), we are left with four unknowns ($\overline{N}_1$, $\overline{N}_2$, $\overline{N}_3$ and τ), and four equations of equilibrium.

We may solve these equations simultaneously to obtain values of the average effective normal stress and the average developed shear stress along surface (2).

The derivation of these equations follows:

First consider WEDGE I

Summing the forces in the vertical direction

$$\Sigma F_v = W_1 - N_1 + T_3 = 0$$

Shear stress has been defined as $\tau = \frac{\bar{c}}{F} + \bar{N} \times \frac{\tan(\bar{\phi})}{F}$

and $N = \bar{N} + U$

Setting F=1.0 for an equilibrium condition and substituting into the above equation, we obtain equation (1)

(1) $$W_1 - \bar{N}_1 - U_1 + \alpha \bar{c}_3 + N_3 \times \tan(\bar{\phi}_3) - U_3 \times \tan(\bar{\phi}_3) = 0$$

Summing the forces in the horizontal direction

$$\Sigma F_H = \tau_1 - N_3 = 0$$

but $\tau_1 = \gamma \bar{c}_1 + \bar{N}_1 \times \tan(\bar{\phi}_1)$, substituting we obtain equation (2)

(2) $$N_3 = \tau_1 = \gamma \bar{c}_1 + \bar{N}_1 \times \tan(\bar{\phi}_1)$$

Substituting equation (2) into equation (1), we eliminate the unknown N_3 (total normal force acting on surface (3)) and obtain equation (3).

(3) $$\bar{N}_1 = \frac{(W_1 - U_1 + \alpha \bar{c}_3 + \gamma \bar{c}_1 \times \tan(\bar{\phi}_3) - U_3 \times \tan(\bar{\phi}_3))}{(1 - \tan(\bar{\phi}_1) \times \tan(\bar{\phi}_3))}$$

Since the values of W_1, W_2, U_1, U_2 and U_3 are determined by the geometry of the problem and we assume values for $\bar{c}_1$, $\bar{c}_3$, $\bar{\phi}_1$ and $\bar{\phi}_3$, we may calculate $\bar{N}_1$.

With a value of $\bar{N}_1$, we may calculate τ_1 and N_3 using equation (2). With this value of N_3, we may calculate τ_3 using the definition of shear stress.

$$\tau_3 = \alpha \bar{c}_3 + (N_3 - U_3) \times \tan(\bar{\phi}_3)$$

So far we have assumed values of $\bar{c}_1$, $\bar{c}_3$, $\bar{\phi}_1$ and $\bar{\phi}_3$ and have been able to calculate corresponding values of $\bar{N}_1$, τ_1, N_3 and τ_3.

Now consider WEDGE II

Summing the forces in the vertical direction

$$\Sigma F_V = W_2 - T_3 - T_2 \times \sin(\theta) - N_2 \times \cos(\theta)$$

substituting $N_2 = \bar{N}_2 + U_2$, and solving for $\bar{N}_2$, we obtain equation (4).

$$(4) \qquad \bar{N}_2 = \frac{W_2 - T_3 - T_2 \times \sin(\theta) - U_2 \times \cos(\theta)}{\cos(\theta)}$$

Summing the forces in the horizontal direction

$$\Sigma F_H = N_3 - N_3 \times \sin(\theta) + T_2 \times \cos(\theta) = 0$$

substituting $N_2 = \bar{N}_2 + U_2$, we obtain equation (5)

$$(5) \qquad N_3 - \bar{N}_2 \times \sin(\theta) - U_2 \times \sin(\theta) + T_2 \times \cos(\theta) = 0$$

Substituting equation (4) into equation (5), such that the unknown $\bar{N}_2$ is eliminated, we may solve for τ_2, obtaining equation (6).

$$(6) \qquad T_2 = \frac{W_2 \times \tan(\theta) - T_3 \times \tan(\theta) - N_3}{\tan(\theta) \times \sin(\theta) + \cos(\theta)}$$

We may now substitute this value of τ_2 back into equation (4) and obtain a value of $\bar{N}_2$ (average effective normal stress acting on surface (2)).

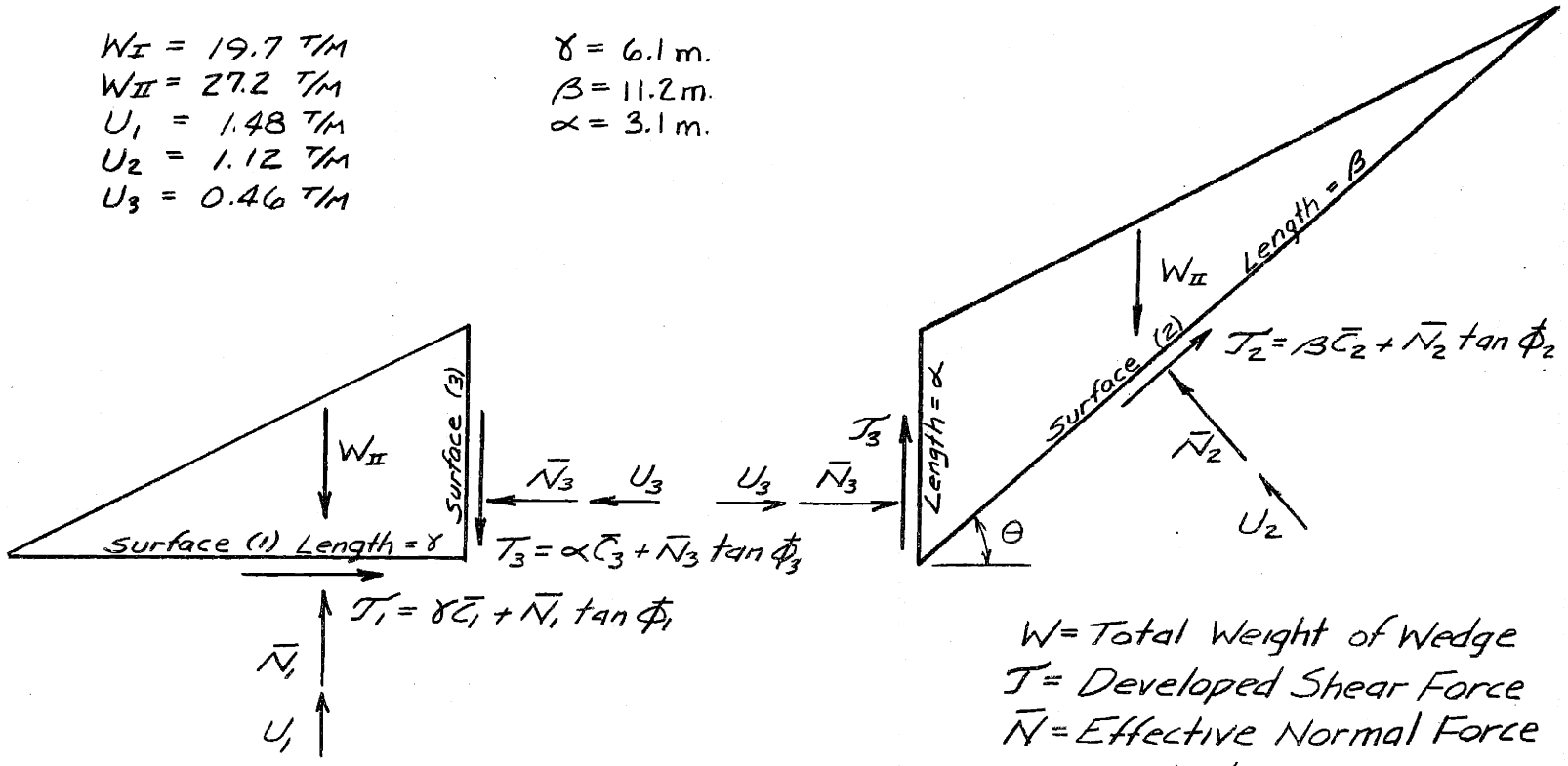

FIGURE B.1 External Forces Acting on Wedges

APPENDIX C

DERIVATION OF THE EQUATIONS OF THE WEDGE ANALYSIS FOR THE F.S.=F ALONG SURFACES (1), (2) and (3).

We have shown in Figure C.1, the external forces acting on the surfaces of the two wedges defined in terms of their corresponding soil parameters and factors of safety.

If we assume values of the cohesion and the angle of friction acting along surfaces (1), (2) and (3), we are left with four unknowns ($\bar{N}_1$, $\bar{N}_2$, $\bar{N}_3$ and F) and four simultaneous equations (summing the forces horizontally and vertically for the two wedges). As shown below, an iteration procedure must be used to solve these equations for the factor of safety (F).

First consider WEDGE I

Summing the forces in the vertical direction

$$\Sigma F_V = W_1 - N_1 + T_3 = 0$$

Shear stress has been defined as $T = \frac{\bar{c}}{F} + \frac{\bar{N} \times \tan(\phi)}{F}$

and $N = \bar{N} + U$

Substituting and solving for $\bar{N}_1$, we obtain equation (1)

(1) $$\bar{N}_1 = W_1 - U_1 + \frac{\alpha \bar{c}_3}{F} + \bar{N}_3 \times \frac{\tan(\phi_3)}{F}$$

Summing the forces in the horizontal direction

$$\Sigma F_H = T_1 - N_3 = 0$$

substituting $$T_1 = \frac{\gamma \bar{c}_1}{F} + \frac{\bar{N}_1 \times \tan(\phi_1)}{F}$$

and $$N_3 = \bar{N}_3 + U_3$$

we obtain equation (2)

(2) $$\bar{N}_3 + U_3 = \frac{\gamma \bar{c}_1}{F} + \frac{\bar{N}_1 \times \tan(\phi_1)}{F}$$

Substituting equation (1) into equation (2), we eliminate the unknown $\bar{N}_1$ (effective normal force acting on surface (1)).

rearranging and combining terms, we obtain equation (3).

$$(3) \qquad \bar{N}_3 = \frac{\left[\gamma \bar{c}_1 + (W_1 - U_1) \times \tan(\phi_1)\right] \frac{1}{F} + \frac{\alpha \bar{c}_3 \times \tan(\phi_1)}{(F)^2} - U_3}{\left(1 - \frac{\tan(\phi_3) \times \tan(\phi_1)}{(F)^2}\right)}$$

Now consider WEDGE II

Summing the forces in the vertical direction

$$\Sigma F_V = W_2 - T_3 - T_2 \times \sin(\theta) - \bar{N}_2 \times \cos(\theta) - U_2 \times \cos(\theta) = 0$$

substituting $\qquad T = \frac{\bar{c}}{F} + \frac{\bar{N} \times \tan(\phi)}{F}$

we obtain equation (4)

$$(4) \qquad W_2 - \frac{\alpha \bar{c}_3}{F} - \bar{N}_3 \times \frac{\tan(\phi_3)}{F} - \frac{\beta \bar{c}_2 \times \sin(\theta)}{F} - \bar{N}_2 \times \frac{\tan(\phi_2) \times \sin(\theta)}{F} - \bar{N}_2 \times \cos(\theta) - U_2 \times \cos(\theta) = 0$$

Summing the forces in the horizontal direction,

$$\Sigma F_H = \bar{N}_3 + U_3 - \bar{N}_2 \times \sin(\theta) - U_2 \times \sin(\theta) + T_2 \times \cos(\theta) = 0$$

substituting

$$T = \frac{\bar{c}}{F} + \frac{\bar{N} \times \tan(\phi)}{F}$$

we obtain equation (5)

$$(5) \qquad \bar{N}_3 + U_3 - \bar{N}_2 \times \sin(\theta) - U_2 \times \sin(\theta) + \frac{\beta \bar{c}_2}{F} \cos(\theta) + \bar{N}_2 \times \tan(\phi_2) \times \cos(\theta) = 0$$

Solving both equation (4) and (5) for $\bar{N}_2$, and equating them, we obtain a very complicated expression (equation (6)) in terms of the two unknowns, F and $\bar{N}_3$.

$$(6) \qquad \frac{(W_2 - U_2 \times \cos(\theta)) \times F - (\alpha \bar{c}_3 + \bar{N}_3 \times \tan(\phi_3) + \beta \bar{c}_2 \times \sin(\theta))}{(\tan(\phi_2) \times \sin(\theta) + F \times \cos(\theta))} =$$

$$\frac{F(\bar{N}_3 + U_3 - U_2 \times \sin(\theta)) + \beta \bar{c}_2 \times \cos(\theta)}{(F \times \sin(\theta) - \tan(\phi_2) \times \cos(\theta))}$$

If we were to substitute equation (3) into equation (6), we would get an expression in terms of the unknown F which could

not readily be solved. Therefore, we must try an iterative approach...

Cross-multiplying the terms of equation (6), we obtain

$$[F\cdot\sin(\theta)-\tan(\phi_2)\cos(\theta)][(W_2-U_2\cos(\theta))F-(\alpha\bar{c}_3+\bar{N}_3\cdot\tan(\phi_3)+\beta\bar{c}_2\cdot\sin(\theta)] =$$

$$[F(\bar{N}_3+U_3-U_2\cdot\sin(\theta))+\beta\bar{c}_2\cdot\cos(\theta)][\tan(\phi_2)\cdot\sin(\theta)+F\cdot\cos(\theta)]$$

Combining and canceling terms, yields equation (7)

$$(7)\quad (F)^2\cdot[W_2\cdot\sin(\theta)-(\bar{N}_3+U_3)\cdot\cos(\theta)]$$
$$+F\cdot[(U_2-W_2\cdot\cos(\theta))\cdot\tan(\phi_2)-\beta\bar{c}_2-(\alpha\bar{c}_3+\bar{N}_3\cdot\tan(\phi_3))\sin(\theta)-(\bar{N}_3+U_3)\tan(\phi_2)\cdot\sin(\theta)]$$
$$+[(\alpha\bar{c}_3+\bar{N}_3\cdot\tan(\phi_3))(\tan(\phi_2)\cdot\cos(\theta))]=0$$

It is readily seen that if we assume an initial value for F in equation (3) and solve for $\bar{N}_3$, we may then plug this value of $\bar{N}_3$ into equation (7) and solve for F using the quadratic equation. Making use of an iterative process with a trial and error procedure, we will converge to a value for the factor of safety. To simplify the solving, numerically, of equation (7) we have assigned the letters A, B, and C to the coefficients of F^2, F and 1 respectively. The final equations and a summary of the method of solving them are given below.

$$\bar{N}_3=\frac{\left[\gamma\bar{c}_1+(W_1-U_1)\cdot\tan(\phi_1)\right]\frac{1}{F}+\frac{\alpha\bar{c}_3\cdot\tan(\phi_1)}{(F_0)^2}-U_3}{\left(1-\frac{\tan(\phi_3)\cdot\tan(\phi_1)}{(F_0)^2}\right)}$$

$$A\cdot(F)^2+B\cdot(F)+C=0$$

$$A=[W_2\cdot\sin(\theta)-(\bar{N}_3+U_3)\cdot\cos(\theta)]$$

$$B=[(U_2-W_2\cdot\cos(\theta))\cdot\tan(\phi_2)-\beta\bar{c}_2-(\alpha\bar{c}_3+\bar{N}_3\cdot\tan(\phi_3))\cdot\sin(\theta)-(\bar{N}_3+U_3)\cdot\tan(\phi_2)\cdot\sin(\theta)]$$

$$C=[(\alpha\bar{c}_3+\bar{N}_3\cdot\tan(\phi_3))\cdot\tan(\phi_2)\cdot\cos(\theta)]$$

$$F_f = \frac{-B \pm \sqrt{(B)^2 - 4 * A * C}}{2A}$$

Solving the Equations:

To obtain a value of the factor of safety for a defined set of soil parameters along the three surfaces:

1) Assume an initial value of the F.S. = F_i and insert this in the equation for $\bar{N}_3$.
2) Using the value of $\bar{N}_3$ obtained, plug into the equations given for A, B and C.
3) Plug the values of A, B and C in the final equation and compute a value of F_f.
4) Repeat this process using a trial and error iteration procedure, until $F_f = F_i$. This is the factor of safety for the defined soil parameters.

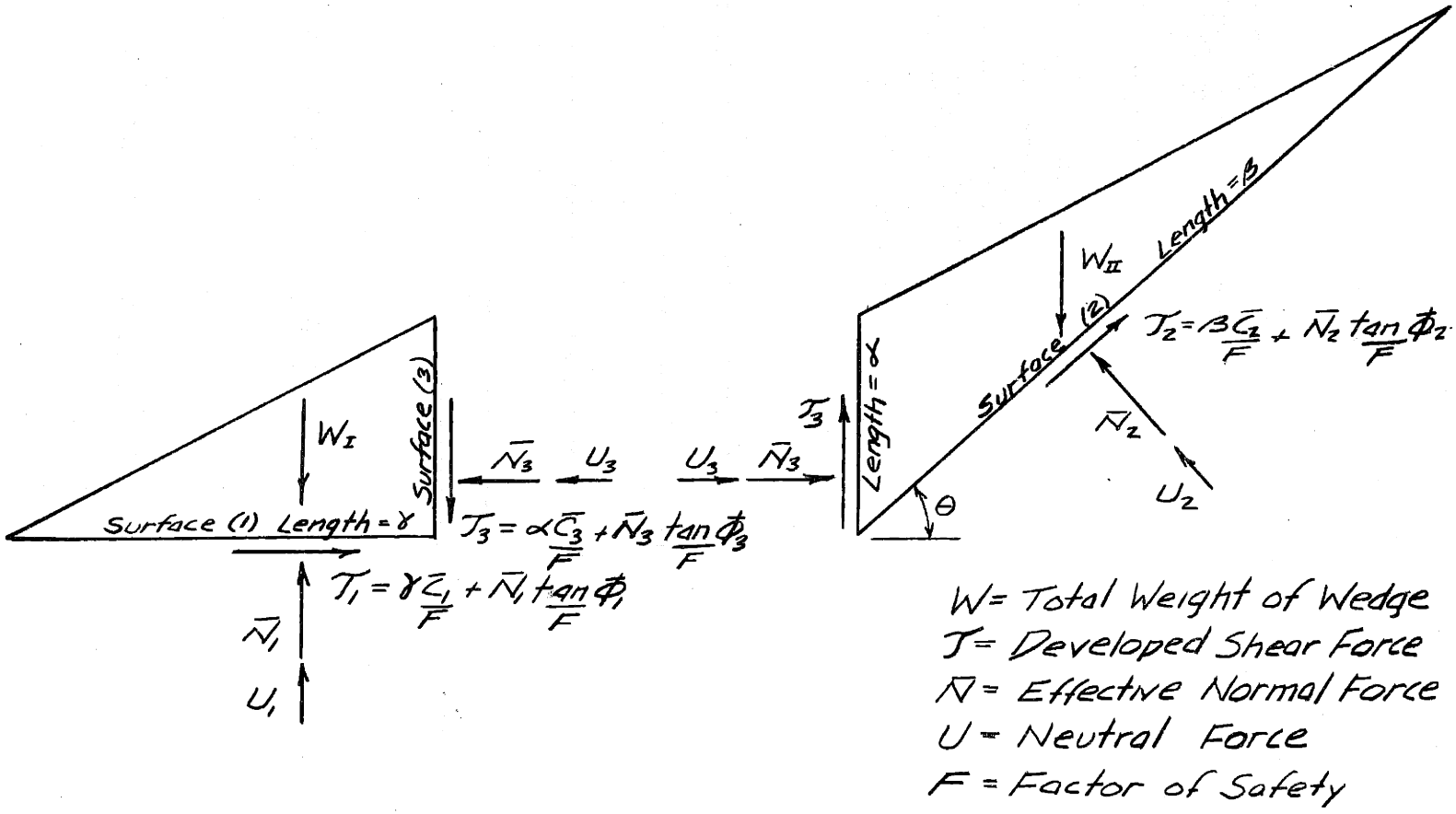

FIGURE C.1 External Forces for FS=F Condition

APPENDIX D

DERIVATION OF THE EQUATIONS OF THE WEDGE ANALYSIS FOR F.S. = 1.0 ALONG SURFACE (1) F.S. = F ALONG SURFACES (2) AND (3)

We have assumed a residual condition along surface (1), but not along surfaces (2) and (3). We have shown in Figure D.1, the external forces acting on the surfaces of the two wedges and defined these forces, as in Appendix C, in terms of their corresponding soil parameters and factors of safety. The only difference between the forces shown in Figure C.1 and those of Figure D.1 is the shear stress which is developed along surface (1). In this analysis, the factor of safety = 1.0 along surface (1) and the shear stress equals:

$$\tau_1 = \frac{\alpha \bar{c}_1}{1.0} + \frac{\bar{N}_1 \times \tan(\phi_1)}{1.0}$$

We must set up and solve the simultaneous equations for translational equilibrium of the two wedges, using an iteration procedure, just as we did in Appendix C.

We find that changing the definition of the shear stress which is developed along surface one only affects the equation for $\bar{N}_3$. All of the terms of the other final equations which we use in the determination of a factor of safety for this analysis are the same as those in Appendix C.

First consider WEDGE I

Summing the forces in the vertical direction

$$\Sigma F_v = W_1 - N_1 + \tau_3 = 0$$

Shear stress has been defined along surface (3) as

$$\tau_3 = \frac{\alpha \bar{c}_3}{F} + \frac{\bar{N}_3 \times \tan(\phi_3)}{F}$$

and $N_1 = \bar{N}_1 + U_1$

Substituting and rearranging, we obtain equation (1)

(1) $$\bar{N}_1 = W_1 - U_1 + \frac{\alpha \bar{C}_3}{F} + \frac{\bar{N}_3 \times \tan(\phi_3)}{F}$$

Summing the forces in the horizontal direction,

$$\Sigma F_H = T_1 - N_3 = 0$$

Substituting $T_1 = \gamma \bar{C}_1 + \bar{N}_1 \times \tan(\phi_1)$

and $N_3 = \bar{N}_3 + U_3$

We obtain equation (2)

(2) $$\bar{N}_3 + U_3 = \gamma \bar{C}_1 + \bar{N}_1 \times \tan(\phi_1)$$

Substituting equation (1) into equation (2), we eliminate the unknown $\bar{N}_1$ (effective normal force acting on surface (1))

$$\bar{N}_3 + U_3 - \gamma \bar{C}_1 = \left(W_1 - U_1 + \frac{\alpha \bar{C}_3}{F} + \frac{\bar{N}_3 \times \tan(\phi_3)}{F}\right) \times \tan(\phi_1)$$

Rearranging and combining terms, we obtain equation (3)

$$\bar{N}_3 \left(1 - \frac{\tan(\phi_3) \times \tan(\phi_1)}{F}\right) = \left(W_1 - U_1 + \frac{\alpha \bar{C}_3}{F}\right) \times \tan(\phi_1) + \gamma \bar{C}_1 - U_3$$

(3) $$\bar{N}_3 = \frac{(W_1 - U_1) \times \tan(\phi_1) + \gamma \bar{C}_1 - U_3 + \frac{\alpha \bar{C}_3 \times \tan(\phi_1)}{F}}{\left(1 - \frac{\tan(\phi_3) \times \tan(\phi_1)}{F}\right)}$$

Now consider WEDGE II

The forces and equations of equilibrium for wedge II are identical to those in Appendix C. The equations are solved and the iteration procedure is set up in the same manner. Substituting $\bar{N}_3$ from the above equation into the expression for F_f (given in Appendix C), we may obtain a factor of safety for this condition.

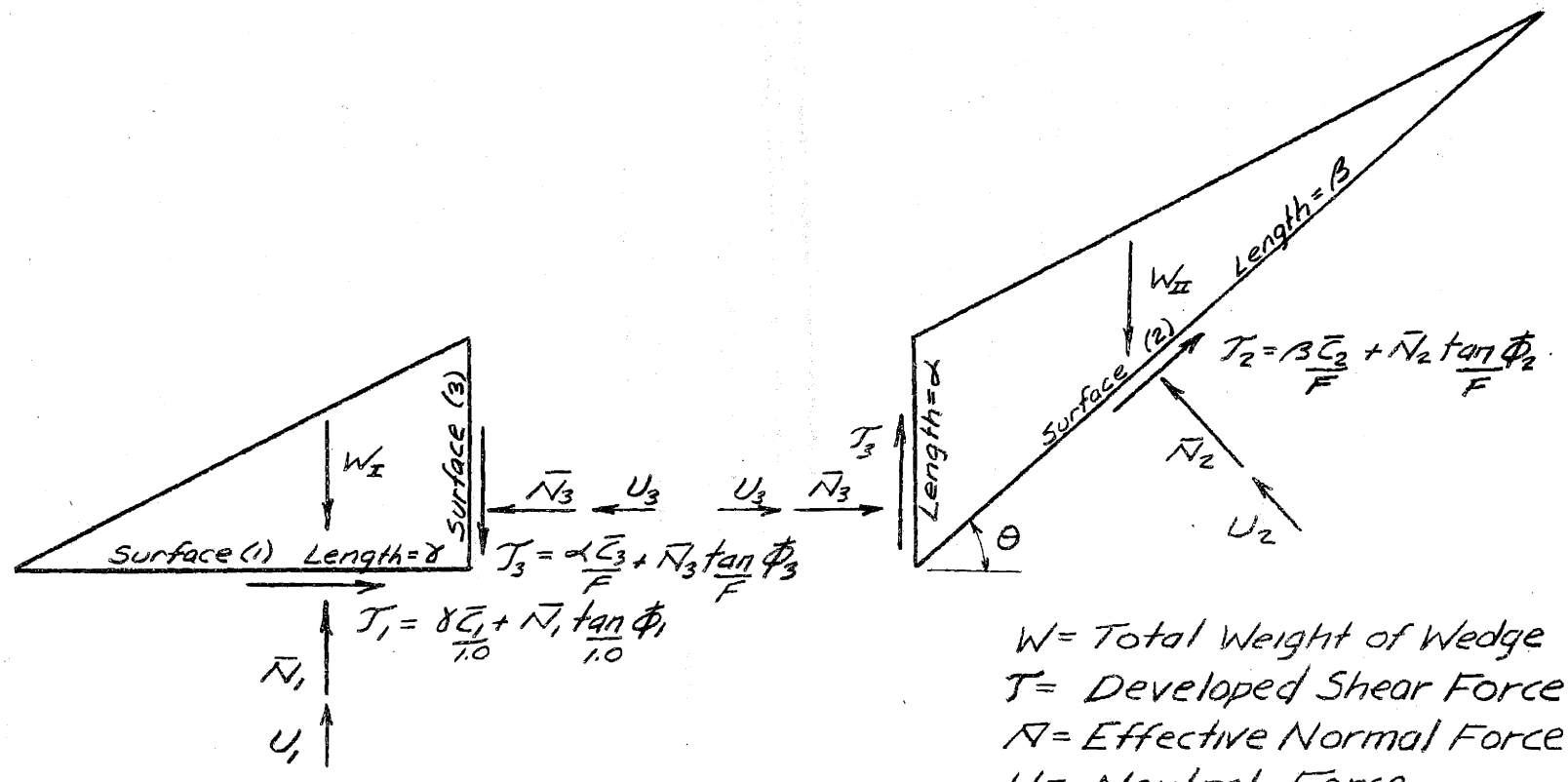

FIGURE D.1 External Forces for FS=1 Along Surface(1) Condition

APPENDIX E

INVESTIGATION OF THE SIDE FORCE ASSUMPTION BY "MGSTRN"

Figure 19 is a cross-section of the geometry and soil conditions (3 zones) which are used throughout this investigation. The parameters of zones (1) and (3) are assumed to be equal to ($\overline{\phi}_1$=7.5, $\overline{c}_1$=0 TSM) and ($\overline{\phi}_3$=25, $\overline{c}_3$=0 TSM) respectively. After obtaining values of $\overline{c}_2$ and $\overline{\phi}_2$ so that the factor of safety was approximately equal to unity (Section VII.2.3), we found that the value of equilibrium cohesion parameter $\overline{c}_2$ (for a fixed value of $\overline{\phi}_2$), was insensitive to the choice of side force function. For eight different assumptions of side force, the factors of safety (using the same soil parameters) came out within 3% of each other (see table E.I for a tabulation of the side force assumption, Lambda, and F.S. of each trial).

The first four assumptions of the side force function are standard choices which the "user" of "MGSTRN" may employ. Trials 5 through 8 were set up by the author.

Figure E.1 thru E.4 include plots of the "MGSTRN" output for these eight different side force assumption trials. The top portion of the figure is a cross-section of the slope geometry showing the phreatic surface, sides of the slices (indicated by a dot), the failure surface and the line of action of the effective side thrust.

The center portion of these figures is a plot of the friction angles which must be developed on the sides of the slices for the failure body to satisfy equilibrium.

The lower portion of the figure is a plot of the side force assumption. In the method of Morgenstern and Price, the side force assumption has been defined as:

$$F(X) = \frac{X}{\lambda * E}$$

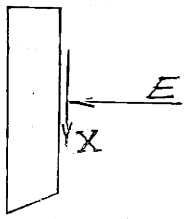

F(X) = side force function

X = shear force developed on the side of a slice

E = total normal force acting on the side of a slice

λ = constant employed in the solving of the equations

(See Bailey, 1966 for further explanation)

A comparison of Figures E.1 to E.4 shows us the effect of changing the side force assumption on the value of $\overline{\phi}$ developed on the sides of the slices and on the position of the effective side thrust.

In this problem, we are primarily concerned with the analysis of a drawdown condition. It would be beneficial in solving later problems, if we could correlate the type of water condition of a problem (submerged, seepage, dry) with a "most correct" side force assumption for that condition.

The first assumption is the side force function equal to a constant (F(X)=1.0). This means that the tangential force and the normal force acting on the side of a slice are related only by the constant Lambda and thus, the inclination of the total side force acting on each slice is the same. Upon examination of case 1 of Figure E.1, we see that the position of the effective side thrust ($\overline{E}$) is in the 1/3 to 1/2 times the height of the slice range until we get to zone (3) (cohesionless rubble), where it is slightly low. The plot of the developed friction angles indicates that in two regions

equilibrium of the wedges by the method of Morgenstern and Price requires a developed $\bar{\phi}$ which is higher than the $\bar{\phi}$ available. In the region of the slide zone toe, discontinuities in defining the soil conditions and selecting the first slice are the cause of a $\bar{\phi}$ being developed. Therefore, in all of our plots, we neglect this developed $\bar{\phi}$ at the toe.

However, the high values of $\bar{\phi}$ developed in the upper region of the slide are reasonable. With a high value of F(X) in this region, we are developing more shear stress on the sides of the slices than we have available in frictional resistance. This calls for a decrease in the side force function. A decrease will result in less shear stress being developed on the sides of the slices and thus a lower value of $\bar{\phi}$ required. It may also raise the position of the effective side thrust in that region by decreasing the inclination of the total side force.

"MGSTRN" places slice boundaries at given intervals of the X coordinate, plus through all points along the failure surface and slope where there is a soil boundary, intersection of phreatic surface, or change in direction of the failure surface or slope. Slice boundaries with X coordinates of 3.92, 7.10 and 10.62 meters are such points along the failure surface. These discontinuities are the reason for the abrupt change in the position of the effective side thrust and the value of $\bar{\phi}$ developed along the sides of the slices. Soil boundaries and changes in direction of the failure surface are readily seen to be the most critical.

A sudden change in the side force assumption does seem to have a great effect, in our problem, on the smoothness of the curve defining the line of the effective side thrust. This is verified in trial 8 of Figure E.4.

It is also found that average $\bar{N}$ along the steep portion of the failure surface is relatively insensitive to the side force assumption. Consequently, the residual factors which we calculate from "MGSTRN" output, will not change appreciably with the side force assumption. Looking over the results of the trials, it seems that trial 6 is the "most correct" side force assumption for the problem (that is, the "most correct" of the trials that we have performed). Side force assumption 6 is a very crude approximation to a trapezoid plus bell, with the peak of the bell occurring at the change in direction of the failure surface. It is thought that an off-centered bell plus trapezoid would be "the" most correct side force assumption for this problem.

TABLE E.I

EFFECT OF SIDE FORCE ASSUMPTION

Soil Properties			
Soil #	γ_t tons/m^3	$\bar{C}$ tons/m^2	$\bar{\phi}$
1	2.08	0.	7.5°
2	2.08	2.2	7.5°
3	2.17	0.	25.0°

TRIAL	SIDE FORCE ASSUMPTION	λ	F.S.
1	F(x)=Constant	0.518	0.990
2	F(x)=Half Sine Wave	0.692	1.005
3	F(x)=Bell Shape	0.795	1.019
4	F(x)=Trapezoid+Bell	0.641	0.998
5	F(x)=KX+M	0.907	1.056
6	"	1.160	1.012
7	"	0.949	1.022
8	"	0.919	0.935

"MGSTRN" OUTPUT

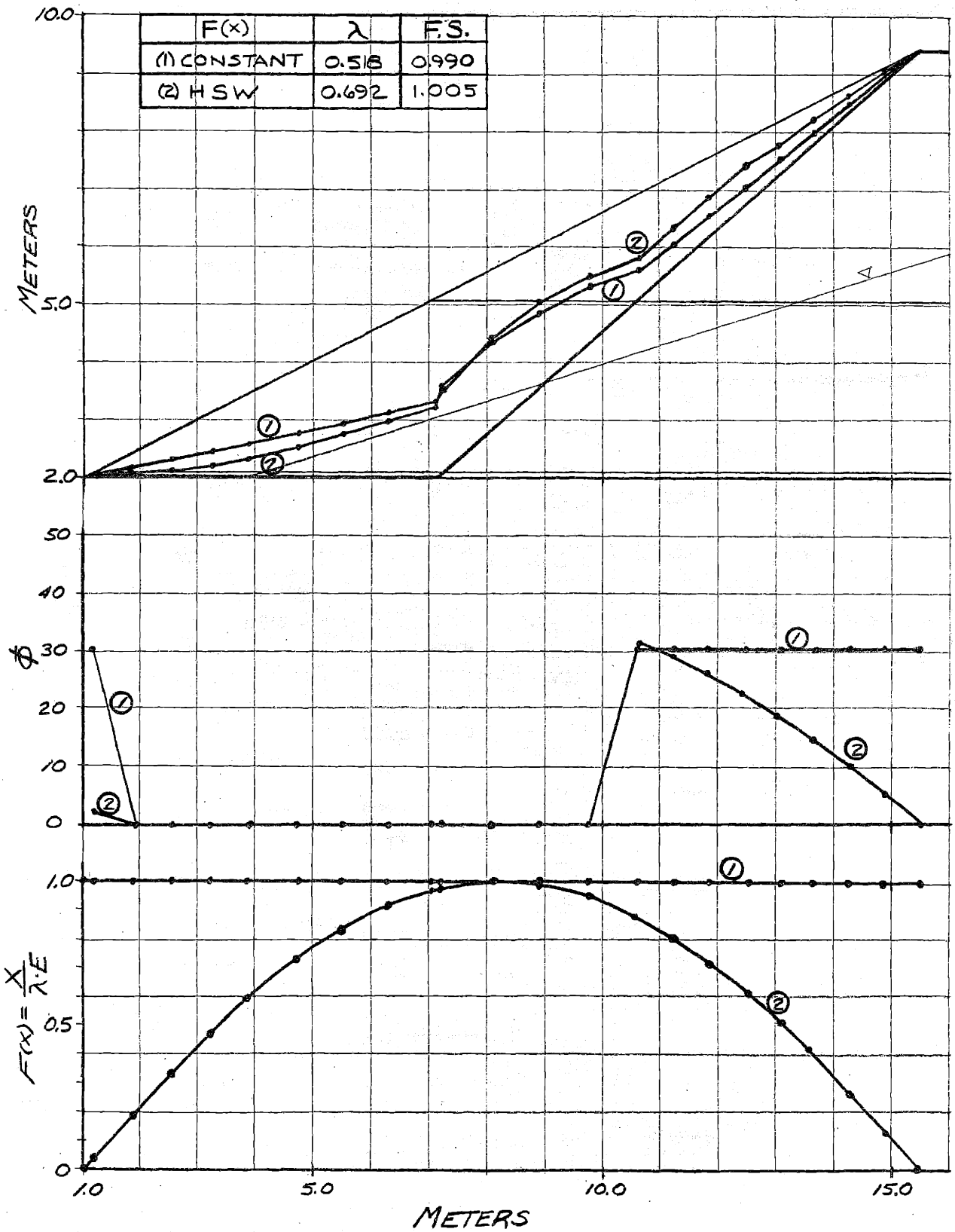

FIGURE E.1

"MGSTRN" OUTPUT

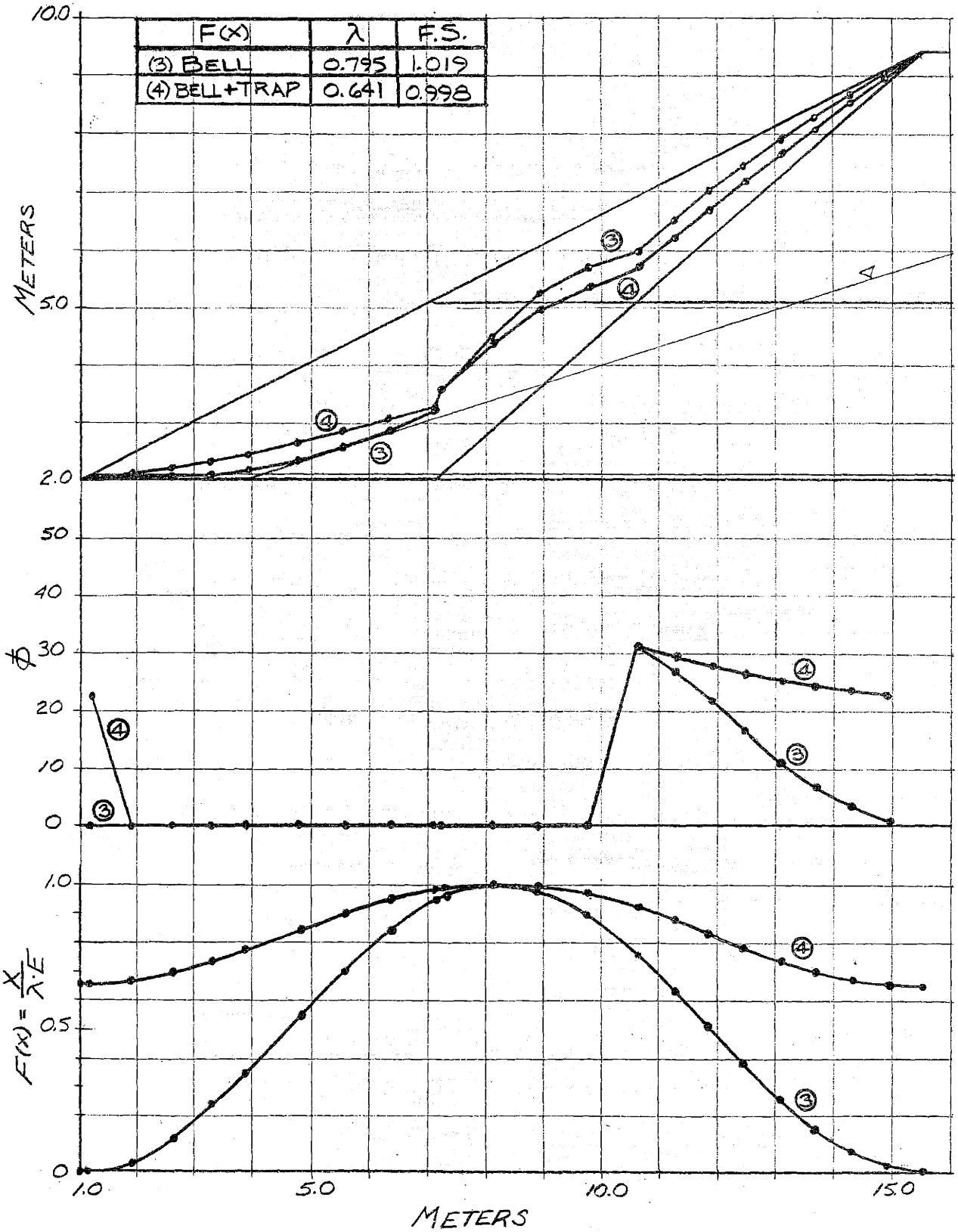

FIGURE E.2

"MGSTRN" OUTPUT

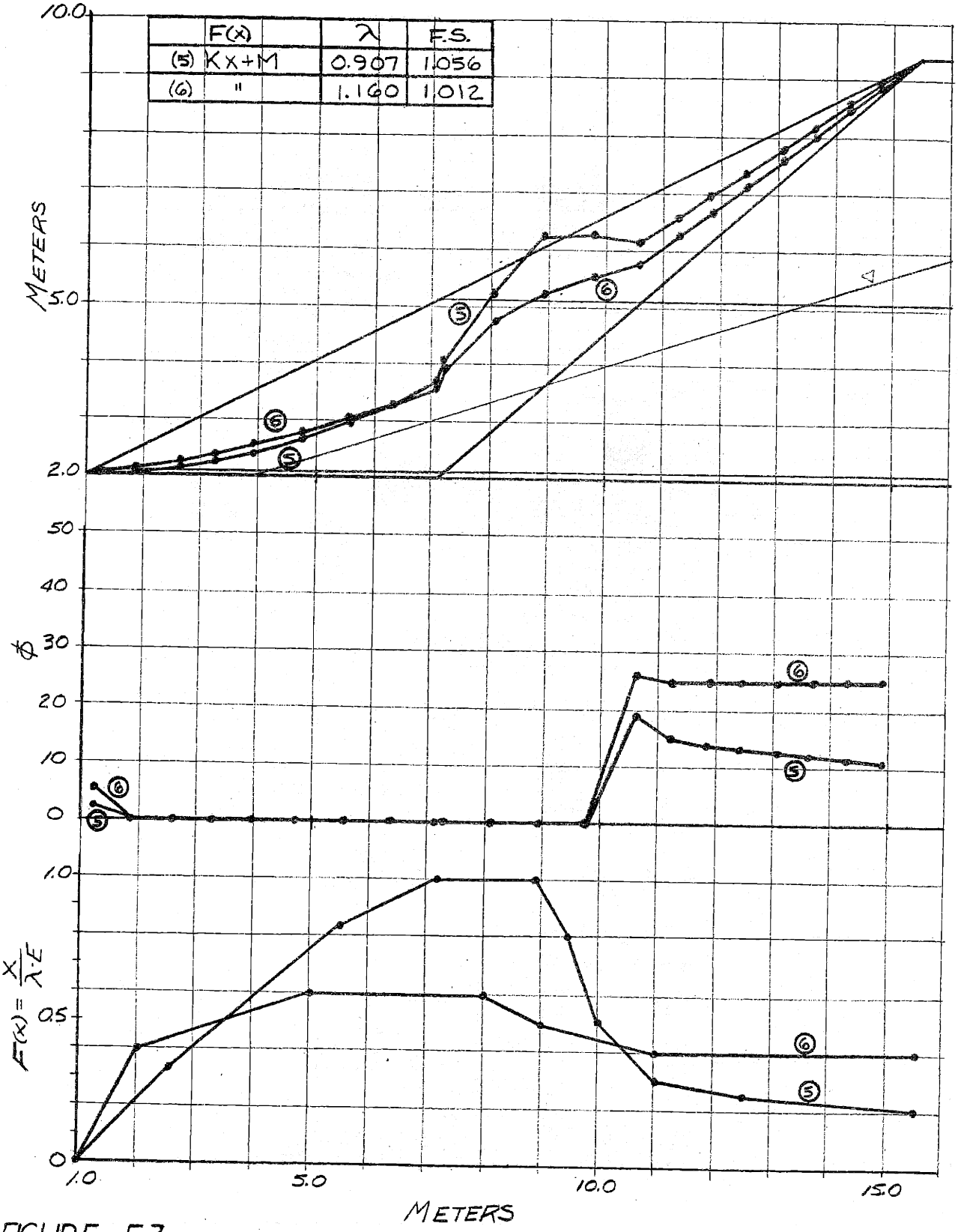

FIGURE E.3.

"MGSTRN" OUTPUT

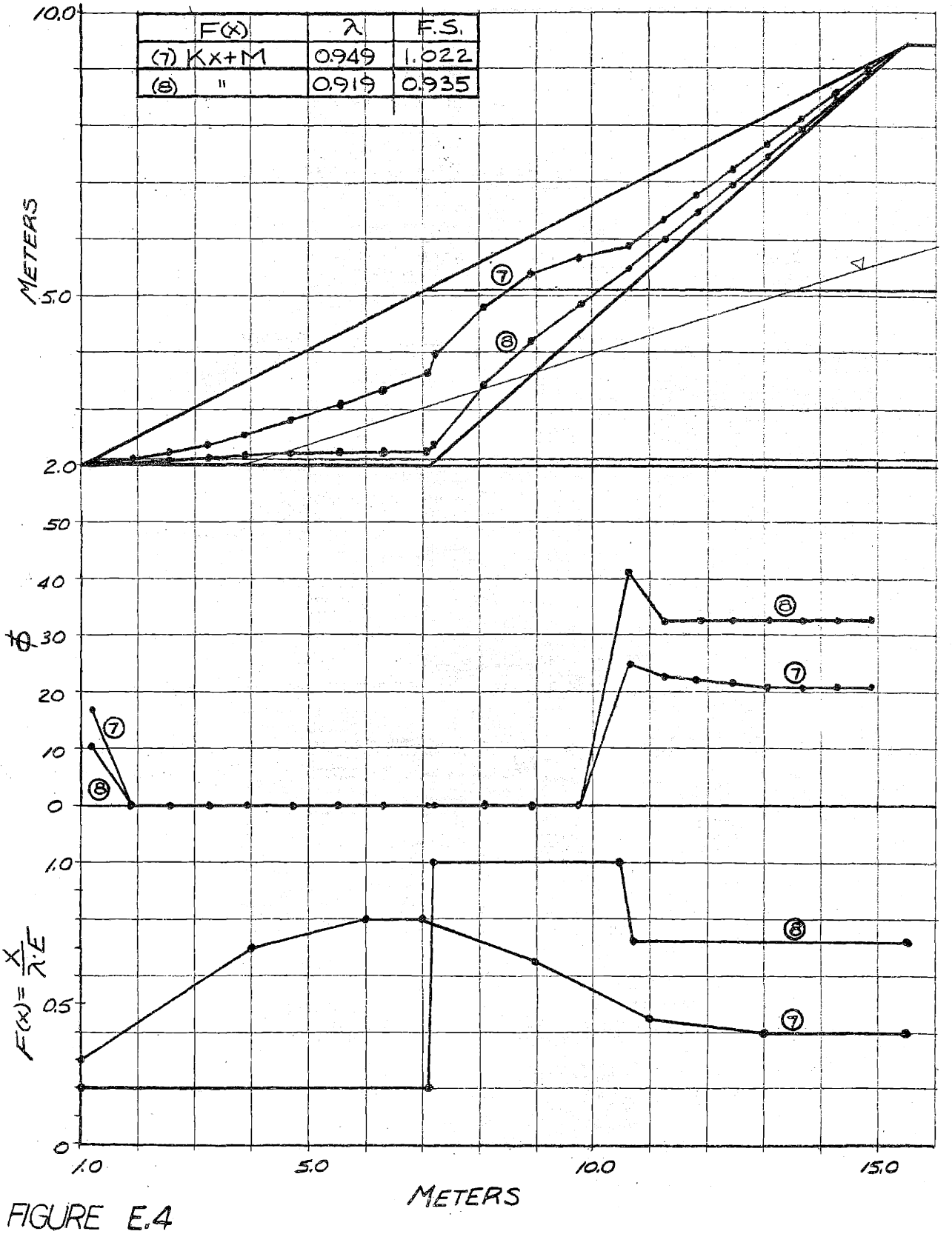

FIGURE E.4